INFORMATION TO USERS

NOTE TO USERS

Page(s) missing in number only; text follows.
Microfilmed as received.

190

This reproduction is the best copy available.

UMI

Neural Correlates of Human Sensorimotor Coordination:

EEG, MEG, and Functional MRI

by

Justine M. Mayville

A Dissertation Submitted to the Faculty of the

Charles E. Schmidt College of Science

In Partial Fulfillment of the Requirements for the Degree of

Doctor of Philosophy

Florida Atlantic University

Boca Raton, Florida

December 2000

UMI Number: 9988029

Copyright 2000 by

Mayville, Justine Meaux

All rights reserved.

UMI®

Neural Correlates of Human Sensorimotor Coordination:
EEG, MEG, and Functional MRI

by

Justine M. Mayville

This dissertation was prepared under the direction of the candidate's dissertation co-advisors, Dr. Armin Fuchs & Dr. J. A. Scott Kelso, Program in Complex Systems and Brain Sciences, and has been approved by the members of her supervisory committee. It was submitted to the faculty of The Charles E. Schmidt College of Science and was accepted in partial fulfillment of the requirements for the degree of Doctor of Philosophy.
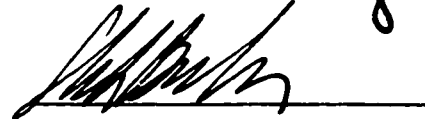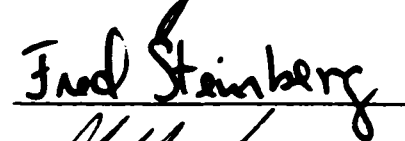
SUPERVISORY COMMITTEE
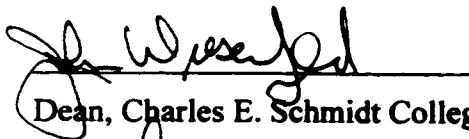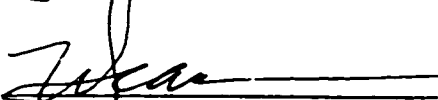
Chairperson   Co-Chairperson

Director, Program in Complex Systems
and Brain Sciences

Dean, Charles E. Schmidt College of Science

Vice Provost   8 Sept., 2000
                                           Date

Acknowledgments

It is a special thing in life to be given an opportunity not only to follow one's passions but also to learn new things. Thank you to my family, especially my parents, for teaching me just how special such opportunities are and for never failing to provide me with the confidence or support I needed to pursue them. I consider myself very lucky to have been able to participate in the Center's doctoral program not only because I was able to contribute to such excellent research but also because of the people I was able to surround myself with. I will be forever grateful to Dr. Scott Kelso and the entire Center faculty for giving me the chance to do so.

I must also thank a large number of people who helped shape my graduate experience and who worked closely with me to teach me the skills I needed to accomplish the research contained in this thesis. No one deserves more thanks, of course, than Dr. Armin Fuchs. Armin, I cannot possibly enumerate all the things you taught me – from getting experiments up and running, to implementing data analyses, to putting together presentations. To do the research in this thesis without your help would have taken at least twice as long! Thank you for all your patience and guidance over the years, for taking the time to sit with me for hours on end and showing me how to program, for all the beers (and nightcaps!) and advice, and finally for always being my strongest supporter. I wouldn't have made it without you. Thanks also to Dr. Steve Bressler and Dr. Kelso for introducing me to neuroimaging by giving me a chance to work in the Center's EEG laboratory and to Dr. Fred Steinberg for making it possible to incorporate

MRI into my research. Finally thanks to Dr. Betty Tuller for all of our conversations, academically and not.

I would also like to acknowledge Arnold Delarisch and Bill McLean, who provided instrumental technical support upon which much of this research depended. Arnold, thank you thank you thank you for always making the EEG lab a priority on your list and answering my questions right away and for ensuring I had plenty of disk space – I'm pretty sure I owe you about a case of beer by now. Thank you also for building an exceptionally stable system from the start – although we tend to take it for granted I am very grateful for the fact that I can count the number of major system problems during my six years here on one hand! Bill, thank you for always dropping everything to help us track problems and for the countless trips to Radio Shack that kept the equipment working.

A number of people helped with data collection and analysis over the years. Specials thanks to Gene Wallenstein for showing me how to use the EEG equipment and for letting me watch over his shoulder for months. Tom Holroyd, I would have been lost without you in that first year. Thank you for taking the time to teach me about computers – I remember asking you what a directory was! Thanks to Rob Lancaster, Fred Carver, and Simon Davis for all their help with the EEG experiments, especially for the many laughs. Thanks to KJ Jantzen for helping me design and collect data for the MRI experiment and for his help and comments with the MEG experiments. Thanks to Dr. Mingzhou Ding for spending time with me and helping me to do some of the MEG analyses. Dinesh Nair and Kari Purcott, thank you for helping to collect and analyze the

MRI data. Finally, thanks to the staff at University MRI and the Department of Neurology at the General Hospital in Vienna, Austria for their help with collecting the MRI and MEG data, respectively.

On a personal note, I would like to thank those who helped to keep me sane during my time here. First and foremost, thank you Ian for all of your support and for always telling me I could do it. Thank you most of all for always listening to my seemingly endless science babble even when there were at least a thousand other things you'd rather be doing! Thanks to Betty Harvey, Sue Rankin, Rhona Frankel and Denise Dorman for making my life a whole lot easier and especially to Rhona for your nice words and goodies every morning. I am grateful to Collin Brown and Dave Engström, both whom I miss very much, for our endless conversations on science and life in general. To Rob Lancaster for being such a good friend and for helping me time and time again with everything. Viktor Jirsa always had a kind word and good advice. Thank you for that Viktor and for being the best canoe partner a girl could ask for. KJ, what can I say, you completely rock! How I wish you'd been here for all of these six years. Thank you also to Phil Fink for the many laughs and for being a great ping-pong partner – I never lost with you on my side (must be the force in you!). Corey Delaplain, I would have died that night in Everglades City without you – thanks for taking care of me then and later (even if you did betray me in Quake). To Tom Ditzinger, the nicest person I have ever met in my life, thank you for always seeing the beauty and kindness in the world and for sharing it with all of us. I will admire you forever.

Last, but certainly not least, there is you Pat Foo. You continue to make me laugh the hardest of all. Thank you for introducing a bit of fun into every day, for making the late hours bearable, for the coffee and slurpee runs, for all your words of encouragement that kept me going this past year and for being my best friend. I am honored to be able to finish with you.

Abstract

Author: Justine M. Mayville

Title: Neural Correlates of Human Sensorimotor Coordination:
                            EEG, MEG, and Functional MRI

Institution: Florida Atlantic University

Thesis Co-Advisors: Dr. Armin Fuchs and Dr. J. A. Scott Kelso

Degree: Doctor of Philosophy

Year: 2000

The ability to coordinate rhythmic finger movement with a metronome is constrained by both the target timing relation and the rate of coordination. For slow metronome rates (< 2 Hz), subjects are able to both *syncopate* (in between successive beats) and *synchronize* (on each beat) with the metronome. At faster rates, however, syncopation becomes unstable and subjects spontaneously switch to synchronization in order to maintain a 1:1 stimulus/response relationship. No switches are observed if subjects start in synchronization, indicating it is an inherently more stable mode of coordination. Patterns of brain activity associated with transitions from syncopation to synchronization as well as synchronization only were examined as the metronome rate was increased from 1.0 to 2.75 or 3.0 Hz. Significant differences in the power of the coordination frequency component of event-related potentials (EEG) as well as the MEG beta (15-30 Hz) rhythm were observed when brain activity associated with syncopation was compared to that accompanying synchronization. These differences were focused over left central and centro-parietal areas and the direction of difference in both cases suggests that syncopation is associated with stronger activation of contralateral

sensorimotor cortex. Similar results were found when subjects only imagined performing each mode of coordination at an increasing rate, indicating that differences in signal power at least partially reflect neural processes associated with motor planning and preparation independent of overt execution. Consistent with these findings, functional MRI revealed syncopation to be accompanied by significantly more activity in a wide array of cortical (e.g., premotor, prefrontal) and subcortical (basal ganglia, cerebellum) areas known to play a role in motor planning and/or timing of behavior. Whereas the neuromagnetic auditory response decreased as function of coordination rate, the motor evoked response remained approximately constant. This was true both when subjects syncopated and synchronized but may reflect changes in auditory-motor integration near movement rates that induce transitions in the former case. A control experiment examined only self-paced movement and showed a second neuromagnetic motor 'readiness' response that was strongly attenuated for rates above 1.0 Hz. This may signify a decreased need for the planning of motor behavior at faster rhythmic rates.

Table of Contents

3.0 Experiment 2: Neuromagnetic activity associated with transitions in sensorimotor coordination

4.0 Experiment 3: Neuromagnetic beta (15-30 Hz) rhythm distinguishes syncopated and synchronized timing patterns in overt and imagined sensorimotor coordination

5.0 Experiment 4: Neuromagnetic motor fields accompanying self-paced rhythmic finger movement of different rates

6.0 Experiment 5: Differences in cortical and subcortical networks associated with syncopated versus synchronized coordinative timing patterns as revealed with fMRI

List of Tables

Talairach coordinates corresponding to the approximate center of voxel clusters in brain areas activated by each control condition and clusters in these same areas which significantly differed between the control and each coordination condition. **6.4a**: Auditory only. **6.4b**: Motor only. Note that for the Synchronize-Motor comparision, the differences found in the cerebellum were negative indicating significantly stronger activation during self-paced movement. Bd: Brodmann's area.

List of Figures

Averaged brain activity and corresponding power spectra for one subject from electrode CP3 (which lies approximately over primary sensorimotor cortex in the left hemisphere) in both coordination conditions. Power is plotted for the first 10 frequency components in the spectrum. (Higher frequencies showed negligible power). Due to the fact that each averaged waveshape is exactly one cycle period in duration, the fundamental frequency in each spectrum corresponds to the labeled coordination frequency. For both conditions, almost all channels showed a concentration of power at this frequency across plateaus. Averages are scaled to $\pm$ 3.25μV and $\pm$ 2.16μV for the Syncopate and Synchronize conditions, respectively. Power spectra are individually scaled to illustrate the prominence of the coordination rhythm; values in the upper right hand corner indicate amplitudes of the largest frequency component in μV^2. Note the difference in power during syncopation versus synchronization at the same plateau frequencies (compare plateaus 1-3 across conditions).

Topographic patterns of grand-averaged EEG power at the coordination frequency for the Syncopate condition (top half), Synchronize condition (bottom half), and flexion frequency for the Motor-only condition (upper right corner). Each plateau is independently scaled from zero to maximal power (unit = μV^2) at that frequency. Coordination frequencies associated with each plateau are shown in the bottom half of the figure. Syncopate condition: The three patterns in the top row (Plateaus 1-3) are associated with syncopated coordination. Note the similar topography across the three different plateau frequencies (1.0 - 1.5 Hz) with maximal power at left centro-parietal, central and antero-frontal sites. Post-transition patterns for this condition (Plateaus 5-9) show maximal power at more frontal sites. These patterns are also consistent across plateau frequencies, indicating a reorganization of cortical activity associated with the switch in coordination mode from syncopation to synchronization. Synchronize condition: Maximal power tends to be focused at left and midline frontal sites. Motor-only condition: power at the flexion frequency (average = 1.0 Hz) is focused at left central sites, consistent with activation of the underlying sensorimotor area during flexion of the right finger.

Chapter 3

Chapter 4

Chapter 5

Chapter 6

A comparison of the coordination and control conditions (see also table 6.4). **Auditory** (top half): Listening to the metronome was associated with activation of the left primary auditory cortex (Brodmann's area 41) in the superior temporal gyrus and right temporal association cortex (Brodmann's area 21) in the middle temporal gyrus (1st row). Within the temporal lobes, syncopation resulted in additional bilateral activation of Brodmann's area 22 (2nd row, left panel). No differences between the Synchronize and Auditory control conditions were found in either temporal lobe (2nd row, right panel). **Motor** (bottom half): Large task-related clusters in the contralateral sensorimotor cortex, SMA and ipsilateral cerebellum were found for self-paced movement (1st row). Neither cortical region showed significant changes in activation levels during coordination (2nd and 3rd rows, 1st panel). Relative to self-paced movement, cerebellar activation increased for syncopation (2nd row, right 2 panels) but decreased for synchronization (3rd row, 3rd panel). All slices are axial: left side – right hemisphere, right side – left hemisphere; slice location along the superior-inferior axis is indicated below.

1.0 General Introduction

One of the fundamental problems faced by any nervous system is the coupling of perception and action. Despite the fact that these processes are often treated as distinct, they are intimately related and, in practice, can be considered to comprise a single system. An integral function of this system is the timing of movement with respect to the external world. The temporal organization of behavior is inherently a problem of coordination, not only of processes within an organism (e.g. between different effector groups) but also between the organism and its environment (e.g. anticipating time to contact) [Arbib, 1985; Kelso & Kay, 1987; Warren, 1998; Lee et al., 1999]. Though the neural mechanisms which integrate these different processes are poorly understood, a guiding principle according to the theory of coordination dynamics [Kelso, 1995] is that coordinative patterns self-organize according to the goal of the organism and constraints of the task situation.

1.1 Transitions in Coordination

A large body of behavioral work demonstrates that one constraint on the ability to perform certain rhythmic timing patterns is the rate of movement. Bimanual coordination experiments have shown that subjects can perform both in-phase (activation of homologous muscle groups) and anti-phase (e.g. flexion of one hand and extension of the other) relations at low movement frequencies [Kelso, 1984; Tuller & Kelso, 1989]. However, increasing the rate of movement causes subjects to spontaneously switch from

anti-phase to in-phase [Kelso, 1984] though transitions in the opposite direction do not occur [Kelso & Scholz, 1985]. Similar effects are observed for unimanual coordination with an external metronome. Under instructions to react to each metronome beat, subjects respond reactively for metronome rates below 1.0 Hz but begin to show anticipatory behavior at higher frequencies [Engström et al., 1996]. Transitions between syncopated (off-the-beat) and synchronized (on-the-beat) response patterns have also been observed. Whereas both timing relations can be successfully performed at rhythmic rates lower than ~2 Hz, beyond this threshold only synchronization is possible [Fraisse, 1982]. Kelso et al., (1990) systematically investigated this phenomenon by asking subjects to perform both timing relations with an auditory metronome whose rate was increased from 1.0 to 3.5 Hz in 0.25 Hz after every 10 beats. When subjects began the trial in a syncopated mode, they spontaneously switched to synchronization once the metronome reached a critical rate. In contrast, for trials that began in a synchronized mode, no transitions were observed. There were also no transitions observed if subjects synchronized with a metronome of decreasing rate (3.5 to 1.0 Hz).

1.2 Coordination Dynamics

Switches between different coordinative timing patterns have been theoretically modeled as phase transitions in a nonlinear dynamical system within the framework of synergetics [Kelso, 1985; Haken et al., 1985]. Synergetics deals with the spontaneous formation of spatial and temporal patterns in nonlinear systems that are far from thermal equilibrium [Haken 1977, 1983]. From this perspective, a given mode of coordination corresponds to a state in a dynamical system that is defined by collective variables or

2

order parameters that both govern and arise from nonlinear interactions of the system's parts. Such order parameters are identified by systematically varying an external control parameter such that qualitative changes in the system's behavior (i.e. switches between different states) occur, a phenomenon that does not exist for linear systems. As stated above, an important concept is that these states are not prescribed explicitly by the control parameter but rather arise in a self-organized fashion. A given state of the system is associated with a certain level of stability that can be probed by measuring the system's response to external perturbation. If the system is near a transition point, the amount of time it takes to relax back into its original state after perturbation increases (known as critical slowing down). In addition, transitions are preceded by an enhancement of fluctuations (i.e. variability in the order parameter) that reflect the system's increasing instability.

In the coordination experiments described in section 1.1, the rate of movement/metronome served as a control parameter whereas the relative phase (between the two hands, or finger and metronome) was identified as an order parameter [Haken et al., 1985, Kelso et al., 1990]. These experiments demonstrate transitions from bistability at low movement frequencies (e.g. both syncopation and synchronization are possible) to monostability at higher rates (only synchronization is stable). An advantage of these transition paradigms is that they can be used to identify features of the spatiotemporal dynamics of brain activity that are uniquely related to a given pattern of behavior.

1.3 Previous Work

During the last decade, transitions from syncopated to synchronized sensorimotor coordination have been shown to be accompanied by temporal and spatial changes in the dynamics of neuroelectric and neuromagnetic brain activity. The first studies [Kelso et al., 1991, 1992; Fuchs et al., 1992] used a 37-channel magnetometer system centered over contralateral sensorimotor areas and revealed a transition in the phase of the MEG signal at the coordination frequency that occurred simultaneously with the transition on the behavioral level. The strongest frequency component of the MEG signal was also observed to undergo a doubling from the coordination frequency to its first harmonic at the transition point. Finally, there was a topographic reorganization of activity such that the dominant spatial pattern pre-transition had a single maximum at the center and post-transition became dipolar. These findings were later theoretically modeled on a phenomenological level using a set of two coupled nonlinear oscillators [Jirsa et al., 1994].

In a later study, whole-head EEG recordings confirmed the existence of a parallel transition in the phase of the coordination frequency component of brain activity [Wallenstein et al., 1995]. Moreover, it was revealed that these phase shifts only occurred in left central recording sites over the contralateral sensorimotor area. Wallenstein et al. (1995) additionally showed an enhancement of fluctuations in this phase measure just prior to the behavioral transition demonstrating a neural correlate of increasing coordinative instability. Evidence of critical slowing down had been found in the earlier MEG studies and was also confirmed.

4

Recently, another MEG study (this time with whole-head sensor coverage) revealed that patterns of brain activity associated with syncopated and synchronized modes of coordination were independent of the target effector group (flexor versus extensor muscles) [Kelso et al., 1998]. A second finding was the existence of a tight coupling between the neuromagnetic motor response and the velocity profile of finger movement. The latter result was theoretically modeled by Fuchs et al. (2000b).

1.4 Measuring Activity in the Human Brain

This thesis contains five separate experiments designed to extend our current understanding of the spatiotemporal dynamics of brain activity associated with syncopated and synchronized modes of sensorimotor coordination. Three imaging techniques that measure different aspects of the spatiotemporal dynamics of neural activity at a macroscopic level were used: Electroencephalography (EEG), Magnetoencephalography (MEG) and functional Magnetic Resonance Imaging (fMRI). All are non-invasive and thus well suited to experiments involving human subjects.

1.41 *Electroencephalography (EEG)*

Human EEG activity is a measure of the collective electrical behavior of neurons. The EEG signal primarily reflects cortical dendritic currents flowing in the *extracellular* space. These currents are carried by ions that flow across the neuronal membrane during states of depolarization/hyperpolarization. Scalp measurements require that a large population of neurons is simultaneously depolarized/hyperpolarized such that these currents sum to produce a measurable signal. In general, action potentials propagating down the axon are not thought to contribute to the EEG signal because they are too brief

(1-2 msec) for appreciable summation to occur. The primary contributing cells to EEG are the pyramidal neurons located in the superficial layers of the neocortex. While it is possible to measure electrical signals at the scalp that were generated in much deeper areas (e.g. the auditory brainstem response), such responses typically have poor signal-noise ratios and require several hundred, even thousands, of trials to extract the signal from an average.

The actual quantity measured in EEG is the difference of the electric potential between two electrodes, one that is located on the scalp surface and a reference located on the head but typically away from the scalp. Common reference choices include the earlobes, nose or mastoid bones located just behind the ears. A conductive bridge is created between each electrode and the skin so that currents can be detected with recording equipment. These currents are extremely weak resulting in small potentials, on the order of 10 μV. Therefore, EEG signals have to be amplified by a factor of about 10^5 to transform them into the volt range for processing with standard electric equipment. Typically the signals are also filtered and then sampled so that they can be digitally analyzed. The temporal resolution afforded by EEG well exceeds typical time scales for neural processes (~10-100 msec) and depends only on one's ability to sample the signal adequately.

In contrast to this excellent ability to measure dynamical changes in patterns of neuroelectric activity on the scalp surface, localizing the sources that generate such EEG patterns is difficult for several reasons. The electric potential itself is not an absolute quantity and therefore can only be measured as a difference between two locations, the

recording electrode and a reference site. Choosing the reference for EEG recording is generally guided by the desire for an 'electrically silent' or 'indifferent' scalp location such that any observed amplitude changes can be attributed to the site of the recording electrode. However, the choice of reference can significantly affect the pattern of activity observed at the scalp [Nunez, 1981] because the EEG signal is subject to volume conduction effects. Moreover, the resistance and dielectric properties of the cerebral spinal fluid, scalp and skull influence the propagation of electric currents. The thickness of these layers is not homogeneous across the entire head surface which means that a signal measured at a given scalp location does not necessarily imply a source in the immediate cortical region [Nunez, 1981]. This happens if, for example, the tissue/fluid layers are relatively thicker above a source causing the current to 'escape' through a thinner, less resistant, portion of the head.

1.42 *Magnetoencephalography (MEG)*

Relatively recent technological advancements have made it possible to detect magnetic fields associated with electric currents within the brain over the head surface. As with EEG, the MEG signal reflects changes in dendritic, not axonal, currents in pyramidal neurons. However, in contrast to EEG signals, the signal detected with MEG is primarily generated by *intracellular* dendritic currents because the majority of magnetic fields caused by diffuse volume current flows or transmembrane currents cancel due to symmetry. Magnetic fields are also differentiated from electric potentials in two other important ways. First, field strength is an absolute quantity and thus is not defined with respect to a separate reference. Second, whereas the electric potential is a scalar

7

field, the magnetic field is a vector field and thus has a directional component in addition to strength.

Magnetic field lines are closed and related to the currents which generate them according to the 'right-hand' rule such that if the thumb of one's right hand points in the direction of current flow, the fingers wrapped around the thumb correspond to the direction of the surrounding magnetic field. This relation implies that currents directed radially to the head surface produce magnetic fields that are externally undetectable because the field lines never exit the head surface. Fortunately all primary sensory and motor areas are located within cortical fissures such that the main current flows are approximately tangential to the scalp. However, the external silence of many other cortical sources is perhaps the main limitation of MEG. Also implied by the relation between currents and magnetic fields is the fact that MEG signals associated with more optimally-oriented current sources have a dipolar structure characterized by field lines exiting in one region of the head surface and entering in another.

A primary advantage of MEG over EEG is the relative insensitivity of magnetic flux to the differing material properties of the cranial tissues. Thus the cerebral spinal fluid, scalp and skull are virtually transparent to magnetic field lines which pass through undistorted. This affords major advantages concerning source localization, which is typically done by finding the one or few 'equivalent current dipoles' that best approximate the MEG signal.

The measurement of magnetic fields associated with neuroelectric activity is difficult for a number of reasons. First, their amplitude is extremely small (10^{-12} or 10^{-13}

Tesla). The only detectors with sufficient sensitivity for the measurement of these fields are so-called SQuIDs (superconducting quantum interference device) [Josephson, 1962; see Hämäläinen et al., 1993 for review], which have to be placed in close proximity to the head surface in order to account for the fact that magnetic field amplitude falls off with the square of the distance from the current source (a major difficulty because the SQuIDs must be cooled to 4 K, the temperature of liquid helium). Second, the relative weakness of these fields with respect to the earth's magnetic field ($\sim 10^{-4}$ T) means that they may be easily swamped by ambient magnetic field variations. These arise from a number of sources including electrical equipment, moving vehicles, elevators, etc. Rejection of such sources of interference is critical. One way to do this is by using gradiometers, which define the MEG signal by comparing field strength at two coil locations (and a set of reference coils in the surrounding). Gradiometer coils are separated by a short distance but wound in opposition. Therefore, background fields that do not change appreciably across such a distance will cancel while the amplitude of magnetic fields generated by the brain (which fall off with the cube of the distance when measuring a gradient) will not.

1.43 Functional Magnetic Resonance Imaging (fMRI)

Magnetic resonance is based on the interaction between an external magnetic field and a particle (in the case of MRI, the nucleus of the hydrogen atom or proton) that possesses a magnetic moment or spin. These spins become aligned with the external field in either a parallel or anti-parallel fashion, with the former corresponding to a lower state of energy. More protons occupy this state, which leads to a macroscopic

9

magnetization of tissue parallel to the external field. The MR signal is produced by applying electromagnetic energy to the tissue at a specific frequency, which is within the range of radio waves and thus called an RF pulse. By applying magnetic field gradients in three orthogonal directions, it is possible to restrict excitation caused by the RF pulse (and thus also the resulting MR signal) to a small volume of tissue, thus allowing 3-D spatial resolution with high accuracy (~ 1 mm^3). The RF pulse has two effects on the net magnetization vector. First, it is turned out of alignment with the external field. The relaxation of the net magnetization back into its resting aligned state is determined by the T_1 relaxation time. Second, the net magnetization vector precesses around the direction of the external field thus emitting electromagnetic waves at the same radio frequency. A second relaxation time is related to this precession. Over time, local inhomogeneities in the surrounding magnetic field differentially affect the precession speed of individual nuclei thus decreasing their net magnetization in directions orthogonal to the external field. The time constant for this decay process is known as T_2^*.

Functional MRI takes advantage of the fact that local field inhomogeneities are introduced by hemodynamic changes that accompany task-related neuronal activation. Though the exact coupling mechanism is not known, excitation of neural tissue is associated with vasodilatation and rapid blood flow increases within the local area, presumably to meet increasing demands for metabolic energy. The increase in blood flow floods the area with oxygenated hemoglobin faster than the rate at which oxygen is extracted by the tissue. This phenomenon (Fick's principle) causes the ratio of oxygenated to deoxygenated hemoglobin to increase [see Cohen et al., 1993; DeYoe et

al., 1994 for discussion]. While oxygenated hemoglobin is a diamagnetic molecule, deoxygenated hemoglobin molecules are paramagnetic and thus introduce stronger variations in a surrounding magnetic field. The change in their ratio therefore *decreases* magnetic inhomogeneities in the local tissue which lengthens the $T2^*$ relaxation time, thus *increasing* the MR signal. In other words, by releasing oxygen hemoglobin acts as a natural contrast agent. This effect is referred to as the BOLD (blood oxygen level dependent) contrast effect.

The main advantage of fMRI over other neuroimaging techniques is its tremendous spatial resolution, which is on the order of cubic millimeters. Furthermore, it is capable of identifying activity in deep cortical and subcortical areas not generally accessible with EEG or MEG. On the other hand, since it is dependent upon the hemodynamic response, fMRI has poor temporal resolution (seconds) which severely limits its ability to track changes in brain activity within the time scale that perceptual, motor and cognitive processes are known to occur (10-100 msec). A second potential drawback is that the fMRI approach is commonly based on subtraction methods in which task-related activity is assessed by computing the difference in MR signal associated with task versus rest (or different task) conditions. This subtraction logic assumes that brain areas involved in a given task or task attribute are *not* involved in the comparison condition, which may not necessarily be true. Finally, since the coupling between neural activity and hemodynamic changes is not known, results must be interpreted with caution. For example, there could be task-related neural activity in other brain areas that

does not result in a hemodynamic response (e.g. lower metabolic demands, different properties of the local vascular structure).

In summary, both EEG and MEG provide excellent temporal resolution that is limited only by one's ability to adequately sample changes in the electric potential or neuromagnetic field. However, volume conduction effects in EEG and the insensitivity of MEG to fields generated by unoptimally oriented current dipoles make it problematic to accurately determine the sources of EEG and MEG activity. Moreover, detecting deep (e.g. subcortical) sources with either technique is extremely difficult, if not impossible in most cases. In contrast, fMRI has far superior spatial resolution and is capable of identifying sources of cortical and subcortical activity that contribute to the performance of certain tasks. Measures of the BOLD effect, on the other hand, are insensitive to rapid dynamical changes in brain activity. Figure 1.1 shows the relation of the spatial and temporal resolutions of EEG, MEG and MRI/fMRI. From their advantages and limitations, it is clear that combining information obtained with each of the techniques can significantly improve one's understanding of the spatiotemporal dynamics of brain activity associated with a given task.

1.5 *Outline of this Thesis*

In the following chapters, five separate experiments on sensorimotor coordination are presented. Experiments 1-3 employed the transition paradigm outlined in section 1.1 to 1) further investigate the reorganization of brain activity that accompanies behavioral transitions from syncopation and synchronization and 2) distinguish changes due to the performed timing pattern from those due to increasing coordination frequency. One of

12

our primary goals in these experiments was to take advantage of technological developments to provide a physiological interpretation of observed effects. In Experiment 1, whole-head EEG recordings were used to measure and describe changes in event-related potential amplitude. In Experiments 2 and 3, we measured whole-head MEG signals and analyzed both event-related field activity as well as amplitude changes in higher frequency bands that are not preserved when ensemble averaging is done in the time domain. In Experiment 3, we examined perceptual transitions from syncopation to synchronization that occur when subjects only imagine coordinating with a metronome and identified neural correlates of mental switching in the brain that parallel the overt case.

Experiment 4 also employed whole-head MEG recordings and was designed to systematically investigate the effects of response rate on motor-related processes in the brain. In this experiment, subjects performed a continuation task that allowed them to successfully self-pace movements at 21 separate rhythmic rates. This made it possible to examine neuromagnetic activity associated with movement in the absence of auditory-related field activity. Such dissociation is desirable since these fields overlap topographically at the head surface with motor fields. Finally, in Experiment 5 we used fMRI to elucidate the contributions of different brain areas to syncopation and synchronization. We primarily focused on cortical and subcortical areas known to be involved in the temporal organization of behavior.

Figure 1.1 (page 15): Temporal and spatial resolution of EEG, MEG and fMRI/MRI imaging technologies. Both EEG and MEG are sensitive to changes in brain activity that occur on a millisecond timeframe. Since fMRI is dependent on the hemodynamic response, the changes it monitors occur over a few seconds. Structural MRI takes much longer, on the order of several minutes. Spatially, structural MRI scans have the best resolution and are capable of imaging tissue volumes near 1 cubic mm in size. Voxel sizes in fMRI are slightly larger (~4mm x 4mm x 7mm) but this resolution still well exceeds that associated with EEG and MEG technologies, which is on the order of one to several centimeters. MEG also has slightly better spatial resolution than EEG because magnetic fields are not subject to volume conduction effects or smearing as a result of passage through the cerebral spinal fluid, scalp and skull.

Figure 1.1
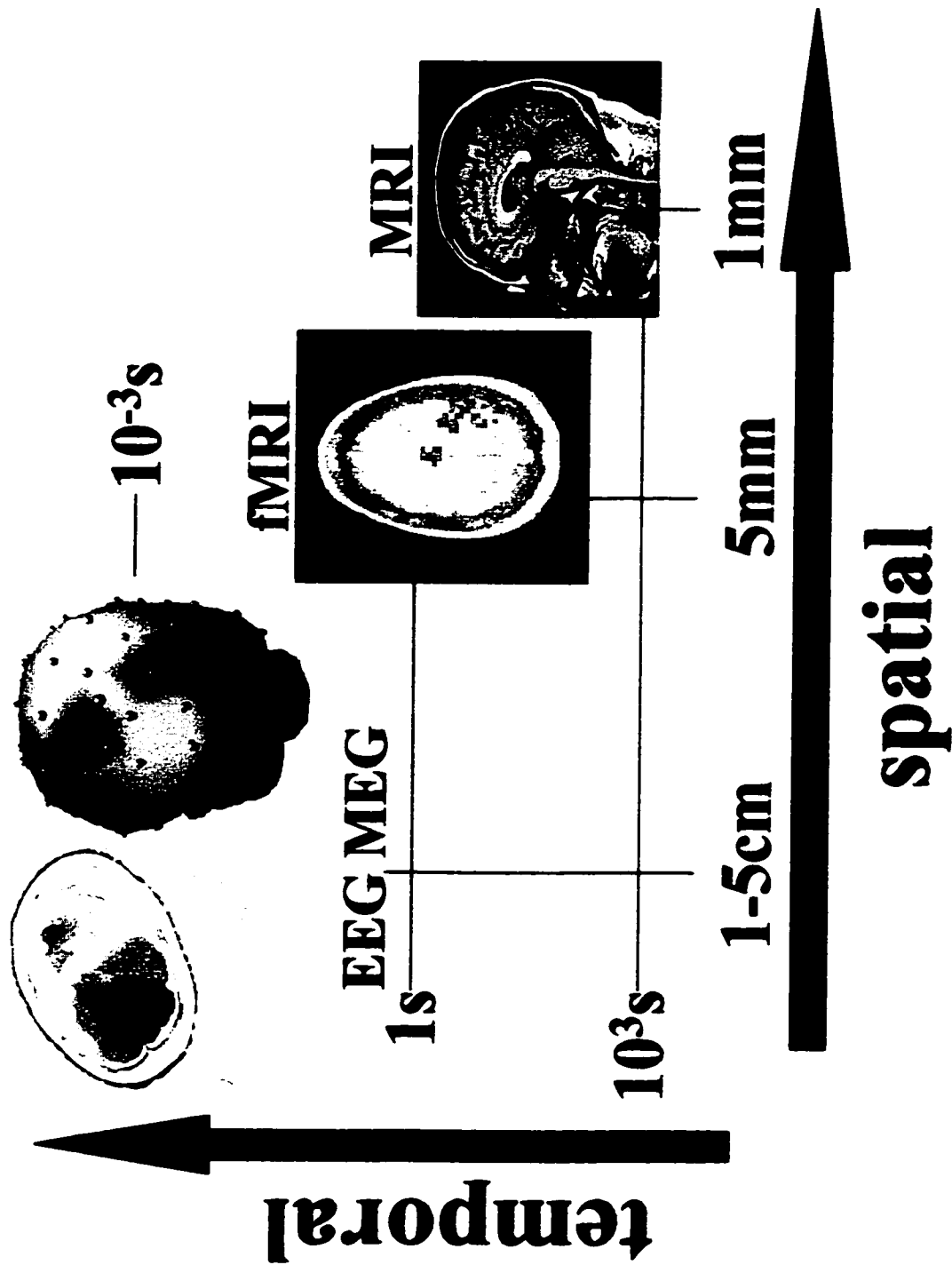
2.0 Experiment 1: Neuroelectric activity associated with transitions in sensorimotor coordination

2.1 Introduction

Rhythmic coordination is common to many activities we encounter in everyday life. For example, dancing, playing a musical instrument, typing, riding a bicycle, all require that the brain integrate incoming sensory information and outgoing motor commands in a regular, patterned fashion. Here we focus on a simplified form of rhythmic coordination, periodic finger flexion paced by an auditory metronome. It is well known from previous studies that the stability of certain coordinative states under these task conditions depends on the frequency of coordination [Kelso, 1984; Kelso et al., 1990; Wimmers et al., 1992]. When subjects are directed to maintain a 1:1 relationship between repeated finger flexion and a periodic external metronome in a synchronized fashion, they are able to do so across a wide range of continuously increasing metronome frequencies (approximately 0.7-4.0 Hz for an auditory metronome). However, under instructions to flex *in between* successive metronome beats (i.e. in an anti-phase or syncopated manner) subjects spontaneously shift to a synchronized mode of coordination when the metronome frequency increases beyond a critical point. If the metronome frequency is subsequently decreased back to its initial rate, subjects do not spontaneously switch back to an anti-phase relation [Kelso et al., 1990], suggesting that synchronization is an inherently more stable timing relation at all frequencies. This conclusion is

supported by the work of Scholz and Kelso (1990) [see also Kelso et al., 1988] which investigated the ability of subjects to intentionally switch between syncopated and synchronized modes of coordination at a single frequency. Their results showed significantly longer switching times when subjects had to go from in-phase to anti-phase coordination when compared to the reverse. Also consistent are recent results demonstrating that a greater degree of attention is required to maintain an anti-phase versus in-phase mode of rhythmic bimanual coordination [Temprado et al., 1999].

Previous studies by our group have used the syncopation-synchronization transition to investigate neural processes (as reflected, e.g., in large-scale electrode or SQuID (Superconducting Quantum Interference Device) recordings) that underlie stability and change in rhythmic coordination. We have consistently observed a periodic component in human brain electrical and magnetic activity at the frequency of behavioral coordination (whether unimanual or bimanual), and have found that qualitative changes in the temporal evolution of that activity accompany the transition from syncopation to synchronization. These changes include a parallel transition in the phase of magnetoencephalographic (MEG) [Kelso et al., 1991, 1992; Fuchs et al., 1992] and electroencephalographic (EEG) [Wallenstein et al., 1995] signals with respect to the metronome. In addition, just prior to the switch in timing, phase measures at brain and behavioral levels show enhanced fluctuations and increased relaxation times [Kelso et al., 1991, 1992; Fuchs et al., 1992; Wallenstein et al., 1995]. These are both key features of instability predicted by theories of self-organization, particularly synergetics [Haken, 1977, 1983].

Here we examine the question of whether the switch to a synchronized timing relation also entails a spatial reorganization of brain activity. Related studies have reported changes in the involvement of active brain areas during performance of rhythmic movement tasks as a function of several task parameters. For example faster movement rates are associated with increased activation in primary sensorimotor cortex (SM1) [Rao et al., 1996; Sadato et al., 1996, 1997; Jenkins et al., 1997], higher-order motor areas, including premotor cortex (on the dorsolateral hemispheric surface) and the supplementary motor area (SMA, in the medial wall of the interhemispheric fissure), as well as the cerebellum [Jenkins et al., 1997]. The way in which the movement is paced is also of importance with self-paced movements resulting in stronger SMA activation than externally-paced movements [Halsband et al., 1993; Larsson et al., 1996; Rao et al., 1997]. A third movement attribute of particular relevance is the complexity of the movement. Several areas are thought to play a greater role in producing more difficult movement patterns including SMA, premotor cortex, posterior parietal cortex, the basal ganglia and ipsilateral SM1 [Lang et al., 1990; Kitamura et al., 1993; Shibasaki et al., 1993; Sadato et al., 1996; Chen et al., 1997; Gerloff et al., 1997; Boecker et al., 1998; Catalan et al., 1998].

We now report evidence that the transition from one stable mode of rhythmic coordination to another involves qualitative changes in the spatial pattern of cortical activity. Employing a full-head EEG electrode array, we found that different rhythmic timing relationships in behavior (syncopation and synchronization) are associated with unique spatial distributions of neural activity. We further show the spatial differences to

.

be localized to left central and centro-parietal recording sites, which most likely reflect changes in activity of the underlying SM1. Finally, we demonstrate that the timing relationship between stimulus and response (anti-phase or in-phase), rather than the rate of coordination, is the key contributing factor that determines the spatiotemporal pattern of electrical activity in this type of rhythmic coordination task.

2.2 Methods

2.21 Subjects

Six male subjects, aged 24 to 47 years, participated in all experimental conditions. All subjects were right-handed according to self-reported responses to the Edinburgh handedness inventory [Oldfield, 1971]. Informed consent was obtained from all subjects prior to the experiment and the study was approved by the institutional review board.

2.22 Task Conditions

Four *conditions* were included in this experiment: two sensorimotor coordination conditions and two control conditions. In the coordination conditions, a series of auditory tones (1.1 kHz, 80 ms duration) were presented at a periodic rate, which increased from 1.0 to 3.0 Hz in increments of 0.25 Hz after every 10 tones. Each series of 10 cycles at a single rate is referred to as a *plateau*; nine plateaus constituted a run. Each subject performed 60 runs of each condition in two 30-run sessions. Instructions for the Syncopate condition were to produce peak flexion halfway between consecutive tones, i.e. with a 180°, or anti-phase relationship. For the Synchronize condition, subjects were told to coincide peak flexion with the tones (0° or in-phase). This condition provided a control for the effect of plateau frequency. In both coordination conditions,

19

subjects were instructed to maintain a 1:1 stimulus-flexion ratio at all times, regardless of whether or not they could do so with the correct phase relation; that is, if they felt their motor pattern begin to change, they should not resist the change at the cost of abandoning the required flexion rate. In the Motor-only control condition subjects were instructed to flex their right index finger at a comfortable pace, with no stimuli being delivered. Finally, in the Auditory-only control condition, subjects were instructed not to respond as they listened to a series of tones presented at a rate of 1.0 Hz.

2.23 Experimental procedure

All subjects were informed of the possible risks and benefits associated with their participation, as well as the nature of the experimental tasks. Subjects were seated in an armchair inside a sound-attenuating chamber (Industrial Acoustics Company). The auditory metronome was presented to subjects binaurally through plastic headphones. Each subject's right arm was abducted approximately 30° at the shoulder with the forearm supported in a pronated position by an armrest. Movement of the right index finger was monitored via an air cushion pressure sensor located beneath the fingertip. The air cushion was inflated such that subjects could not depress it all the way in order to ensure definition of peak flexion (i.e. maximal displacement). Since the tasks required timing of peak flexion with an external stimulus, it was not necessary to monitor EMG activity associated with contraction of the flexor muscles. Pilot work, however, revealed a consistent temporal delay (120 ± 15 msec) between the onset of EMG activity in the flexor carpi radialis muscle of the subject's right arm and peak flexion measured with the same pressure device used in this experiment.

20

The onset of each run was cued with three rapid auditory tones. Subjects were instructed to maintain fixation on a marked point approximately one meter in front of the eyes, and to refrain from all body and facial movements. Short breaks were provided between runs and longer breaks after each block of five runs. To familiarize subjects with the experiment, the coordination tasks were demonstrated before recording began.

2.24 Data Collection

Electroencephalographic (EEG) activity was recorded during task performance from 61 electrodes placed on the scalp according to an expanded 10/20 International System of Electrode Placement (figure 2.1). Electrode impedance was reduced to less than 10 KΩ. During recording, each electrode was referenced to a left mastoid electrode and then later, off-line, rereferenced to the average of the left mastoid and electrode T8 (on the right side of the head) in order to minimize lateral bias. Signals were amplified (gain = 10^5) using Grass 12A5 amplifiers (-6 dB at 0.1 and 30 Hz, 4.5 dB per octave falloff), and sampled at 128 Hz (12-bit A/D conversion using two VAXlab ADQ32s). Eye movements were monitored by referencing the upper medial to lower lateral portions of the orbital rim. Auditory stimuli and finger pressure data were also digitized at a rate of 128 Hz as described above.

2.25 Behavioral Analysis

The relative phase between peak flexion and stimulus onset was calculated for each cycle per run in the coordination conditions and then used as the basis for segregating cycles according to the type of coordination performed. Two modes of coordination were studied: syncopation and synchronization. Syncopation cycles were
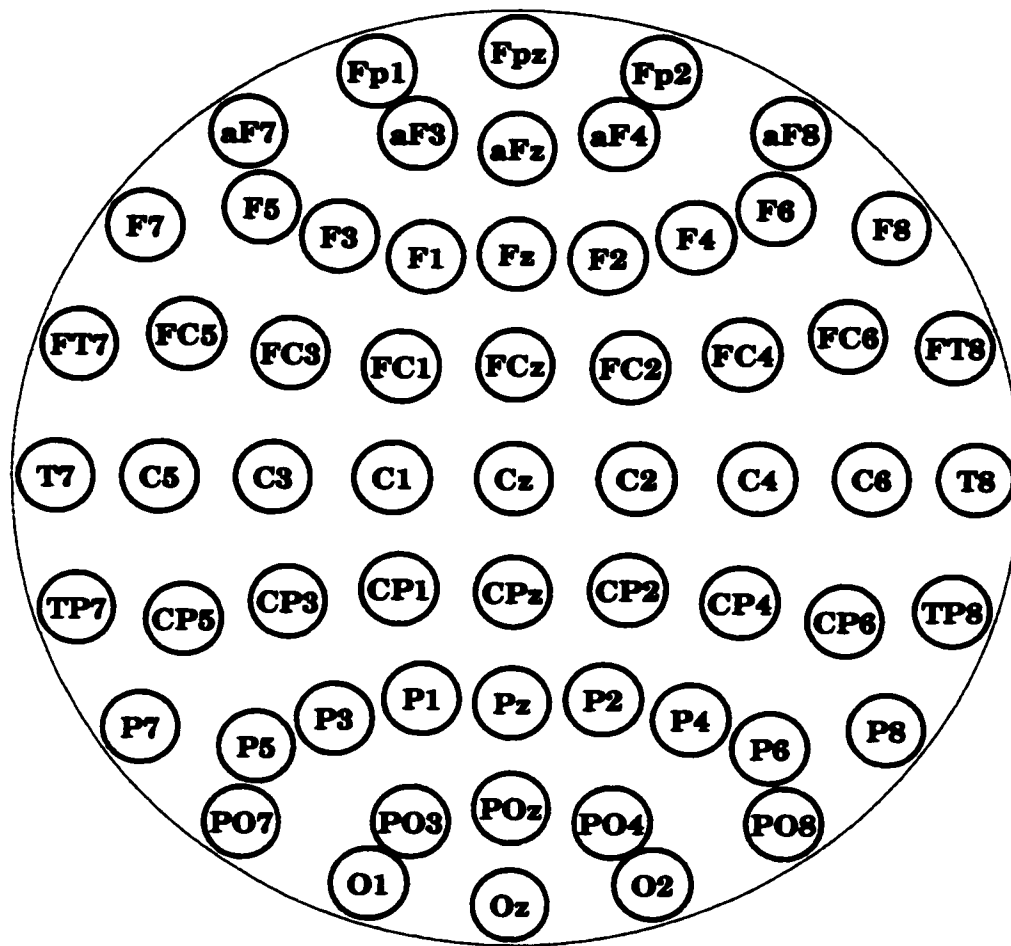
Figure 2.1: Projected top view of electrode positions. The subject's nose would be in front of Fpz.

Figure 2.1

classified as those whose relative phase fell within a ± 50° window centered on the mean relative phase value averaged across the subject's first three plateaus in the Syncopate condition. Syncopation phase values ranged from 120° to 220° across subjects. For all subjects, synchronization cycles were defined as those within a ± 50° window around 0° (with 0° representing exact coincidence of peak flexion with the stimulus). At least five consecutive cycles with consistent coordination were required to classify them as syncopated or synchronized. Where indicated, transition cycles refer to any cycle occurring in the transient region between stable episodes of syncopation and synchronization.

2.26 EEG Analysis

2.261 Averaging and Topographic Mapping

First, cycles for which the EEG was free from artifacts due to eye or other movements were selected and grouped into sets according to condition, coordination mode (syncopation or synchronization), plateau and subject. Second, brain neuroelectric activity was averaged relative to stimulus onset for each set which contained at least 50 artifact-free cycles. Third, the Discrete Fourier Transform was applied to the averaged waveshape to obtain power spectra. Because the duration of each averaged waveform equaled the metronome cycle period, the fundamental frequency in each spectrum was the required coordination frequency. Finally, power spectra were averaged across subjects (weighted according to the number of cycles) for combinations of condition, coordination mode and plateau having averages from at least five of the six subjects. Grand-averaged power spectral values at the coordination frequency were mapped at

standardized electrode locations on a three-dimensional model head. Map values for locations between electrodes were spline-interpolated.

Grand-averaged power spectra from the Auditory-only and Motor-only control conditions were computed relative to stimulus onset and peak flexion, respectively, in similar fashion. Due to the self-paced nature of the Motor-only condition, each subject produced cycles having a characteristic inter-peak interval. The fundamental frequency component in the resulting power spectra thus corresponded to each subject's preferred flexion frequency.

2.262 Statistics

Topographic similarity between power maps was assessed with a Pearson correlation using power values at each channel as observations. Power values were also subjected to two-way analysis of variance (ANOVA) to investigate statistical differences in the spatial distribution of power. These values were pooled across subjects and plateaus and weighted the same way as when calculating grand-averaged power. Post-hoc pairwise channel comparisons for significant interactions were computed using the conservative Tukey's HSD procedure [Kirk, 1968].

2.3 Results

2.31 Behavior

All subjects were able to maintain syncopated coordination in the early plateaus of the Syncopate condition, and synchronized coordination throughout the entire run in the Synchronize condition. Figure 2.2 illustrates the stimulus and finger pressure time series (top and bottom rows, respectively) from representative runs in the Syncopate and

Behavior: Stimulus & Response

A: Syncopate Condition

| 1 | 2 | 3 | 4 | 5 | 6 | 7 | 8 | 9 |
| 1.0 Hz | 1.25 Hz | 1.5 Hz | 1.75 Hz | 2.0 Hz | 2.25 Hz | 2.5 Hz | 2.75 Hz | 3.0 Hz |

Plateau

B: Synchronize Condition

| 1 | 2 | 3 | 4 | 5 | 6 | 7 | 8 | 9 |
| 1.0 Hz | 1.25 Hz | 1.5 Hz | 1.75 Hz | 2.0 Hz | 2.25 Hz | 2.5 Hz | 2.75 Hz | 3.0 Hz |
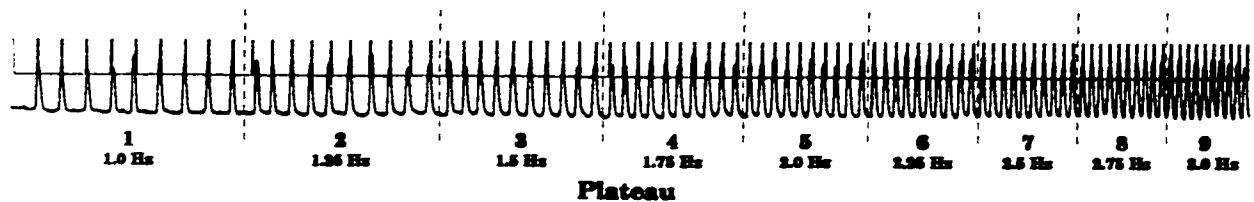
Plateau

Figure 2.2: Stimulus (top trace) and finger-pressure (bottom trace) channels from single runs for both coordination conditions. A: Syncopate, B: Synchronize. Note the loss of syncopated coordination beginning around plateau 5 in the Syncopate condition, followed by a synchronized mode of coordination. There is no transition in the Synchronize condition.

25

Figure 2.2

All Subjects   Syncopate Condition
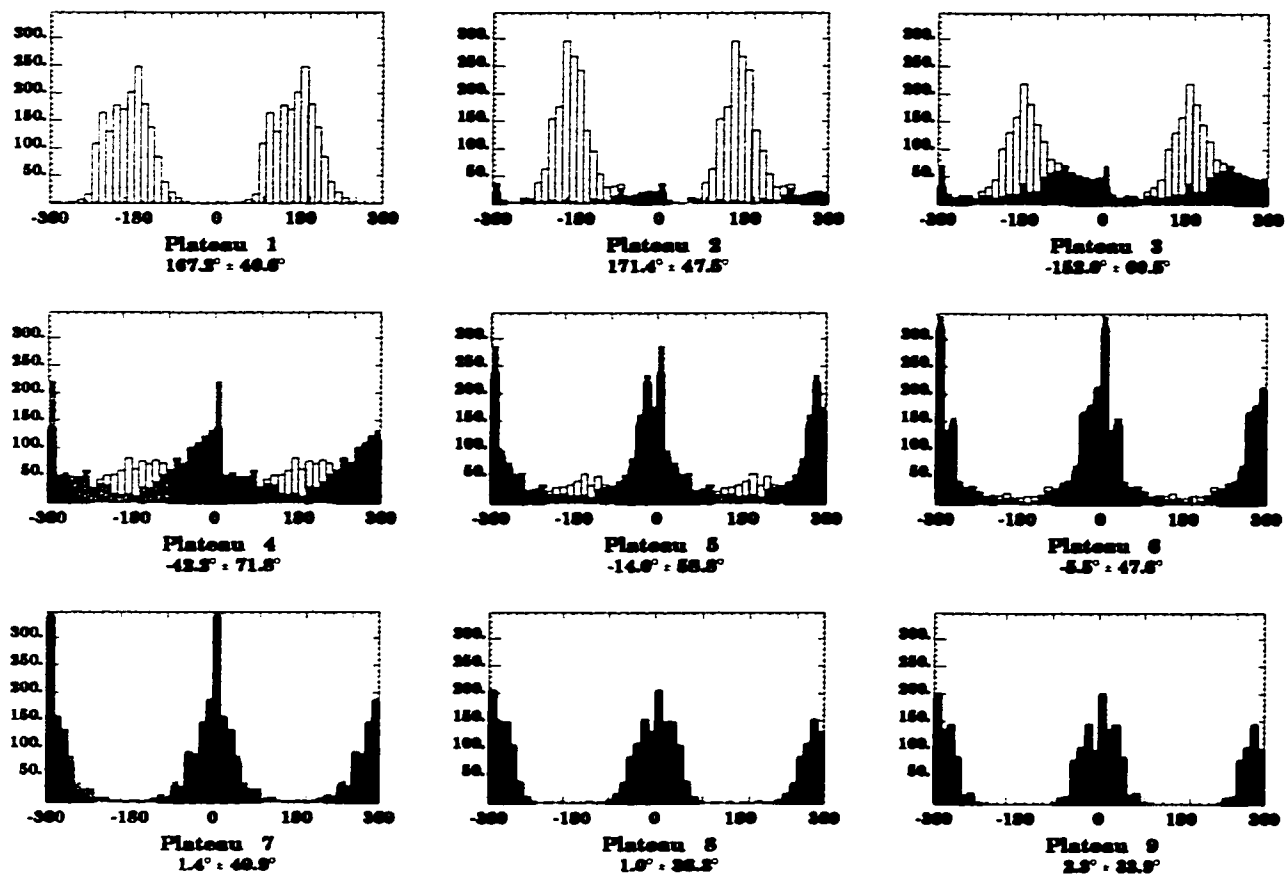
Figure 2.3: Group relative phase distributions for the Syncopate condition. Bars are shaded according to coordination mode: syncopation - white, transition - gray, synchronization - black. Note the onset of transitions as early as plateau 2 and as late as plateau 7.

Figure 2.3

Synchronize coordination conditions. In the run shown for the Syncopate condition, a transition from syncopated to synchronized coordination occurred during plateaus 5 and 6 (figure 2.2A). Approximately 65% of all runs from this condition showed a transition to synchronization, although the plateaus in which the transitions occurred varied somewhat across runs and subjects. For example, one subject switched to synchronized coordination as early as plateau 2 (1.25 Hz), while another subject maintained syncopated coordination as late as plateau 7 (2.5 Hz) before switching. The majority (72%) of transition regions, though, included plateaus 4 or 5 (1.75 - 2.0 Hz). In the runs that did not exhibit a clear-cut transition, subjects either failed to syncopate from the beginning or were unable to settle into any stable pattern after losing syncopated coordination.

The distribution of relative phase values from the Syncopate condition is broken down by plateau in figure 2.3. Mean values were $174°$ ($\pm$ $37°$) for syncopated coordination (shown in white), $-75°$ ($\pm$ $74°$) during the transition régime (shown in gray), and $-4°$ ($\pm$ $32°$) for the synchronized mode (shown in black). The greater variability in the transition mode reflects the presence of phase wrapping during the transition, that is when the 1:1 stimulus/flexion relationship was lost.

For the Synchronize condition, no transitions in coordination mode were observed (figure 2.2B). Approximately 4% of the runs in this condition were excluded due to unstable coordination, which typically occurred at higher plateau frequencies. The average phase between peak flexion and tone onset for this condition was $-8°$ ($\pm$ $32°$). No noticeable differences were observed in the ability of subjects to maintain synchronization across plateaus. These results confirm the established result [e.g. Kelso

et al., 1990] that, in this type of task, coordination for low stimulus rates is bistable (both syncopation and synchronization are possible), whereas only synchronized behavior is stable at higher movement frequencies.

2.32 EEG

2.321 Syncopate Condition

Grand-averaged power spectra were computed in the Syncopate condition for syncopated coordination on plateaus 1 to 3 (1.0-1.5 Hz) and for synchronized coordination on plateaus 5 through 9 (2.0-3.0 Hz). Figure 2.4 shows one subject's averaged EEG and corresponding power spectra for these plateaus from a left centro-parietal electrode (CP3). The predominance of power at the coordination frequency, reflecting the prominent rhythmic component at this frequency in the brain activity, was observed in 86% and 91% of the channels averaged across pre-transition and post-transition plateaus, respectively. The dominance of the coordination frequency in the brain activity is further illustrated by comparing the overlap of this single component with the averaged waveshape (figure 2.4). Note that the time series of the coordination frequency component shifts in phase by approximately 180° when the behavior switches from syncopation to synchronization (compare left and right side of figure 2.4 top). The prominence of the coordination frequency in the brain activity as well as the parallel phase shifts on both neural and behavioral levels are consistent with previous results [Kelso et al., 1991, 1992; Fuchs et al., 1992; Wallenstein et al., 1995].

Topographic mapping of power at the coordination frequency was used to examine differences in involvement of brain areas associated with syncopated versus

Subject 2, Channel: CP3

Syncopate Condition

Pre-Transition

Post-Transition

3.25 μV Plot 1   Plot 2   Plot 3   Plot 5   Plot 6   Plot 7   Plot 8   Plot 9

-3.25 μV

1.0 Hz   1.25 Hz   1.5 Hz   2.0 Hz   2.25 Hz   2.5 Hz   2.75 Hz   3.0 Hz

Synchronize Condition

2.16 μV Plot 1   Plot 2   Plot 3   Plot 4   Plot 5   Plot 6   Plot 7   Plot 8   Plot 9

-2.16 μV

1.0 Hz   1.25 Hz   1.5 Hz   1.75 Hz   2.0 Hz   2.25 Hz   2.5 Hz   2.75 Hz   3.0 Hz
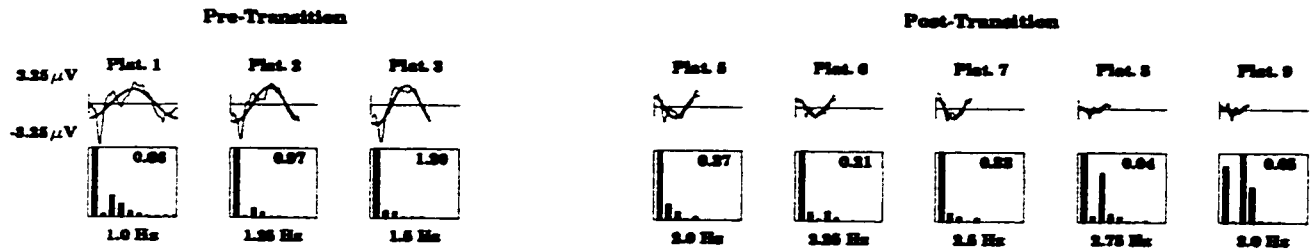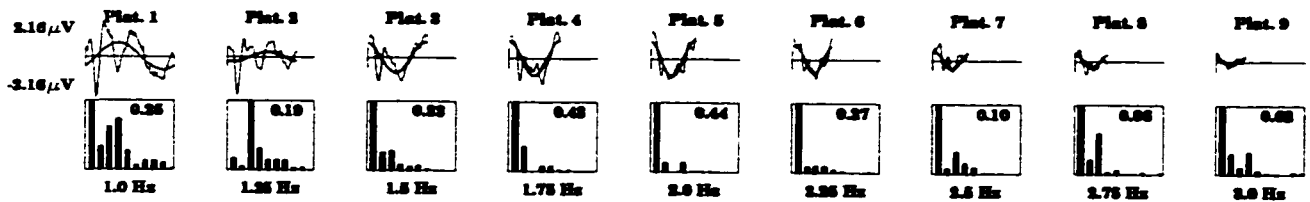
Figure 2.4: Averaged brain activity and corresponding power spectra for one subject from electrode CP3 (which lies approximately over primary sensorimotor cortex in the left hemisphere) in both coordination conditions. Power is plotted for the first 10 frequency components in the spectrum. (Higher frequencies showed negligible power). Due to the fact that each averaged waveshape is exactly one cycle period in duration, the fundamental frequency in each spectrum corresponds to the labeled coordination frequency. For both conditions, almost all channels showed a concentration of power at this frequency across plateaus. Averages are scaled to ± 3.25μV and ± 2.16μV for the Syncopate and Synchronize conditions, respectively. Power spectra are individually scaled to illustrate the prominence of the coordination rhythm; values in the upper right hand corner indicate amplitudes of the largest frequency component in μV^2. Note the difference in power during syncopation versus synchronization at the same plateau frequencies (compare plateaus 1-3 across conditions).

Figure 2.4

Figure 2.5 (page 31): Topographic patterns of grand-averaged EEG power at the coordination frequency for the Syncopate condition (top half), Synchronize condition (bottom half), and flexion frequency for the Motor-only condition (upper right corner). Each plateau is independently scaled from zero to maximal power (unit = μV^2) at that frequency. Coordination frequencies associated with each plateau are shown in the bottom half of the figure. Syncopate condition: The three patterns in the top row (Plateaus 1-3) are associated with syncopated coordination. Note the similar topography across the three different plateau frequencies (1.0 - 1.5 Hz) with maximal power at left centro-parietal, central and antero-frontal sites. Post-transition patterns for this condition (Plateaus 5-9) show maximal power at more frontal sites. These patterns are also consistent across plateau frequencies, indicating a reorganization of cortical activity associated with the switch in coordination mode from syncopation to synchronization. Synchronize condition: Maximal power tends to be focused at left and midline frontal sites. Motor-only condition: power at the flexion frequency (average = 1.0 Hz) is focused at left central sites, consistent with activation of the underlying sensorimotor area during flexion of the right finger.

Syncopate Condition

Motor-only Condition

0.0 0.43	0.0 0.41	0.0 0.64		0.0 0.42
1.0 Hs	1.25 Hs	1.5 Hs		

0.0 0.34	0.0 0.36	0.0 0.30	0.0 0.23	0.0 0.35
2.0 Hs	2.25 Hs	2.5 Hs	2.75 Hs	3.0 Hs

Synchronise Condition

0.0 0.56	0.0 0.57	0.0 0.35	0.0 0.36
1.0 Hs	1.25 Hs	1.5 Hs	1.75 Hs

0.0 0.33	0.0 0.36	0.0 0.32	0.0 0.31	0.0 0.24
2.0 Hs	2.25 Hs	2.5 Hs	2.75 Hs	3.0 Hs

31
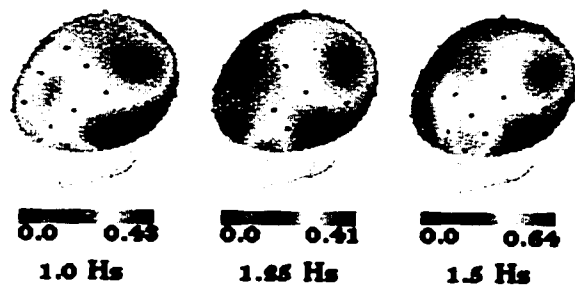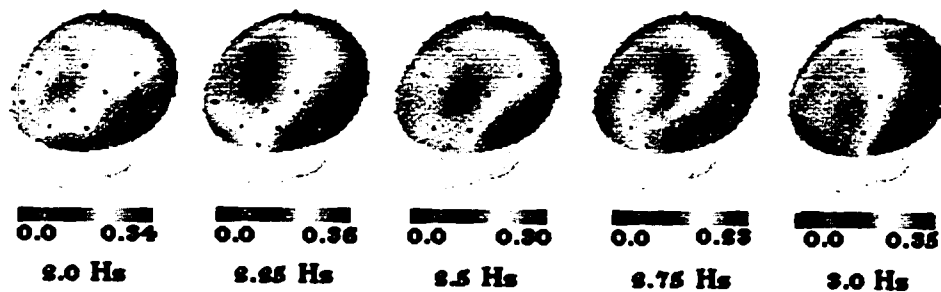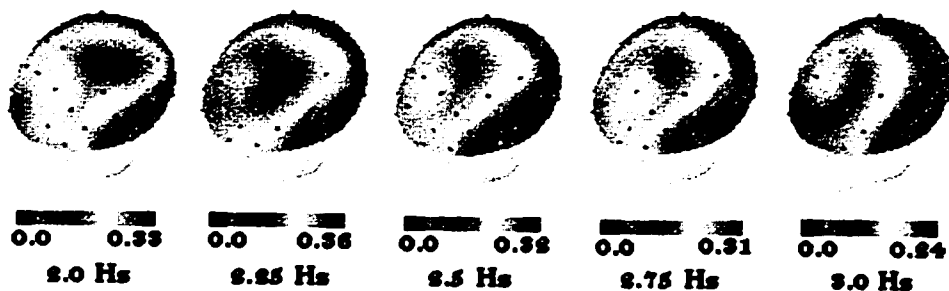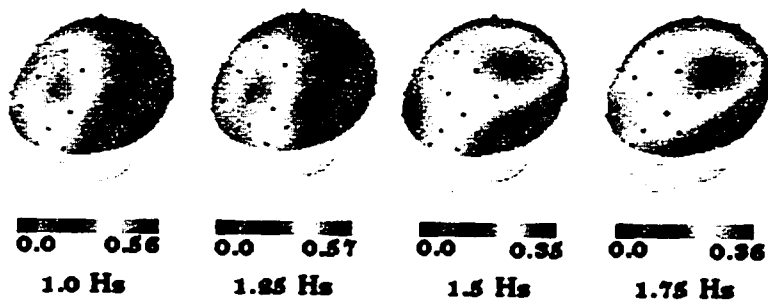
Figure 2.5

synchronized coordination. During syncopated coordination, power was focused at left centro-parietal, central and frontal sites (figure 2.5, top row, and table 2.1, top left). High power in the left central region suggests activation of the underlying sensorimotor cortex (contralateral to the finger flexion). This suggestion is supported by significant correlation between patterns from plateaus 1-3 and the Motor-only pattern (figure 2.5, top right) (r(59) = 0.57, 0.60, and 0.59 respectively -- all p< 0.001). After the transition to synchronized coordination, maximal power at the coordination frequency dropped in intensity and covered a broader left and midline frontal region (figure 2.5, second row, and table 2.1, top right). This shift in spatial distribution resulted in much weaker correlations with the Motor-only control pattern (average r value = 0.35).

Statistical evaluation of this difference in the spatial distribution of power by a two-way ANOVA, with coordination mode (syncopated or synchronized) and electrode location as factors, showed main effects of both coordination mode [F = 120.11] and electrode site [F = 10.01] as well as a significant interaction [F = 1.91] (all p < 0.0001). Post-hoc tests revealed that power at the coordination frequency decreased in the transition from syncopated to synchronized behavior at left centro-parietal, central and prefrontal sites (table 2.2, left). No electrodes showed an increase in power after the transition. These results suggest a spatiotemporal reorganization of cortical activity coincident with the behavioral transition in timing from syncopated to synchronized coordination, but do not rule out the rate of coordination as a contributing factor.

Syncopate Condition

Syncopated Coordination			Synchronized Coordination				
1.0 Hz	*1.25 Hz*	*1.5 Hz*	*2.0 Hz*	*2.25 Hz*	*2.5 Hz*	*2.75 Hz*	*3.0 Hz*
C3 (0.43)	C3 (0.41)	C3 (0.64)	F1 (0.34)	F1 (0.36)	F3 (0.30)	FC1 (0.23)	FP1 (0.35)
CP3 (0.37)	CP3 (0.37)	CP3 (0.60)	FC1 (0.29)	FCz (0.36)	FC1 (0.28)	F3 (0.23)	F3 (0.34)
FC1 (0.34)	aF7 (0.36)	aF7 (0.49)	FCz (0.26)	FC1 (0.34)	FC3 (0.27)	Fz (0.22)	aF7 (0.33)
aF7 (0.33)	CP1 (0.33)		F3 (0.26)	F3 (0.32)	F1 (0.27)	aFz (0.22)	Fz (0.31)
				Fz (0.31)	aFz (0.25)	FPz (0.21)	F1 (0.30)
				aFz (0.27)	C3 (0.23)	FC3 (0.20)	FC1 (0.30)
					aF7 (0.23)	FCz (0.20)	aF3 (0.30)
					FCz (0.23)	FP2 (0.19)	aFz (0.30)
					aF3 (0.22)	FP1 (0.19)	FPz (0.28)
							FCz (0.27)
							F5 (0.27)

Synchronize Condition

1.0 Hz	*1.25 Hz*	*1.5 Hz*	*1.75 Hz*	*2.0 Hz*	*2.25 Hz*	*2.5 Hz*	*2.75 Hz*	*3.0 Hz*
F1 (0.56)	F1 (0.57)	FP2 (0.35)	C3 (0.36)	C3 (0.33)	FC1 (0.36)	FC1 (0.32)	FC1 (0.31)	F3 (0.24)
F2 (0.50)	aF4 (0.52)	aFz (0.33)	FC3 (0.32)	FC1 (0.32)	F3 (0.36)	F3 (0.29)	FCz (0.28)	FC1 (0.24)
FCz (0.45)	FP1 (0.50)	C3 (0.32)	FC1 (0.32)	aFz (0.24)	FC3 (0.35)	FCz (0.29)	F3 (0.28)	aFz (0.23)
aF4 (0.42)	aF3 (0.46)	FPz (0.32)	aFz (0.30)	F3 (0.30)	FCz (0.34)	F1 (0.26)	FC3 (0.26)	aF3 (0.22)
FC1 (0.42)	F2 (0.45)	FC1 (0.30)	F3 (0.29)	FC3 (0.29)	aFz (0.33)	aF3 (0.25)	Fz (0.25)	FPz (0.22)
	FPz (0.44)	aF4 (0.27)	FPz (0.29)	FPz (0.28)	F1 (0.32)	FC3 (0.24)	aFz (0.25)	FP2 (0.20)
		CP3 (0.26)	FP2 (0.27)	FP2 (0.28)	C3 (0.30)	aFz (0.24)	aF3 (0.23)	FP1 (0.20)
		F2 (0.26)		FCz (0.27)	Fz (0.29)			F2 (0.20)
				Fz (0.25)	F2 (0.29)			FCz (0.19)
					aF3 (0.29)			aF7 (0.19)
								FC3 (0.19)

Motor-only Condition

C3 (0.42)
C1 (0.37)
FC3 (0.32)

Table 2.1: Electrode sites whose power at the required coordination frequency exceeded 75% of the maximum value for that plateau and coordination mode. Actual power values (unit = μV^2) are indicated in parentheses next to each electrode name. Electrodes are listed in order of decreasing amplitude.

2.322 Synchronize Condition

The lack of a behavioral transition in the Synchronize condition allowed us to disambiguate effects due to the timing relationship from those due to increasing coordination frequency. Grand-averaged power spectra were calculated for all nine plateaus in the Synchronize condition. As in the Syncopate condition, the dominant power spectral component was at the frequency of coordination (at an average of 92% of the channels across all 9 plateaus; see figure 2.4, bottom row). The corresponding topographic patterns are illustrated in the middle and bottom rows of figure 2.5. To determine whether significant differences in power occurred with increasing rate of coordination, data were divided into two frequency classes: low (plateaus 1-3) and high (plateaus 5-9) and subjected to a two-way ANOVA (frequency class vs. electrode location). Both main effects were again strongly significant [frequency: $F = 157.35$; electrode site: $F = 19.26$, $p < 0.0001$] but the interaction between factors barely reached significance [$F = 1.33$] at $p < 0.04$. Furthermore, although post-hoc statistical tests revealed a decline in power from low to high frequency plateaus at frontal and prefrontal sites (particularly in the right hemisphere), there were no significant differences at left centro-parietal or central sites (table 2.2, middle). Together, these results indicate that the decrease in power at left central and centro-parietal sites observed in the Syncopate condition was due to the change in coordination timing rather than in coordination frequency.

34

Pre- vs. Post-Transition	Low vs. High Plateau Freq.	Bistable Plateau Freq.
AF7**	AF4**	C3**
C5**	AF8**	CP3**
C3**	F1**	
CP5**	F2**	
CP3**	F4*	
CP1**	F6*	

** $p < 0.01$, * $p < 0.05$

Table 2.2: Listed are electrode sites having significant differences in power at the coordination frequency for the following cases: *ANOVA I* - Syncopated (pre-transition, 1.0 - 1.5 Hz) vs. Synchronized (post-transition, 2.0 - 3.0 Hz) coordination in the Syncopate condition; all sites shown had higher power values during syncopation (i.e., none of the 61 electrodes showed significant increases in power at the coordination frequency following the behavioral transition). *ANOVA II* - Low frequency (1.0 - 1.5 Hz) vs. High frequency (2.0 - 3.0 Hz) synchronized coordination in the Synchronize condition; power at the coordination frequency was significantly higher in the Low than in the High frequency plateaus at all sites listed. With one exception, the sites with significant differences in this comparison were in the right hemisphere suggesting a stronger bilateral activation of frontal areas for synchronized coordination at low frequencies. *ANOVA III* - syncopated vs. synchronized coordination at low frequencies (1.0 - 1.5 Hz from both coordination conditions); only two sites showed significant differences between coordination modes, both having larger power at the coordination frequency during syncopation. This implies that the drop in power at left central and centro-parietal sites observed for post-transition plateaus in the Syncopate condition was due to the change in timing relation from anti-phase to in-phase rather than an increase in coordination frequency.

To further quantify the existence of frequency-independent topographic differences between states of syncopated and synchronized coordination, a final ANOVA was performed to compare the low frequency plateaus (1-3) of each condition, at which coordinative bistability was observed. This test confirmed that the topographic power patterns during syncopated coordination were significantly different (p < 0.0001) from those in synchronized coordination [F = 2.31]. Post-hoc tests showed that the difference was due to two electrode sites, left central and centro-parietal (see table 2.2, right), both of which exhibited higher power during syncopated coordination. The topographic power spectral density patterns for plateaus 5 and higher in the Synchronize condition were highly correlated with the corresponding post-transition Syncopate patterns (mean r(59) = 0.84) as expected since both coordination mode and frequency were the same (compare figure 2.5, 2nd and bottom rows).

2.323 Control Conditions

Unlike the coordination conditions, the strongest grand-averaged power spectral values in the Auditory-only and Motor-only control conditions were not, for most electrode sites, at the fundamental (rhythmic) frequency (i.e. the stimulus and flexion frequencies, respectively). Figure 2.6 illustrates why this was the case for the Auditory-only condition. Shown on the left is the grand-averaged event-related potential from a fronto-central electrode (FCz). The characteristic N1-P2 evoked response to an auditory event can be clearly identified. The dashed line marks the return of the P2 component to zero at approximately a 330 msec latency. The N1-P2 complex was reflected in the spectral decomposition as can be seen by the largest concentration of power being at the

36

Auditory-only

1.35

-1.35

0.12

Figure 2.6: A sample grand-averaged ERP from the Auditory-only control condition (recorded over FCz) is shown on the left. Since the metronome rate used for this condition was 1 Hz the entire time series is 1 second (one cycle) in length. The dashed line marks the end of the N1-P2 complex evoked by an auditory event and is 330 msec after stimulus onset. To the right is the corresponding DFT power spectrum. Note the maximum power value at the third frequency component in the spectrum which is centered at 3 Hz (corresponding to the second harmonic of the fundamental cycle frequency, 1 Hz).

second harmonic, 3 Hz (i.e. 3 Hz corresponds to one cycle (N1-P2) in 330 msec; see figure 2.6, right). Across all channels, the amplitudes of this component, although the largest in the spectrum, were still small relative to the maximal power values observed in the other three conditions, despite similar signal amplitudes for all conditions. This reflects a wider distribution of power across higher harmonics in the Auditory-only control condition that was less prevalent during the coordination tasks.

For the Motor-only control, however, signals recorded from left central electrodes did have a relatively large amount of power at the flexion frequency (see figure 2.5, top right, and table 2.1, bottom). As discussed above, these locations are consistent with activation of contralateral SM1, as expected for right finger movements.

2.4 Discussion

This study demonstrates a spontaneous large-scale reorganization of neuroelectric activity associated with the transition between two modes of coordinative timing. The rhythmic nature of the coordination tasks was evident in the concentration of EEG power at the coordination (fundamental) frequency over large portions of the head. Concentration of power at the fundamental, or rhythmic, frequency was less prevalent for self-paced finger flexion and absent during passive listening to a auditory 1 Hz metronome. This suggests that the rhythmic EEG component during the coordination tasks is a dynamically emergent property of the integration of sensory and motor information and emphasizes the need for examining the timing of behavior with respect to the action-perception cycle rather than each component individually [Arbib, 1985; Warren & Kelso, 1985; Kelso et al., 1990; Pribram, 1991].

Our main finding is a strong reduction in power at the coordination frequency at left central and centro-parietal recording sites when behavior undergoes a transition from syncopation to a more-stable synchronized mode of coordination. Since there were no observable shifts in power to other frequencies, this finding suggests a decrease in activity of SMl contralateral to the performing hand. This conclusion may appear to contradict previous reports showing increased activity of primary motor areas with faster rates of repetitive movement [Rao et al., 1996; Jenkins et al., 1997; Sadato et al., 1997]. However, the coordination task used in this experiment additionally involves a change in the inherent stability of the timing relation as well as the rate of flexion. Subjects report experiencing increasing difficulty in maintaining syncopated coordination as the plateau frequency increases, and continue to satisfy task requirements (i.e. preserving the 1:1 stimulus/flexion ratio) by switching to flexion on the beat. The instability presumably arises because of centrally based constraints, e.g. an inability to prevent the auditory stimuli from entraining the central motor signals at higher coordination frequencies. Were it due to inherent biomechanical limitations, one would not expect subjects to be able to synchronize at higher rates either.

Empirical support for the hypothesis that syncopation involves a higher degree of central "effort" has been provided by several behavioral studies. For example, Scholz and Kelso (1990) demonstrated that, although subjects could intentionally switch from an in-phase to an anti-phase timing relation if expressly asked to do so, it took them longer than doing the reverse at the same metronome rate. Furthermore, in a recent dual-task study by Temprado et al. (1999), subjects showed significantly slower reaction times

39

during maintenance of an anti-phase pattern of bimanual coordination when compared to an in-phase timing relation. This suggests that a greater degree of attention is required to maintain an anti-phase mode of rhythmic coordination, consistent with the hypothesis [Kelso, 1994, 1995] that syncopation is less-automatic, requiring more conscious control.

One possible explanation, then, for the decline in power of post-transition activity of the left SM1 is that the power reflects the degree of conscious control exerted in producing the motor output. The greater effort required to move at higher rates (previously associated with increases in SM1 activation; see above) may thus be masked by an even greater reduction in effort resulting from the switch in timing. This explanation is in agreement with the observation that, even at the same low plateau rates, two left central electrode sites showed significantly lower power when subjects performed a synchronized mode of coordination. The decline in amplitude may reflect a transfer of movement control from cortical to subcortical structures. Both the cerebellum and basal ganglia have been shown to be important for timing behavior [Ivry & Keele, 1989; Rao et al., 1997].

An alternative explanation for the spatiotemporal reorganization is a "superposition" of auditory and motor event-related activity during synchronization that is not present during anti-phase behavior. Given that the EEG reflects extracellular current flows, which are subject to volume conduction in the cerebral spinal fluid, it is possible that currents generated in distinct sources cancel each other before reaching electrodes at the scalp. While we cannot eliminate the possibility of such an interference effect, we do know from previous work [Fuchs et al., 1992] that, for the case of MEG,

superimposing an auditory-evoked field with a motor-evoked field (with either an anti-phase or in-phase relation) fails to account for the spatiotemporal patterns that accompany auditory-motor coordination. This finding has limited usefulness, however, when one accounts for the effects of rate on brain activity known to exist for both auditory stimulation [Hari et al., 1982; Binder et al., 1994] and movement tasks (see section 2.1). The latter consideration raises concerns about using evoked field patterns (associated with very transient events) to interpret rhythmic (steady-state) activity. Clearly, an experiment with ramped frequency controls is warranted. In addition, the auditory-evoked field described by Fuchs et al. (1992) was incomplete since sensor coverage was limited to the centro-lateral region of the left hemisphere.

A second finding in this report is the widespread left and mesial fronto-central and anterior frontal distribution of EEG power during both modes of coordination. This topography likely reflects activity in several cortical areas, possibly including left premotor cortex, SMA and prefrontal areas, that contribute to the temporal organization of behavior. Preserving any rhythmic coordinative timing relationship in a stable fashion entails the ability to internalize the external rhythm so that one can anticipate the arrival of each metronome beat and plan one's movement to coincide with a particular phase of the rhythmic cycle. Lesion studies suggest that the timing and motor-control mechanisms which support rhythmic movements involve the cerebellum [Ivry & Keele, 1989] and basal ganglia [Harrington & Haaland, 1998] subcortically as well as frontal cortical areas to which they connect, including premotor cortex, SMA, and prefrontal cortex [Halsband et al., 1993; Truelle et al., 1995]. Additional support for premotor cortex, SMA, and

prefrontal cortex involvement in rhythmic motor tasks comes from electrophysiological scalp recordings [Lang et al., 1990; Bressler et al., 1996; Gerloff et al., 1998] and fMRI imaging [Rao et al., 1997]. In most of these studies, effects were significantly more pronounced during internally paced movement (e.g. reproduction of rhythms from memory) or when the rhythm was complex rather than simply repetitive (as in the Lang et al., 1990 study), thus indicating that the magnitude of premotor cortex and SMA activity relates directly to the degree to which a movement pattern must be preplanned. The present results do not differentiate between syncopated and synchronized movement patterns with respect to lateral frontal and frontocentral electrode sites suggesting that the instability in syncopated timing is due to changes in activation on a different level of the motor control system (perhaps in subcortical timing mechanisms). Further investigations with better spatial resolution (e.g. fMRI) will help to address this issue.

In conclusion, stable performance of anti-phase and in-phase rhythmic coordinative patterns appears to require cortical involvement of a number of central and frontal brain areas. The areas involved and the degree to which they participate depend on the specific timing relationship required between motor and perceptual processes, and may relate to the amount of central control necessary for maintenance of the coordinative pattern. An important feature of the task employed in this study was the spontaneity with which the coordination behavior and the EEG activity reorganized. This reorganization was a necessary consequence of the task requirement that the subject continue to successfully maintain an externally imposed rhythm under the cognitive load imposed by increasing frequency. To our knowledge, few studies have shown such spontaneous

large-scale reorganization induced in real time by parametric task control. We suggest that the exploitation of such instabilities in behavior is a powerful way to more deeply understand the underlying neurodynamical mechanisms that contribute to flexibility in coordination behavior.

3.0 Experiment 2: Neuromagnetic activity associated with transitions in sensorimotor coordination

3.1 Introduction

When people are directed to coordinate unimanual finger flexion with an external metronome in a 1:1 fashion, their ability to do this depends on when they time their movement within the metronome cycle. A synchronized (on-the-beat) mode of coordination is typically established very rapidly (one to two cycles) if the range of metronome frequencies is within what one would normally call rhythmic, ~ 0.6–4.0 Hz [Fraisse, 1982]. Below this range, anticipation of the metronome is difficult whereas for faster rates, there exist both perceptual and biomechanical limitations. Off-the-beat timing relations, however, are much more difficult and can typically only be performed successfully for lower rhythmic rates (< 2.0 Hz). An interesting consequence of this fact is that if people are asked to syncopate with a metronome (i.e., move between-the-beats), and the rate of the metronome is then systematically increased, a spontaneous transition to synchronization occurs at a critical metronome frequency [Kelso et al., 1990]. Two key dynamical features precede this transition. First is an increase in the variability of the phase relationship between the subject's response and metronome onset (180° would be perfect syncopation). The second is an increase in the amount of time it takes for subjects to recover a syncopated pattern in response to external perturbations (e.g. via a torque motor), also known as critical slowing down. Both of these signatures of

instability are hallmark features of self-organization in nonlinear dynamical systems. [see Kelso 1995; Haken 1996 for reviews].

The reason why syncopation becomes unstable is not known. It may be due to the fact that synchronized patterns are learned from childhood whereas 'between the beats' timing patterns are less common. However, it is clearly not a biomechanical problem resulting from faster movement rates since synchronization is still possible. Likewise, subjects are perfectly able to perceive distinct metronome events in this frequency range. Therefore, the answer must somehow lie in the way the perception of the metronome is coupled to the motor response. Given that this coupling occurs centrally an obvious question is whether differences between syncopated and synchronized coordination translate into differences in the spatiotemporal dynamics of brain activity.

Research conducted over the last ten years using both EEG and MEG demonstrates that there are several observable changes in patterns of neural activity that accompany a transition from flexion off-the-beat to flexion on-the-beat induced by increases in the rate of a pacing auditory metronome. The earliest studies to address this issue employed a 37-SQuID (Superconducting Quantum Interference Device) system centered over the contralateral hemisphere [Kelso et al., 1991, 1992; Fuchs et al., 1992]. Results showed a topographic reorganization of the dominant pattern of magnetic field activity coincident with the shift in timing on the behavioral level. In addition, there was a parallel 180° shift in the phase of the event-related field relative to the rate of coordination. Unfortunately, the limited sensor coverage made physiological interpretation difficult by precluding knowledge as to whether these effects were

observable over other regions of the scalp. Furthermore, the lack of a transition-free condition made it impossible to determine whether these topographic effects were due to the change in coordinative timing or simply the increase in coordination rate.

Later work addressed these limitations by using a whole-scalp 61-channel EEG recording system that provided homogeneous coverage over the entire scalp surface. Differences in event-related potential signal power and phase at the coordination frequency were found to uniquely relate to the mode (syncopate vs. synchronize) rather than the rate of coordination [Wallenstein et al., 1995; Mayville et al., 1999]. These differences were confined to electrodes located over contralateral central and centro-parietal recording sites suggesting a change in the dynamics of activity in the underlying sensorimotor cortex (SM1) though effects of volume conduction inherent to EEG technology made it problematic to segregate auditory from motor-related brain activity.

Our aim here is to develop a physiological interpretation of spatiotemporal changes in brain activity that occur when subjects transition from syncopated to synchronized coordination. Through the use of a 143-SQuID whole head system we gain not only the advantage that MEG signals are not subject to smearing or volume conduction but also a tremendous increase in sensor coverage. Together these advantages afford the spatial resolution necessary to separate auditory and motor-related neural events. We examine differences in neuromagnetic activity associated with a condition in which subjects transitioned from syncopation to synchronization as well as a second transition-free condition in which subjects synchronize through the same range of

frequencies. The second condition serves as a control for the effects of frequency versus mode of coordination.

We further extend our analyses to include an investigation of high frequency oscillations, which though event-related, are typically not phase-locked and thus tend to average out in event-related magnetic fields (or electric potentials). Several brain rhythms are known to exhibit movement-related changes in amplitude. For example, both the mu (8-12 Hz) and beta (15-30 Hz) rhythms show a decrease in power prior to movement over contralateral sensorimotor and midline premotor areas as well as during movement bilaterally. This phenomenon is referred to as event-related desynchronization (ERD) [Pfurtscheller & Aranibar, 1977; Pfurtscheller, 1981]. ERD is thought to reflect a shift from 'idling' to task-related activity in underlying thalamocortical and corticocortical networks [Pfurtscheller & Lopes da Silva, 1999], an interpretation supported by the fact that both rhythms 'resynchronize' after termination of movement. [Salmelin & Hari, 1994; Pfurtscheller et al., 1996].

The majority of studies on motor-related changes in non-phase locked rhythms have examined self-paced, discrete finger movements. The dependence of these amplitude changes on movement parameters such as rate or task complexity is not well understood. Recent work by Manganotti and colleagues indicates that suppression of high frequency brain rhythms is stronger for more complex movement tasks [Manganotti et al., 1998], especially for rhythms in the mu frequency range. In contrast, Nashmi et al. (1994) found that drawing tasks resulted in significant increases in gamma (30-50 Hz) activity if subjects were instructed to focus on accuracy of the movement trajectory.

Both effects were stronger over contralateral sensorimotor areas and presumably reflect the degree of motor planning and/or attention necessary to perform more difficult task conditions. A correlation between high frequency oscillations and attention has also been observed in animals recordings [Lopes da Silva et al., 1970; Lopes da Silva, 1991; Murthy & Fetz, 1992; MacKay, 1997].

Here we ask whether the strength of rhythms in the mu (8-12 Hz), beta (15-30 Hz) and gamma (30-50 Hz) ranges has any dependence on whether subjects are coordinating in a syncopated versus a synchronized manner. Given the inability of subjects to syncopate at higher rates, it is reasonable to conclude that off-the-beat relations are more difficult in general, requiring greater attentional focus. This conclusion is supported by recent behavioral work showing that anti-phase coordination in a bimanual task (analogous to syncopation in a unimanual situation) is associated with slower responses in a simultaneous probe reaction time task as compared to in-phase (synchronized) movements [Temprado et al., 1999; see also Carson et al., 1999]. Of particular interest is whether differences in the amplitude of these rhythms are observable over contralateral sensorimotor areas since the prior EEG and MEG studies conducted by our group indicate large-scale reorganization of neuronal activity in this region when subjects switch from syncopation to synchronization.

3.2 Methods

3.21 Subjects

This experiment was in compliance with all standards of human research outlined in the Declaration of Helsinki as well as by the Institutional Review Board. Four subjects

(3 male, 1 female) whose ages ranged from 27-41 participated. All subjects reported being right-handed. Informed consent was obtained from all subjects prior to any MEG recording. Data from three subjects is reported here; the MEG signals from one of the male subjects were corrupted because of dental fillings.

3.22 Task Conditions

The experiment consisted of two auditory-motor coordination conditions and two control conditions. In the coordination conditions, subjects listened to an auditory metronome (1 kHz, 60 msec tones) and were instructed to time *peak* flexion of their right index finger exactly between-the-beat (Syncopate condition) or on-the-beat (Synchronize condition). The rate of the metronome was systematically increased on each trial from 1.0 Hz to 2.75 Hz in 0.25 Hz increments every ten cycles. Each set of 10 cycles at a constant rate is referred to as a *plateau*. Subjects were further told to maintain a 1:1 stimulus/response ratio throughout the entire trial and not to intervene even if they felt the primary timing pattern begin to change. These rates (1.0-2.75 Hz) were chosen because it is known that subjects are unable to maintain a syncopated mode of unimanual sensori-motor coordination across this range [Kelso et al., 1990, 1992]. Each subject performed 16 trials of both coordination conditions.

In the first control condition (Auditory condition), subjects listened to tones (approximately 80) presented with randomized intervals of 2-4 seconds. In the second control condition (Motor condition), subjects were asked to self-pace flexion movements with inter-response intervals of 2-4 seconds; around 60-80 responses were collected for

each subject. These controls were included so that evoked responses to the component events in the coordination task could be measured.

3.23 Experimental Procedure

Experiments were carried out at the Department of Clinical Neurology at the University of Vienna. Subjects participated in all conditions while seated inside a magnetically shielded room (Vacuum Schmelze, Hanau) and with their heads held firm within the helmet of the magnetometer. The metronome was delivered binaurally through plastic headphones at a volume that the subjects reported to be comfortable. Subjects responded with almost-isometric right index finger flexions against a sensitive air pressure cushion that was connected to a pressure-voltage transducer located just outside the room. Due to the length of tubing which connected the cushion to the transducer (10 meters) response signals were corrected off-line for a delay of 33 msec which is the time it took for pressure changes to arrive at the transducer (given by the length of tubing divided by the speed of sound in air). Subjects were asked to fixate at a point located approximately two meters in front of them and to confine all eye or extraneous body movements to breaks between trials.

3.24 Data Acquisition

MEG activity during all four conditions was recorded using a whole-head magnetoencephalograph (CTF Inc., Port Coquitlam, Canada) comprised of 143 SQuID (superconducting quantum interference device) sensors distributed homogeneously across the scalp (figure 3.1). Conversion to third-order gradiometers was performed in firmware using a set of reference coils. MEG, metronome and response signals were bandpass
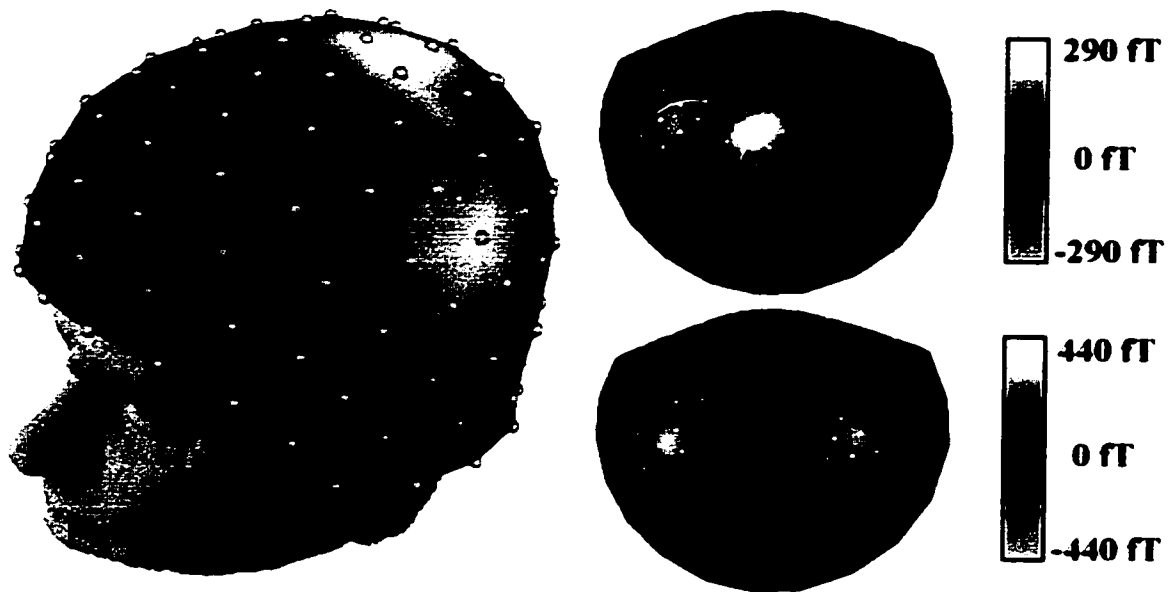
Figure 3.1: Distribution of 143 MEG sensors across the scalp surface. Shown on the left is a sample field pattern over the left hemisphere with the sensor positions indicated by orange dots. Projecting the sensor coordinates into two dimensions yields a topographic distribution like those shown on the right. The view is from above the head with the nose at the top. White dots again indicate sensor positions and the white circle over the left hemisphere shows the extent of coverage in previous MEG studies that examined syncopated/synchronized coordination [Fuchs et al., 1992; Kelso et al., 1991, 1992]. Blue and yellow signify field lines entering and leaving the head, respectively. The two-dimensional topographic plots on the right are of field patterns associated with flexion (top) and auditory (bottom) events.

Figure 3.1

(0.3-80 Hz) and notch filtered (50 and 100 Hz – the European line frequency and its harmonic). Digitization was done at a rate of 312.5 Hz. A coordinate system for each subject's head was defined with respect to three fiduciary points: the nasion, left, and right preauricular points (whose three-dimensional coordinates were measured prior to each experiment using a set of reference coils). Finally, sensor coordinates were projected into two dimensions for topographical mapping (figure 3.1).

3.25 Behavioral Analysis

Metronome and response signals from the coordination conditions were used to determine the timing relationship employed by subjects on a cycle-by-cycle basis. One cycle was defined as one period of the metronome, i.e. tone onset to following tone onset. First, two points in each cycle were marked: the onset of the metronome tone and the peak of the response (corresponding to point of maximal flexion). Second, the relative phase between these two points was calculated. Finally, these phase values were subjected to criteria which segregated each cycle into one of three categories: 1) syncopated coordination ($180° \pm 60°$), 2) synchronized coordination ($0° \pm 60°$), or 3) other. Cycles classified as 'other' were excluded from further analysis.

3.26 MEG Analysis: Control Conditions

The purpose of these conditions was to obtain the primary field pattern evoked by either an auditory tone or flexion event. All MEG data were manually inspected for eye blinks or other artifacts. Contaminated segments were marked and discarded from averaging procedures. Ensemble averaging (i.e. across trials) was done separately for each subject using a one-second window centered at tone onset for the Auditory

condition and at peak flexion for the Motor condition. The principal field patterns were obtained by applying the Karhunen-Loève decomposition technique (also known as Principal Components analysis) to the ensemble average and taking the top eigenvector, i.e. the spatial pattern that accounted for most of the signal variance. Topographic mapping of field patterns was done by projecting three-dimensional sensor coordinates into two-dimensional space and then interpolating between sensor positions with a spline of 3rd order (see figure 3.1 for example).

3.27 MEG Analysis: Coordination Conditions

MEG signals were again manually inspected for artifacts. If any portion of a cycle was contaminated, the entire cycle was discarded from further analysis. Remaining cycles were then separated into groups according to subject, coordination condition, plateau frequency (i.e. metronome rate) and timing mode within plateau (syncopation or synchronization). Ensemble averages were computed separately for each group of cycles resulting in event-related fields (ERFs). Timing differences in ERF components were investigated by applying a discrete Fourier transform (DFT) and plotting the phase of the fundamental frequency in the resulting spectra. Since each ERF was one cycle (metronome period) in length, the fundamental frequency in Fourier space always corresponded to the coordination or plateau frequency in the experiment. Amplitude changes were examined by plotting total spectral power. In order to assess the contribution of auditory and motor-related patterns to the ERFs, patterns obtained from the control conditions performed by each subject were projected onto ERFs from the

53

coordination conditions using a dual-basis projection technique [Friedrich & Uhl, 1996; Fuchs et al., 2000c].

MEG data from the coordination conditions were also analyzed without ensemble averaging in the time domain in order to investigate whether task-related effects are observable for higher frequency bands (e.g. alpha, beta) that are not necessarily phase locked cycle to cycle. The raw cycles in each data group were first preprocessed by subtracting the corresponding ERF in order to meet stationarity requirements for spectral estimation [see Bendat & Piersol, 1986 for discussion]. They were then multiplied by a ½ sine tapering window and transformed into the frequency domain with a DFT. Finally, power spectra were averaged across cycles in each data group and banded by calculating the average of components in each of the following frequency bands: mu (8-12 Hz), low beta (15-20 Hz), high beta (20-30 Hz) and gamma (35-45 Hz). Resulting values for the Syncopate condition were subtracted from those of the Synchronize condition (same plateau only) and then converted to z-scores to test for significant differences between the conditions. Significance levels were adjusted for multiple comparisons (143 channels) using a Bonferroni correction.

3.3 Results

3.31 Task Performance

Figure 3.2 shows a sample of the metronome and response time series from a single run for both the Syncopate (top row) and Synchronize (bottom row) conditions. For low metronome frequencies (figure 3.2, left side), subjects were able to successfully time peak flexion in between the beats in the Syncopate condition and on the beat in the
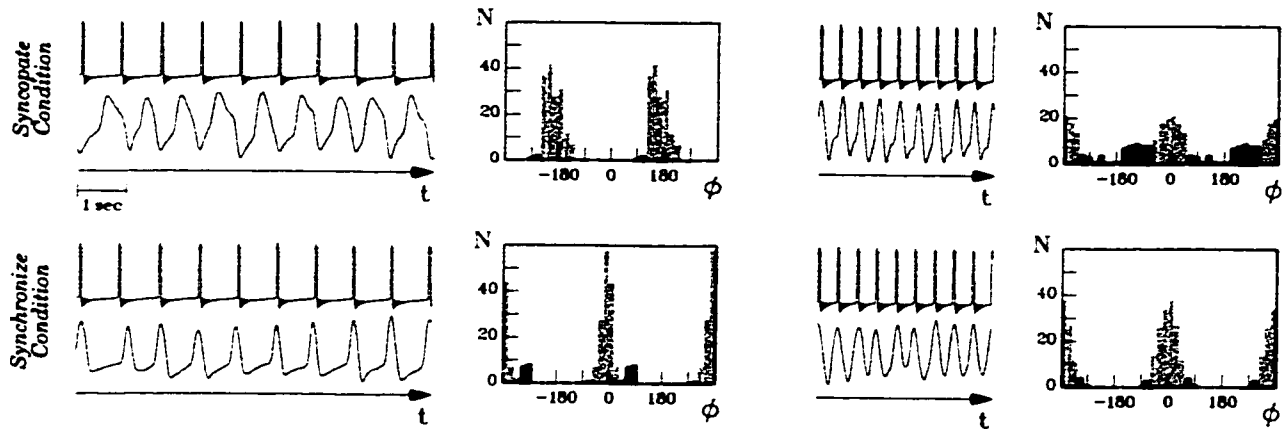
Figure 3.2: Samples of the metronome (top) and response (bottom) channels from one subject for the Syncopate and Synchronize conditions. The left side shows data from plateau 2 for which the coordination rate was 1.25 Hz and the right side from plateau 7 (2.5 Hz). Peaks in the response data indicate points of maximal flexion. Note that at the lower movement rate, these peaks occur in between the metronome beats in the Syncopate condition and on the beat in the Synchronize condition whereas at the higher movement rate, they are synchronized with the beats in both cases. The distributions shown contain all relative phase values for these plateaus for this subject (double plotted for ease of viewing). The switch in the distribution mean in the Syncopate condition is clearly observable. Grey indicates cycles that were kept for MEG analysis while black indicates cycles that did not meet behavioral editing criteria.
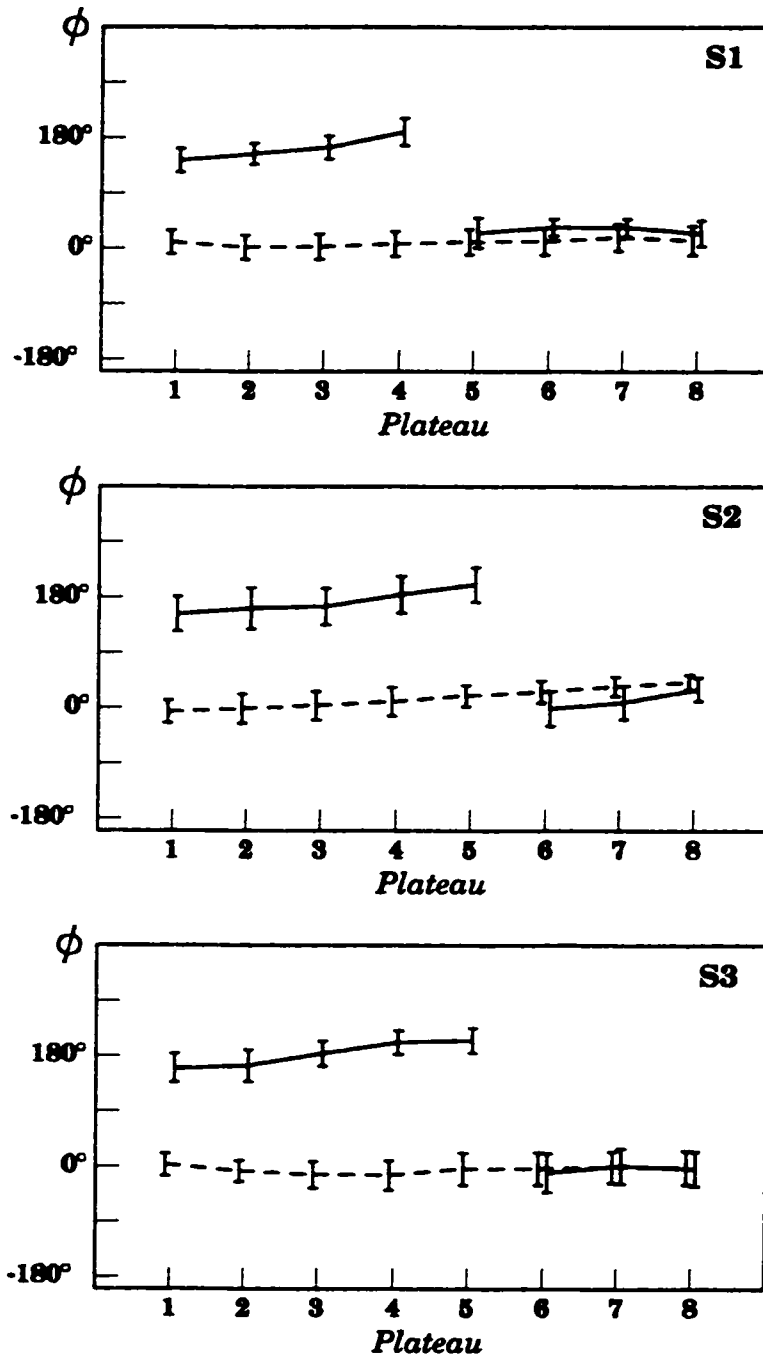
Figure 3.2

Figure 3.3: Average relative phase values (± std. dev.) versus plateau # for the distributions of cycles that were kept for MEG analysis. The solid and dashed lines are for the Syncopate and Synchronize conditions, respectively.

Figure 3.3

Synchronize condition. However, at high metronome rates, all subjects showed a synchronized mode of timing regardless of the task condition (figure 3.2, right) replicating previous behavioral findings [Kelso et al., 1990]. In other words, once the rate of coordination became too high in the Syncopate condition subjects switched to synchronization in order to keep a 1:1 stimulus/response ratio as required by the task instructions. In general, subject 1 switched at a rate of 2.0 Hz (plateau 5) while subjects 2 and 3 were able to maintain syncopation up to 2.25 Hz. Figure 3.3 shows the average relative phase values versus plateau # for the cycles that were kept for MEG analysis. Grand average relative phase values before and after the transitions in the Syncopate condition were 172.9° (± 23.7) and 12.7° (± 24.3), respectively. For the Synchronize condition, the average relative phase value throughout the trial was 6.7° (± 21.2).

3.32 Control Conditions: Dominant Patterns of Activity

Spatiotemporal decomposition of the ERFs from the control conditions yielded the spatial patterns shown in figure 3.4. All subjects showed clear dipolar patterns for both the auditory (figure 3.4, left) and motor (figure 3.4, right) conditions. The auditory-related field consisted of bilateral dipolar patterns, presumably reflecting activation of the primary auditory cortex in each hemisphere. The motor-related patterns, on the other hand, consisted of a single dipolar structure in the left central region, corresponding to activation of the sensorimotor area (SM1) associated with movement of the right index finger.
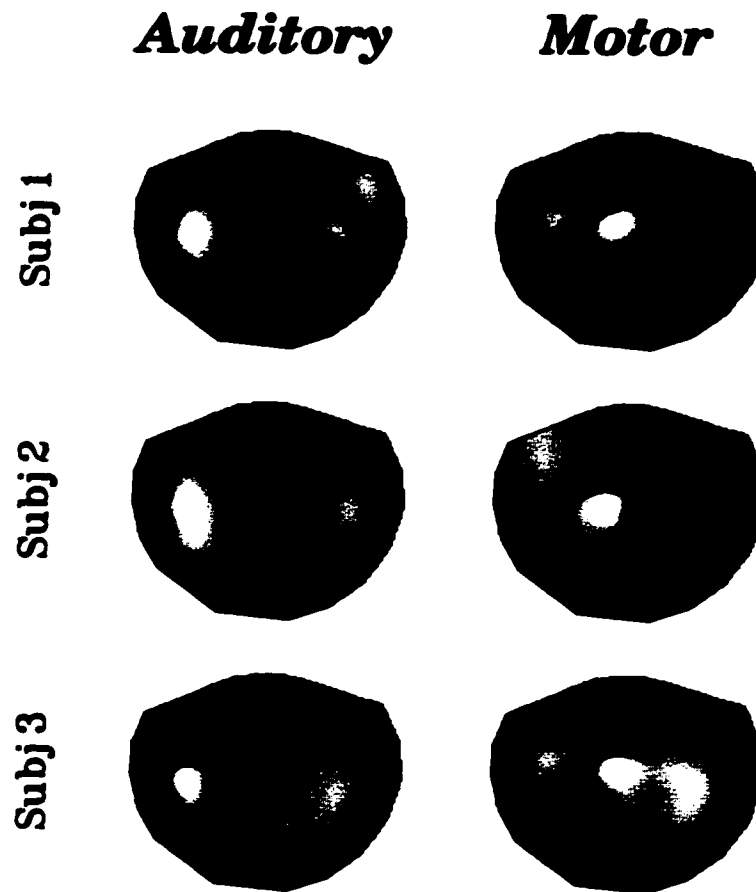
Figure 3.4: Spatial patterns from a Karhunen-Loève decomposition that accounted for most of the signal variance in the ERFs computed from the Auditory (left) and Motor (right) control conditions. All three subjects show dipolar structures that are bilateral in the auditory case and lateralized to the left side in the Motor case (reflecting movement of the right index finger). The scale here is in arbitrary units (since the patterns were obtained with a Karhunen-Loève decomposition); see figure 3.1 for approximate values in terms of femtoTesla.

Figure 3.4

Figure 3.5 (page 60): Topographic maps sampled every 19.2 msec from the ERFs associated with syncopation (top) and synchronization (bottom) on plateau 2 (1.25 Hz). The head is viewed from above with the nose on top. Topos are scaled to ± 227.53 fT for the Syncopate condition and ± 290.17 fT for the Synchronize condition. The green and blue lines beneath each map show the corresponding averaged metronome and response time series, respectively, with the red line indicating the time point at which each map is sampled. Yellow boxes highlight the appearance of the two main patterns in each ERF, the auditory and motor-related field patterns. As expected, the motor pattern is shifted in time depending on whether the subject's response was syncopated or synchronized with the metronome.

Figure 3.6 (page 61): Same as figure 3.5 but for plateau 7 (2.5 Hz) during which the subject was in a synchronized state of coordination in both the Syncopate (top) and Synchronize (bottom) conditions. The amplitudes are scaled to ± 133.04 and ± 107.47 fT for the Syncopate and Synchronize conditions, respectively.

Event-Related Fields: Plateau 2 - 1.25 Hz
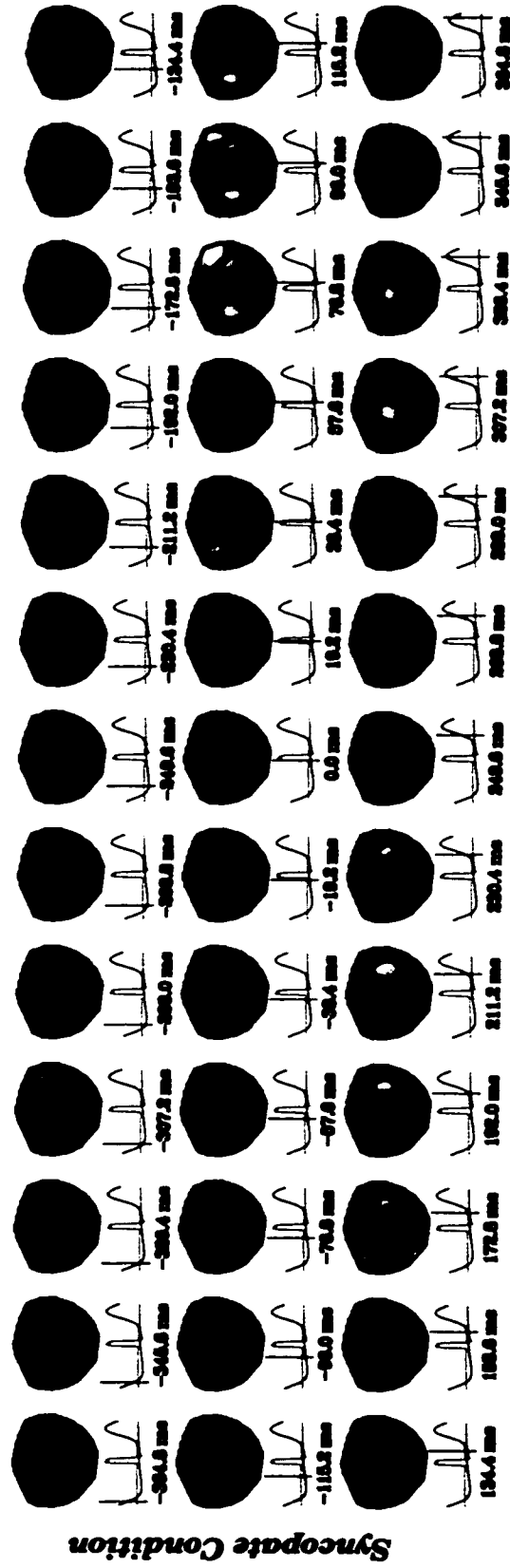
Figure 3.5

Event-Related Fields: Plateau 7 - 2.5 Hz
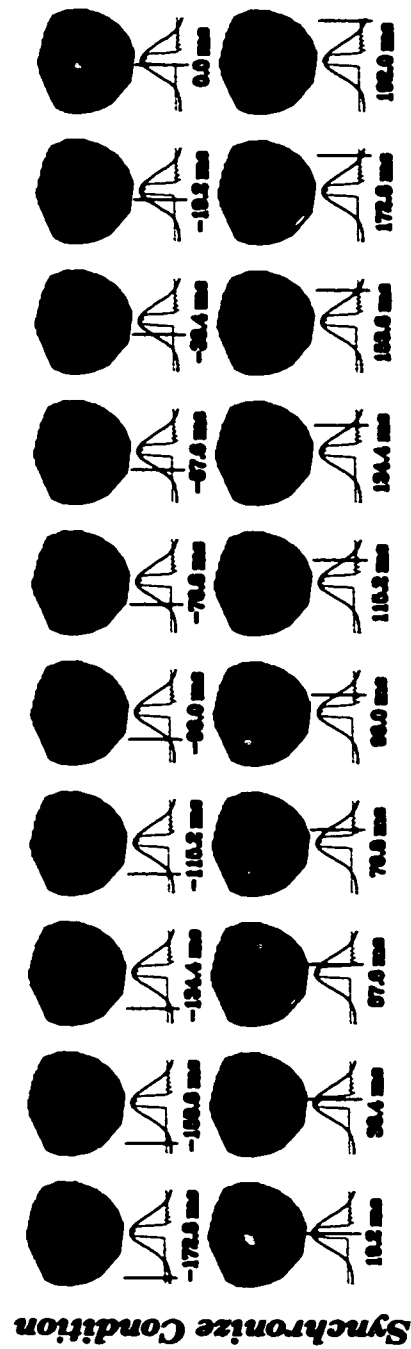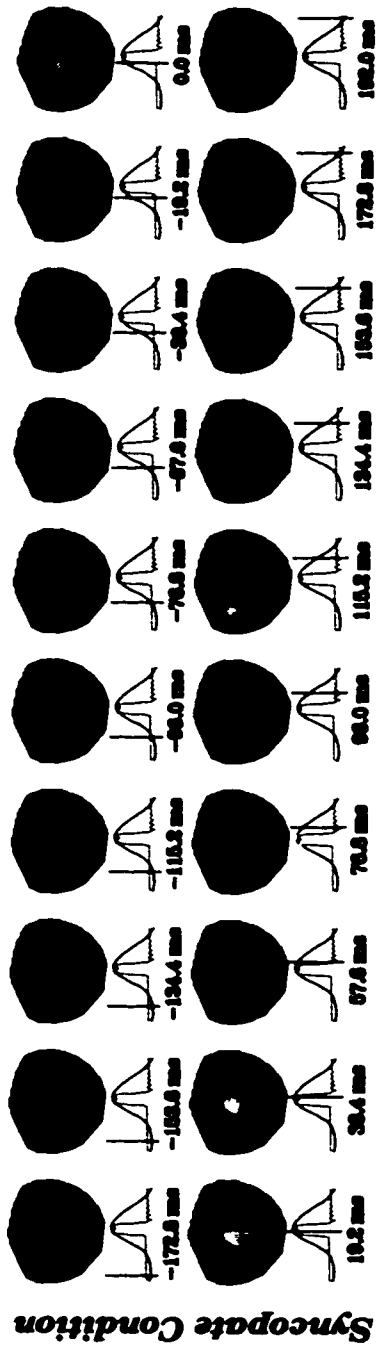
Figure 3.6

3.33 Coordination Conditions: ERFs

We investigated both timing and amplitude characteristics of event-related field activity associated with each plateau from the two coordination conditions. Figure 3.5 shows ERF data from subject 1 for a low frequency plateau (1.25 Hz). In both conditions, maximal activity occurs over bilateral temporal areas around 80 msec after tone onset, consistent with the N1m, the primary magnetic auditory response [Näätänen & Picton, 1987]. Also observable is the P2m, the polarity reversal of this auditory component that occurs approximately 70-120 msec later. The next strongest component in the ERFs is a motor-related pattern that occurs during the flexion phase of the response. The strongest amplitude for this pattern actually occurs at the point of maximal *velocity* in the flexion direction and thus precedes peak flexion [Kelso et al., 1998]. Due to the different timing of the response, this pattern emerges approximately one ½-cycle length after tone onset during syncopation (figure 3.5, top) and just prior to tone onset during synchronization (figure 3.5, bottom). The direct relation between the onset of this pattern and the motor response is further evident in figure 3.6, which shows the same plot for a high frequency plateau (2.5 Hz). There is no difference in the onset of motor-related cortical activity (compare figure 3.6, top and bottom) since subjects were now synchronizing in both conditions, i.e. the transition in the Syncopate condition had already occurred.

The timing of the motor-related pattern within each cycle can be tracked by plotting the phase of the coordination frequency component of the ERF. This is shown in figure 3.7, which plots this phase value for each of the eight plateaus from the Syncopate

Figure 3.7 (page 64): Phase of the brain signal with respect to tone onset versus plateau frequency (double plotted). Sensor #s are indicated in the upper left-hand corner. The two lines indicate phase relationships of ±180°. Data shown are from the Syncopate condition for subject 1 who switched to a synchronized mode of coordination at plateau 5. There is a clear 180° transition in sensors overlying left central areas (gray circles). The direction of the transition (180° to 0° or vice versa) differs depending on which side of the motor dipole the sensor sits (i.e., it depends on the polarity of the ERF). No transitions are visible over other areas suggesting that the phase of the coordination frequency in the ERF tracks the shift of the motor response in time.

Figure 3.8 (page 65): Same as figure 3.7 but for the Synchronize condition. Sensors that showed phase shifts in the Syncopate condition have a constant phase value across all plateaus reflecting the fact that the subject was able to maintain a synchronized mode of coordination across the entire range of plateau frequencies.

Syncopate Condition

φ

Plateau

64

Figure 3.7

Synchronize Condition

Figure 3.8

65
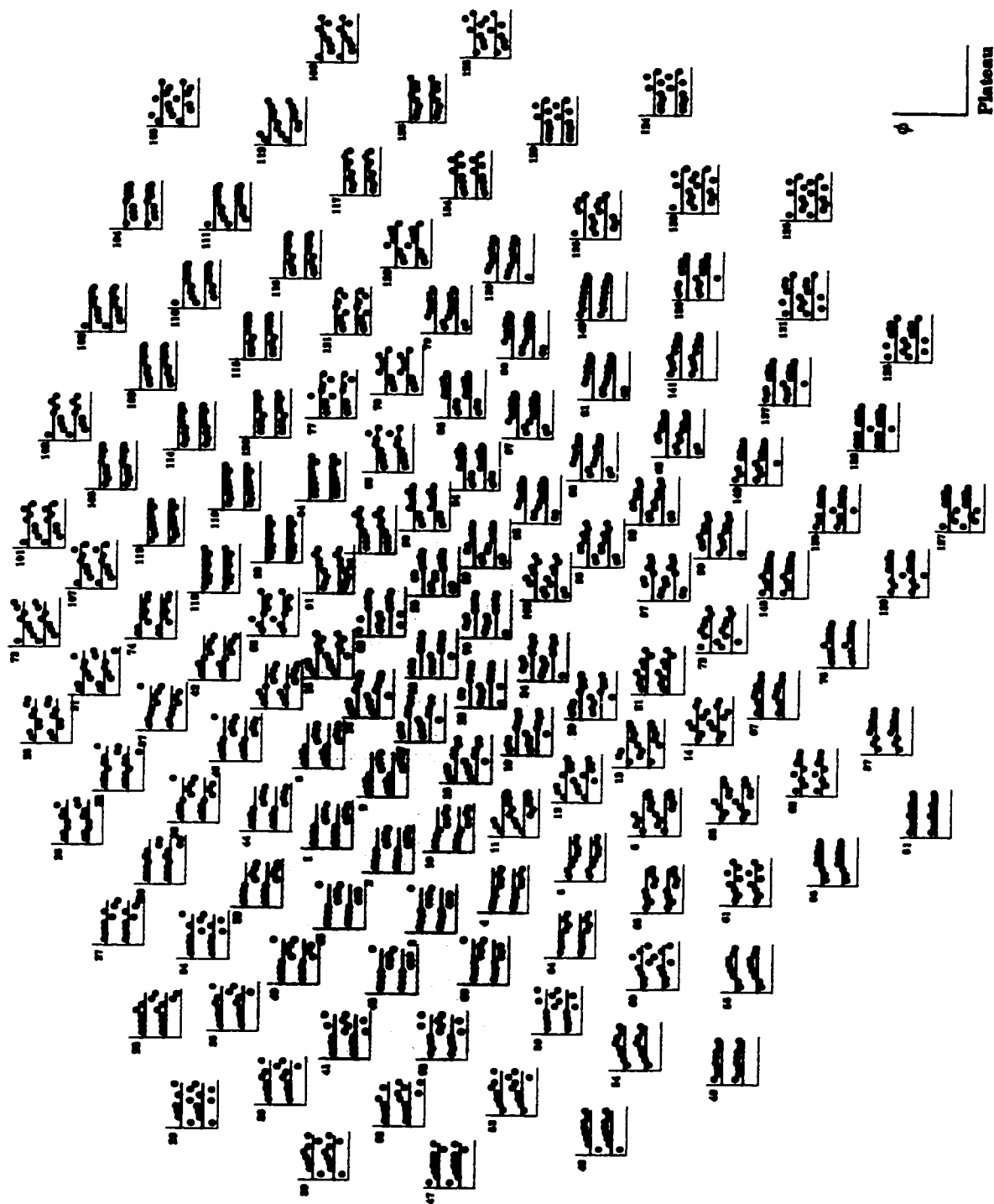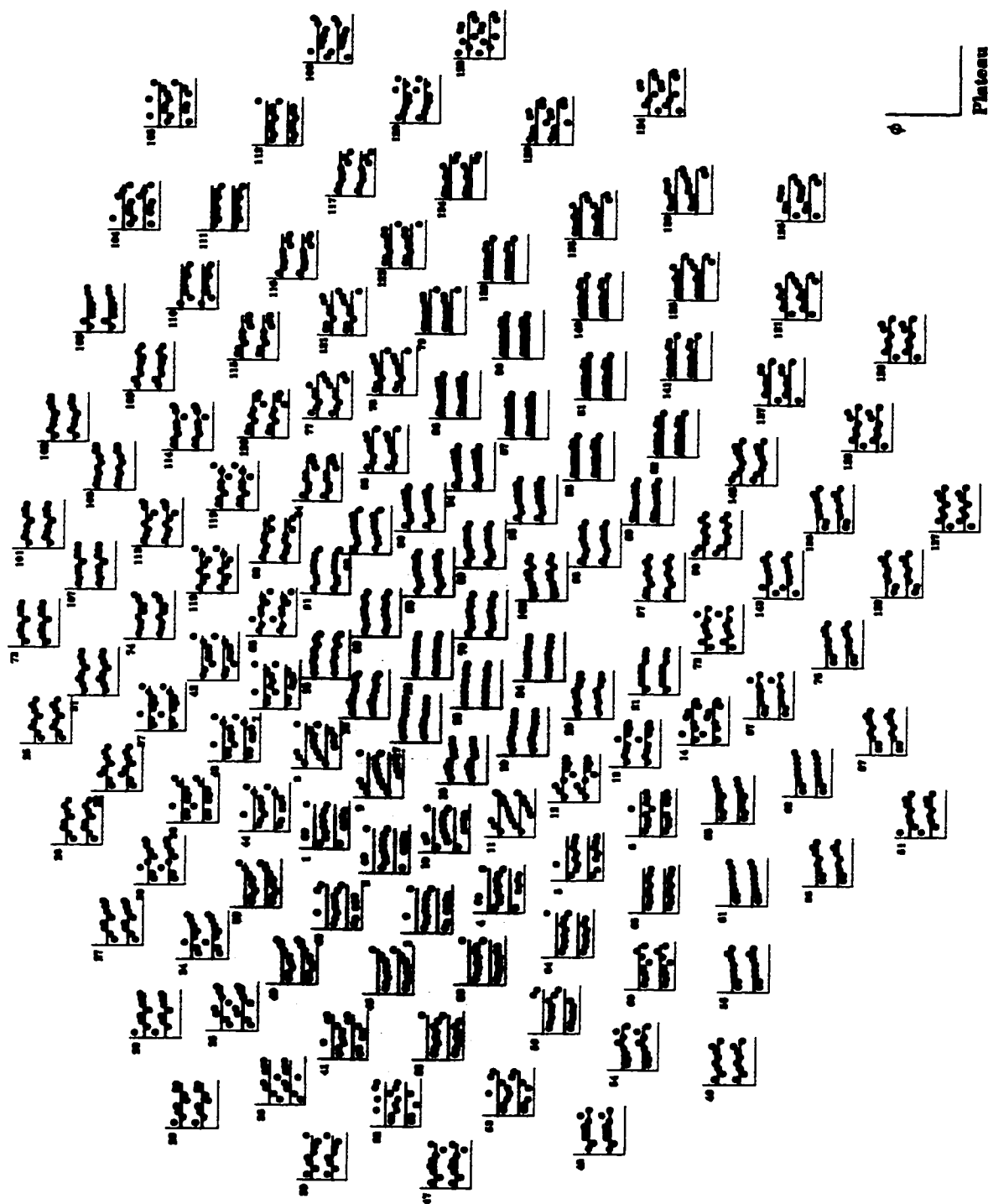
condition. The data shown are from subject 1 who switched to synchronization at plateau 5 (2.0 Hz). Coincident with the transition on the behavioral level is a 180° switch in phase measures in left central sensors, thus replicating earlier work using a 37-SQuID array [Kelso et al. 1991, 1992; see also Daffertshofer et al., 2000; Fuchs et al., 2000ac]. A comparison of the gray highlighted areas with the motor-related pattern in figure 3.4 shows that these are the sensors that pick up activation during a motor response. None of the other sensors show a clear-cut transition in phase that parallels the transition on the behavioral level (i.e. occurs at plateau 5). Figure 3.8 shows the same plot for data from the Synchronize condition. Since there were no changes in the timing of the motor response with increasing plateau frequency, the phase values over these same 'motor' sensors remain approximately constant. This phenomenon has also been previously observed in full-head EEG recordings [Wallenstein et al., 1995].

Amplitude differences in the ERFs were first examined by plotting total power of the MEG signal (figure 3.9). There was practically no difference in ERF amplitude between conditions as can be seen by comparing the bottom two rows in figure 3.9. Signal power was initially concentrated bilaterally in sensors that detected the brain's response to an auditory event (compare first columns of figures 3.4 and 3.9). As the plateau frequency was increased, the power decreased in these areas, especially in the right hemisphere. The focus of power in the left hemisphere at high plateaus reflects activation of the left SM1. Together these results indicate an interaction in frequency dependence of the auditory and motor-related contributions to the ERF. However, it is difficult to discern whether motor areas have higher power at fast coordination

frequencies because they show more activation with increasing rate or because their activation at low rates is swamped by the auditory response.

To obtain further insight into the relative contributions of auditory and motor-related processes to the ERFs, we employed a dual-basis projection technique [Friedrich & Uhl, 1996; Fuchs et al., 2000c] in which the principal field patterns from the two control conditions were projected onto each ERF. This projection resulted in time-dependent amplitudes (TDA) for each pattern that reveal their temporal evolution in the ERF. Together, the two control field patterns accounted for an average of 65% of the ERF variance (across plateaus) in both conditions. Figure 3.10 shows the auditory and motor TDAs from the data of subject 1 (top half figure 3.10). Waveforms for the auditory pattern show a qualitative transition on plateau 4 at which point the N1m-P2m complex reverses in polarity. The motor pattern also shows a qualitative change that results in a strong oscillation at about twice the cyclic frequency at high plateaus. This results in a frequency doubling of the ERF signal, which has been previously reported [Fuchs et al., 1992, 2000ac; Kelso et al., 1992; see also Daffertshofer et al., 2000].

The maximum (absolute) amplitudes of these time series are shown in the bottom half of figure 3.10 for all three subjects. It is clear from these graphs that while the amplitude of the auditory pattern decreases throughout each trial, the contribution of the motor pattern remains approximately constant. Where the auditory pattern amplitude flattens out corresponds approximately to the plateau at which subjects switch to synchronization in the Syncopate condition. This explains previous results which show that the dominant field pattern in the ERF undergoes a topographic change at the

Figure 3.9 (page 69): Total power of the ERFs from the Syncopate condition for each subject. Each row is scaled independently. Grand averaged (normalized) data are shown on the bottom for both conditions. There is very little difference in MEG power between conditions. Initially power is concentrated bilaterally reflecting the brain's auditory response but then decreases as the plateau frequency is increased. At high plateaus power is focused over the left side, associated with movement of the right finger.

Figure 3.10 (page 70): Top half: Examples of time-dependent amplitudes (TDA) of the auditory and motor-related field patterns calculated from a dual-basis projection procedure. Each TDA is independently scaled for ease of viewing. Bottom half: Maximum TDA amplitude (in arbitrary units) versus plateau frequency. All three subjects (solid, dashed, dashed-dotted lines) show a frequency-dependent decrease in the contribution of the auditory pattern to the ERF whereas the contribution of the motor pattern remains approximately constant throughout the entire run.

ERF: Total Power   Syncopate Condition
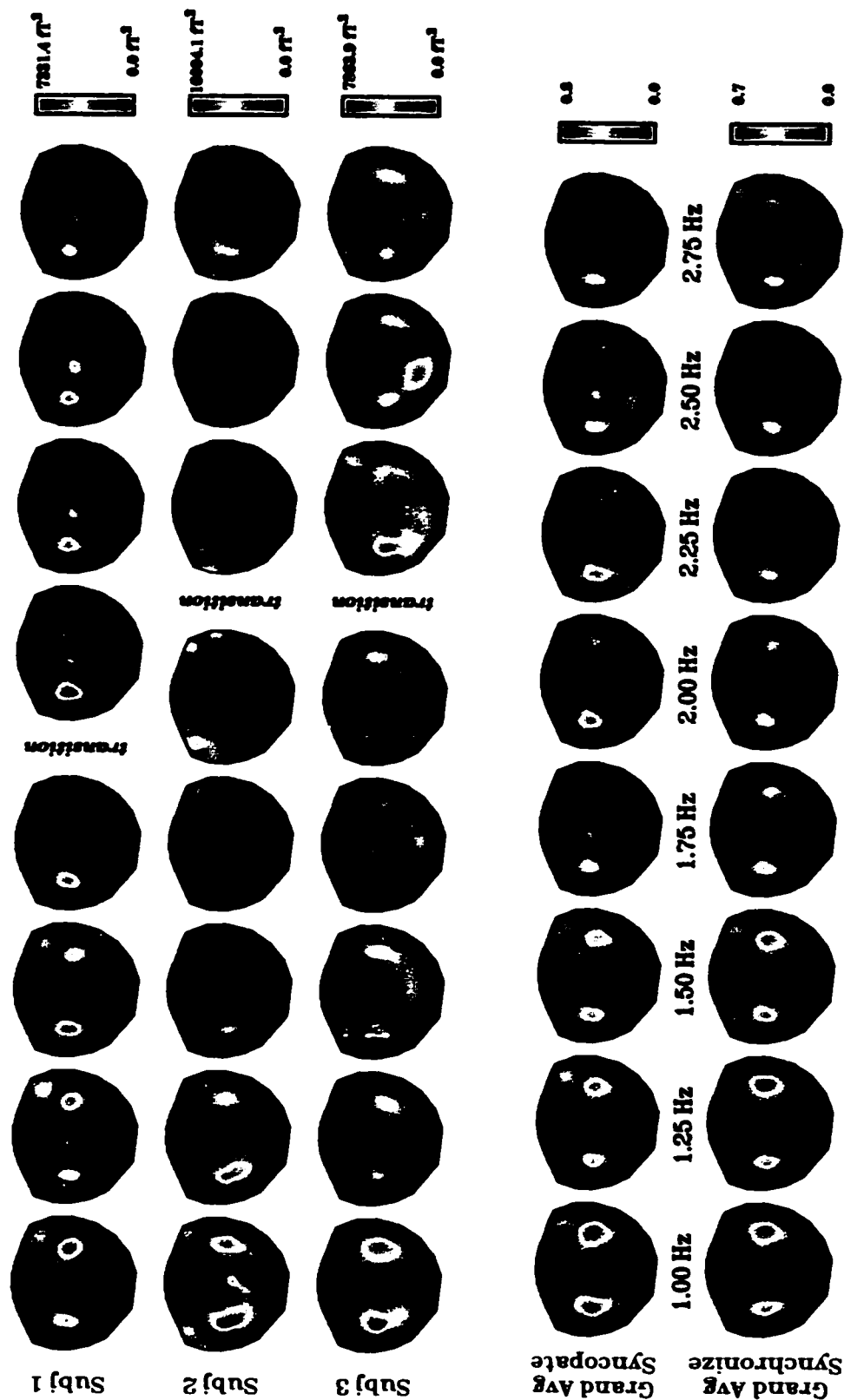
Figure 3.9
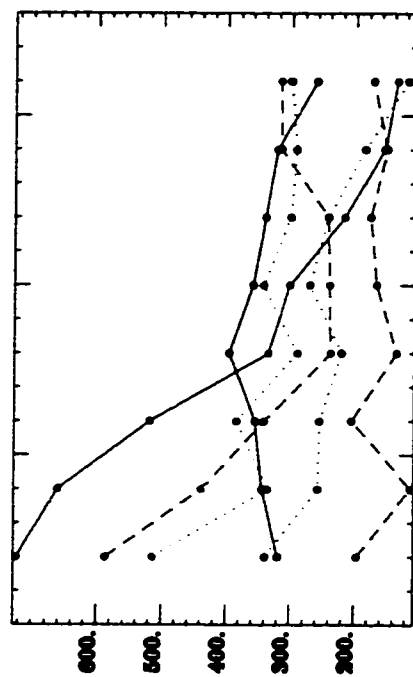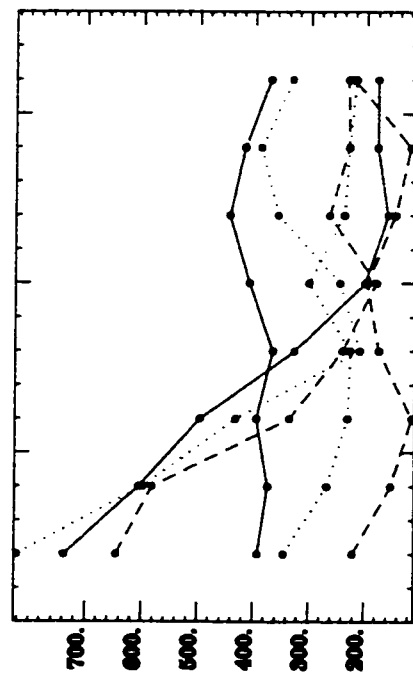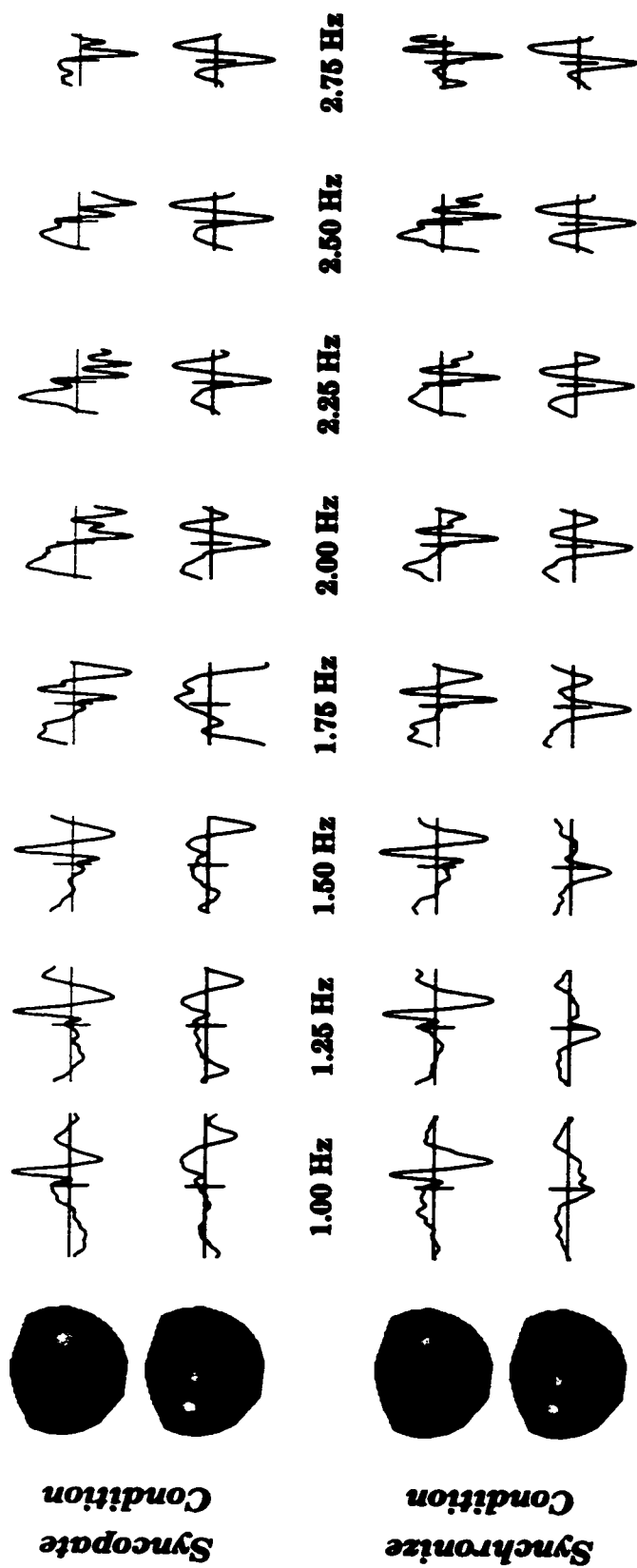
Figure 3.10

70

transition point [Kelso et al., 1991, 1992; Fuchs et al., 1992]. For low plateaus, the ERF is dominated by an auditory pattern whereas for higher plateaus the contribution of the motor-related pattern becomes stronger, even surpassing the auditory pattern amplitude for one of the subjects. Here we show this pattern shift is largely a function of coordination rate rather than mode of coordination since the Synchronize condition exhibits the same relation.

3.34 Coordination Conditions: Task-related activity in higher frequency bands

A growing body of research associates changes in higher frequency bands with the performance of a variety of perceptual and motor tasks [Gray et al., 1989; MacKay, 1997; Classen et al., 1998; Pfurtscheller & Lopes da Silva, 1999; Vanni et al., 1999]. These high frequencies are not necessarily phase-locked to any task event and thus often average out if ensemble averaging is done in the time domain. We investigated whether MEG signal power in higher frequency bands differed depending on whether subjects were performing syncopated or synchronized coordination. Figure 3.11 shows averaged power spectra associated with both modes of timing. The sensors shown are those that have maximal amplitude in the motor-related field pattern. Though there is a peak in the mu rhythm range (~10 Hz) and its first harmonic for both conditions, there is no difference in the power levels at these peaks. This was true not only for contralateral sensorimotor sensors, but all over the head. Gamma band (35-45 Hz) frequencies also showed no consistent significant differences in any area of the head. This indicates that the neurons that generate mu and gamma rhythms are either not involved in performing

syncopated or synchronized coordination or respond to parameters that are similar across the two conditions (e.g. movement duration, muscles activated, etc.).

In contrast, very consistent significant differences between conditions were found in the beta range. These differences were broadband in nature ranging from 15-30 Hz. Figure 3.12 shows the topography of significant differences in the 20-30 Hz range for all plateaus. Results from the 15-20 Hz range were nearly identical and are not included. Two observations are particularly relevant. First, prior to the transition in the Syncopate condition (on average, plateau 5 and below), there are highly significant differences in sensors over central and pre-central areas. These differences are concentrated over the left hemisphere though they do extend across the midline and even into the right hemisphere. This suggests that activity in the contralateral sensorimotor cortex and perhaps also premotor (e.g. supplementary motor area) and ipsilateral sensorimotor areas changes in association with the mode of coordination. Secondly, where there are differences, they are always in the same direction, with more power in the Synchronize condition, indicating a greater suppression of beta activity during syncopation, the more difficult coordinative pattern.

A third interesting observation is what happens after the transition in the Syncopate condition for subjects 1 and 2's data. Despite the fact that these subjects were synchronizing in both conditions, similar regions still show strongly significant differences in beta power, suggesting a "carryover" or history effect of syncopation. The strength of beta rhythms thus depends not only on the mode of coordination currently being performed but also on previously performed coordinative patterns. Together these

72

Figure 3.11 (page 74): Examples of averaged power spectra from plateau 2 of both conditions. Spectra shown are from the sensors indicated in black (lower right corner), which overlie the left sensori-motor area (the sensor # is indicated in the upper right hand corner of each graph; see figures 3.7 and 3.8 for exact location). Clear differences in the two curves are found throughout the beta frequency range (15-30 Hz).

Figure 3.12 (page 75): Topographic maps showing areas of significant differences in MEG signal power in the high beta (20-30 Hz) frequency range. Maps of the 15-20 Hz range were similar and are not shown. The transition point is indicated for each subject; pre-transition the timing mode differed between the two conditions whereas post-transition subjects were synchronized in both cases. Difference values were converted to z-scores before plotting; any z-score that did not exceed a confidence level of $\alpha=0.001$ is shown as black. All differences are positive indicating that higher power levels were always found for the Synchronize condition.

Subj 2
Plateau 2
1.25 Hz

Synchronise
Syncopate

Log(Power) v. Freq.

Figure 3.11

74

Figure 3.12

75
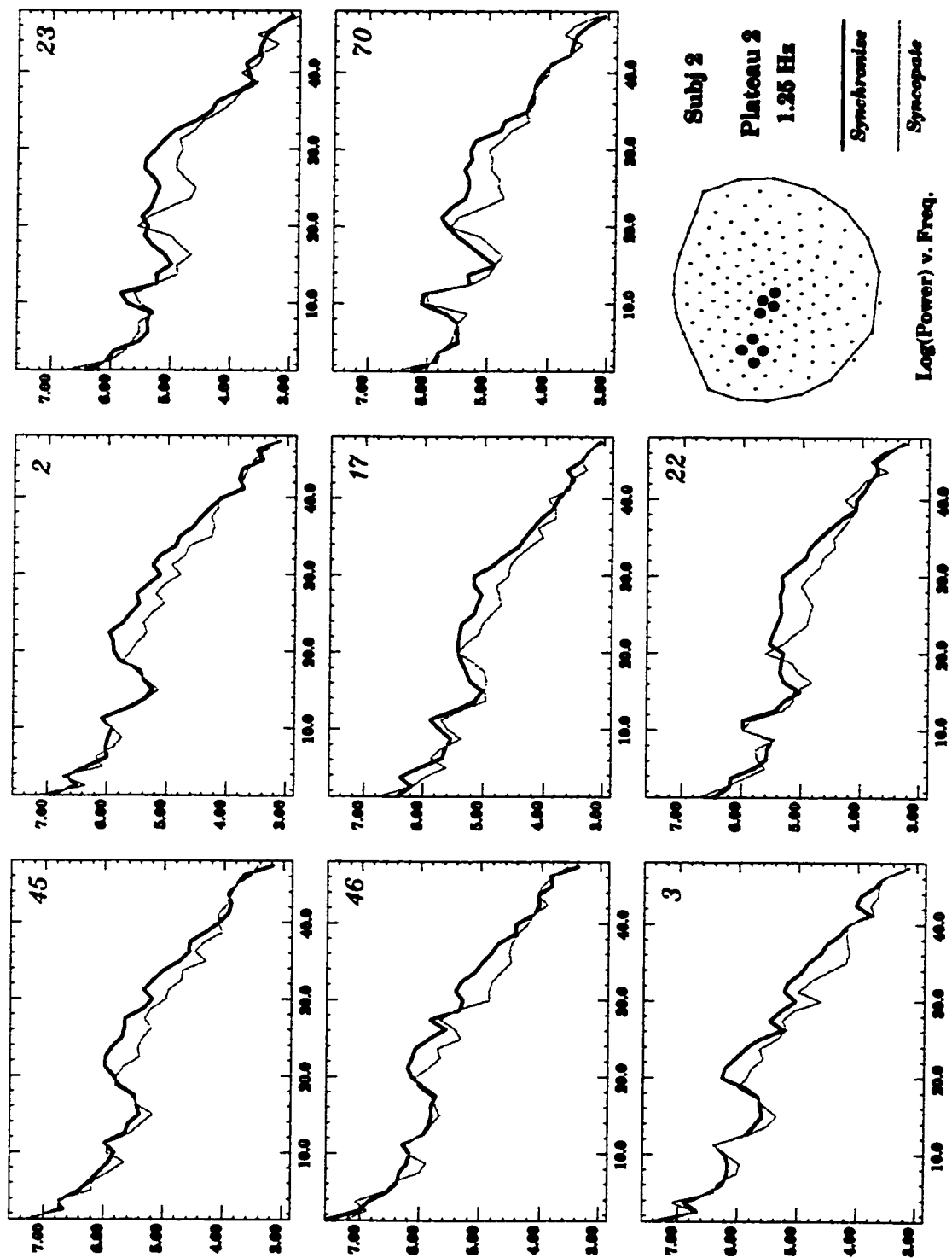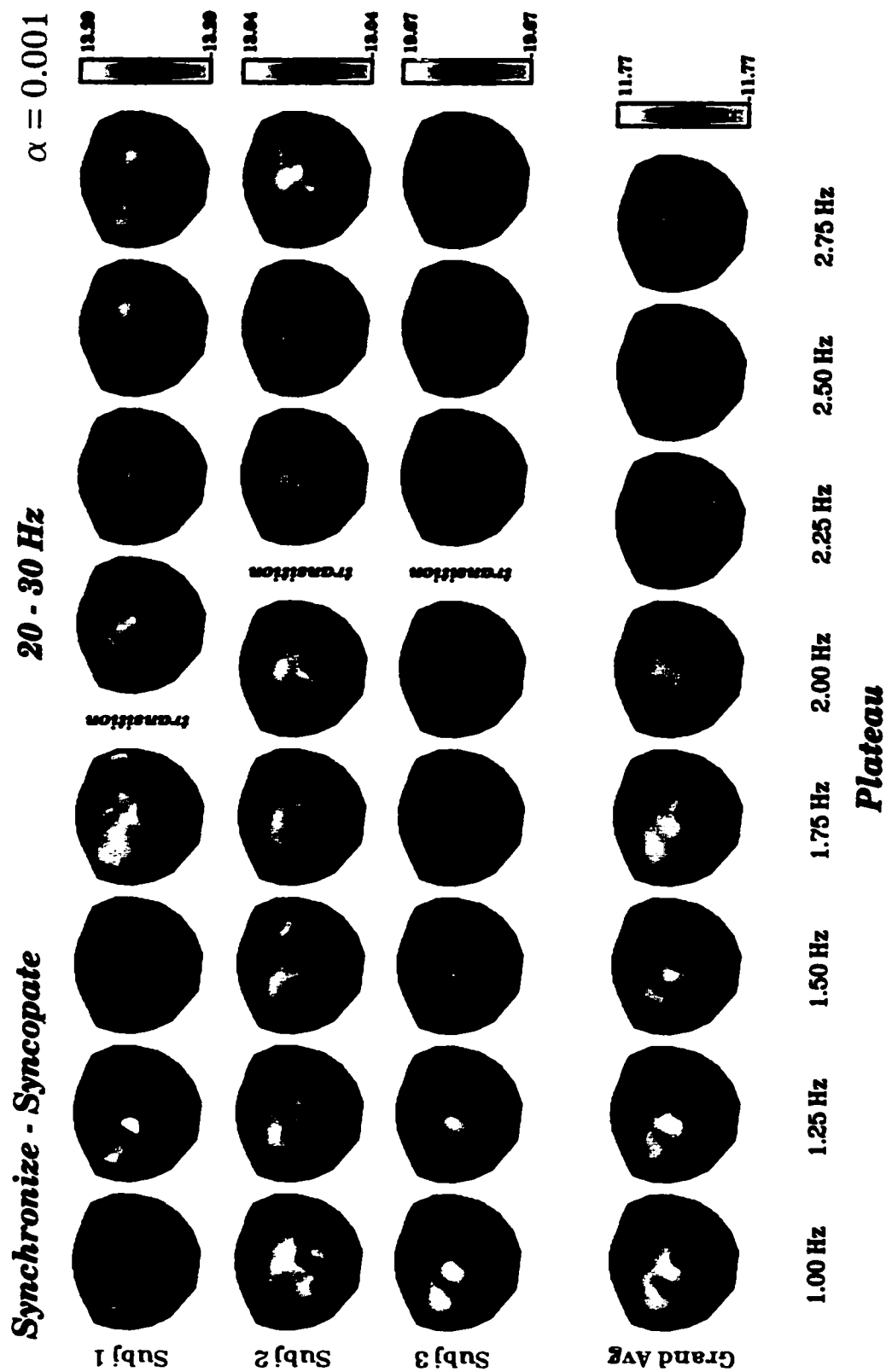
results suggest that neural populations responsible for generating beta rhythms in sensorimotor and premotor areas react to the way in which movement is organized in a given environmental context.

3.4 Discussion

The strongest components in the ERFs reflect auditory and motor-related field activity. The characterization of these two patterns presented here explains previous results [Fuchs et al. 1992, 2000c; Kelso et al., 1992] that demonstrate spatiotemporal shifts in neuromagnetic activity when subjects switch from syncopation to synchronization with an auditory metronome in a ramped frequency task. Regarding temporal ERF features, we have confirmed previous results [Kelso et al., 1991, 1992; Fuchs et al., 1992; Wallenstein et al., 1995] showing that 180° transitions occur in parallel on brain and behavioral levels in the Syncopate condition. We further show these transitions to be restricted to sensors that overlie contralateral sensorimotor areas. This topography plus the lack of transitions in the brain signals from the Synchronize condition suggest that the coordination frequency component of ERP/ERFs tracks the timing of the brain's motor response (here signified by the motor field) within each cycle.

Spatial reorganizations of activity previously observed with MEG recordings [Fuchs et al., 1992, 2000c; Kelso et al., 1992] can also be explained. Increasing the metronome rate leads to a decrease in amplitude of the brain's auditory response. On the other hand, the amplitude of the motor field is relatively unaffected by increasing coordination frequency. This interaction in frequency dependence causes low plateau neuromagnetic activity to be dominated by an auditory-related pattern whereas for high

plateaus, the strongest pattern is a motor-related dipolar field. There are at least two possible explanations for the decrease in amplitude of the auditory pattern. One is that after the transition to synchronization, a superposition of auditory and motor-related activity causes field cancellation. We reject this explanation because the same frequency-amplitude relationship is observed in the Synchronize condition during which the two responses are superimposed at all plateaus. A more likely explanation is a change in the way the brain processes auditory information.

The dependence of the brain's auditory response on inter-stimulus interval (ISI) is well known for both EEG [see Näätänen & Picton, 1987 for review] and MEG [Hari et al., 1982; Liu et al., 1998]. However, this phenomenon has not been systematically investigated in the ISI range used here. Rather much of the work on auditory event-related activity has focused on either slower, transient evoked responses (ISI > 2 sec) or much faster steady-state responses (40 Hz) [see Lins & Picton, 1995 for review]. The range that affords syncopated or synchronized coordination is in the middle; it must be fast enough to allow anticipation of the next stimulus but still remain within the limits of biomechanical operation [see, e.g. Engström et al., 1996]. We speculate that the changes in auditory-related activity observed here reflect a transition to an increasingly steady-state response that results not only in the habituation of auditory cortical neurons, but also in a reorganization of sensorimotor integration networks leading to an inability to separate the motor response from each tone event. In other words, the motor response becomes entrained to the increasingly predictable series of tones, leading to synchronized coordination at faster metronome rates.

Though the results described above may relate to why syncopation becomes unstable, the only ERF features that uniquely distinguish between a syncopated and synchronized mode of coordination (i.e. between conditions) appear to be related solely to the timing of the motor response itself within each cycle. This is in contrast to previous analyses of EEG data, which demonstrate that significant differences in event-related potential (ERP) signal power at the coordination frequency exist in electrodes over contralateral central and antero-parietal areas [Mayville et al., 1999]. Specifically, in Mayville et al. (1999) syncopation was associated with stronger ERP power at these sites when compared to synchronization either post-transition within the same condition or at the same plateau rates in a synchronize control condition. This previous work suggests that activation of contralateral sensorimotor cortex varies with the coordinative pattern. Our finding here of significant differences in the power of beta oscillations (15-30 Hz) in sensors located over contralateral sensorimotor areas is consistent with this hypothesis. Differences exist between plateaus 1-5 of each condition, the range of frequencies across which subjects syncopated in one condition and synchronized in the other. However, in contrast to the ERP study, synchronized coordination is associated with higher power than syncopation. This discrepancy in the direction of difference probably reflects the fact that in the former situation we examined power at the coordination frequency whereas in this experiment we examined non phase-locked activity in much higher frequency ranges.

Desynchronization of oscillations in the beta range during motor activity is a well-documented phenomenon in both EEG [Pfurtscheller & Berghold, 1989; Pfurtscheller & Neuper, 1992; Pfurtscheller et al., 1996, 1998; Leocani et al., 1997] and MEG [Kristeva-Feige et al., 1993; Salmelin and Hari, 1994; Hari et al., 1997]. Current theories posit that decreases in beta rhythm amplitude at the scalp signify a shift from an 'idling' state to task-related activation [Pfurtscheller et al., 1996; Pfurtscheller & Lopes da Silva, 1999]. Such amplitude changes, however, are typically defined with respect to baseline levels of activity associated with rest or some non-movement control condition. In our case, the ramped nature of the task precluded a comparison between each frequency plateau and some baseline period. Therefore we do not have a direct measure of how rhythmic activity changed in response to either type of auditory-motor coordination, i.e. whether it increased or decreased as compared to rest. Nevertheless, it is reasonable to conclude that the differences in rhythmic activity that we observe between the Syncopate and Synchronize conditions reflect similar differences in the functional organization of underlying neural networks. From this perspective, then, syncopated coordination is associated with a stronger event-related desynchronization (i.e. more task-related activity) than synchronization.

Changes in beta activity may, in some cases, reflect changes in mu rhythm oscillations to which frequencies in the beta range are harmonically related. Indeed, figure 11 shows clear peaks around both 10 Hz and its first harmonic. However, neither peak differentiates between conditions. Rather, the second peak splits the beta range into a low (15-20 Hz) and high (20-30 Hz) range, both of which show significant differences

between syncopated and synchronized coordination. This suggests that there are at least two distinct neuronal mechanisms associated with auditory-motor coordination, one that relates to the spectrally-focused mu rhythm and one which generates broad-band beta oscillations. Previous work in both EEG [Pfurtscheller et al., 1996] and MEG [Salmelin and Hari, 1994] indicates that mu rhythms are generated in somatosensory cortex whereas beta rhythms reflect activity in pre-central areas, including not only primary motor areas but also possibly premotor cortical areas. Our results are consistent with these studies. Since we are subtracting power between two conditions which both involve movement, it is not surprising that a rhythm generated in somatosensory areas (mu rhythm) shows no significant differences.

On the other hand, the fact that differences exist for the 15-30 Hz range suggests that beta oscillations are generated by neural populations that respond to how motor behavior is organized within a given environmental context. This hypothesis is also supported by the fact that two of the three subjects in this experiment show a history effect; even after the transition to synchronization, these subjects still show a difference in beta power between conditions. Neural processes relating to movement generation or somatosensory stimulation cannot explain this result. Rather, the task context is the differentiating factor. In one case subjects have been synchronizing the whole time whereas in the other they have recently switched from a more difficult pattern. The former situation is certainly more automatic. Subjects establish a rhythm very quickly and thereafter must only attend to the modification of movement rate in response to perturbations introduced by increases in plateau frequency. In the Syncopate condition,

however, subjects must also attend to the change in the timing pattern that accompanies the transition. In other words, they have to concentrate on reestablishing a 1:1 stimulus/response relation as required by the task in addition to modifying their coordination rate in response to perturbation.

One factor that is likely to differ with task context is the amount of attention/effort required to maintain a given pattern of sensorimotor coordination. Lower levels of beta power during syncopation (or post-transition synchronization) as compared to (transition-free) synchronization may thus reflect the fact that subjects must concentrate harder to maintain a syncopated mode of coordination. While there is behavioral support for the hypothesis that syncopated (anti-phase) modes of coordination require more attention [Carson et al., 1999; Temprado et al., 1999], there is little evidence that scalp-recorded oscillations in the 15-30 Hz range show stronger decreases in amplitude when the task condition requires more attention. A recent study by Manganotti et al. (1998) reports that beta (13-20 Hz) decreases tended to be stronger with motor sequences of increasing complexity but these differences were not found to be significant. The authors do state, however, that focal decreases in 16-19 Hz power were observed over contralateral centro-parietal regions. On the other hand, Murthy and Fetz (1992) showed that bursts of beta (25-35 Hz) oscillations in sensorimotor cortex were more frequent when monkeys performed a task that apparently required more attention and sensorimotor integration (reaching for a raisin versus repetitive wrist flexion/extension). Such increases in beta activity are in contrast to the decreases we observe but could reflect differences between scalp and intracortical recording techniques. Whereas EEG and MEG activity measure

the summed activation of many neuronal populations, microelectrodes pick up only local field activity. Increased arousal and/or action may act to split large synchronized neural populations into smaller functional groups which could simultaneously cause a decrease in amplitude of the aggregate signal measured at the scalp and an increase in oscillatory bursts within local populations.

4.0 Experiment 3: Neuromagnetic beta (15-30 Hz) rhythm distinguishes syncopated and synchronized timing patterns in overt and imagined sensorimotor coordination

4.1 Introduction

One of the fundamental problems faced by the nervous system is the timing of movement with respect to the environment. The temporal organization of behavior is thought to involve a wide array of cortical and subcortical areas [e.g. Halsband et al., 1993; Ivry, 1996, 2000; Rao et al., 1997; Harrington et al., 1998; Harrington & Haaland, 1999] but little is known about the dynamical mechanisms through which they operate. Studies on rhythmic sensorimotor coordination indicate, for example, that the ability to match one's movement with a metronome is constrained by both the timing relation and the rate of coordination. Engström et al. (1996) demonstrated that there is a transition from reactive to anticipatory behavior at a movement rate of about 1.0 Hz. Transitions in coordinative timing have also been observed for higher movement rates. Whereas both syncopated (off-the-beat) and synchronized (on-the-beat) response patterns are possible for rhythmic rates below about 2 Hz, beyond this threshold only synchronization is stable [Fraisse, 1982; Kelso et al., 1990]. Therefore, when subjects are instructed to respond between successive beats and the rate of the metronome is systematically increased they spontaneously switch to a synchronized timing relation in order to stay 1:1 with the

metronome. No such switching, of course, occurs if subjects start in a synchronized mode.

Transitions from syncopation to synchronization are accompanied by two key dynamical phenomena. Just prior to the timing switch, measures of the phase relationship between stimulus and response at brain and behavioral levels show enhanced fluctuations and increased relaxation times [Kelso et al., 1991, 1992; Fuchs et al., 1992; Wallentstein et al., 1995]. These features indicate that transitions to synchronization occur because of emerging coordinative instability [see Kelso, 1995; Haken, 1996 for discussion] and suggest the hypothesis that off-the-beat patterns are controlled by a distinct network of neural areas which then reorganizes as its dynamical interactions become increasingly unstable. One area whose activity has been shown to be uniquely related to the performed timing relation is contralateral sensorimotor cortex. The amplitude of both neuroelectric [Mayville et al., 1999] and neuromagnetic [Fuchs et al., 1992, 2000c] signals recorded at scalp locations over this area was found to significantly differ depending on whether subjects were syncopating or synchronizing, independent of the rate of coordination.

These results demonstrate that there are constraints on the brain's ability to time behavior with respect to external events and moreover that these lead to changes in the spatiotemporal dynamics of brain activity. An interesting question is whether or not such constraints on the temporal organization of behavior are dependent upon the presence of movement. It is possible that switches from syncopated to synchronized coordinative patterns result from central changes in the representation of temporal information that

occur even in the absence of movement execution. Previous work on motor imagery indeed supports the hypothesis that behaviorally relevant temporal information is centrally stored and can be accessed and modified without motor execution. Similar time courses for mental and actual movements have been shown in several studies using a variety of tasks including drawing, writing and walking [see Decety, 1996 for review] and a growing number of studies are showing that mental practice can improve performance of skilled motor tasks significantly more than no practice at all and, in some cases, even to the extent that actual physical practice does [see Decety & Ingvar, 1990 for discussion]. There is even evidence that mental movements are also governed by a speed-accuracy tradeoff in accordance with Fitts' law [Decety, 1996; Georgopoulos & Massey, 1987].

Further support for the hypothesis that motor planning mechanisms operate independent of actual execution comes from several neuroimaging studies that have shown activation of brain areas thought to be involved in the temporal organization of behavior during motor imagery. These include both cortical (e.g. prefrontal cortex, premotor cortex, supplementary motor area (SMA)) [Ingvar & Philipsson, 1977; Roland et al., 1980; Decety et al., 1994] and subcortical (cerebellum) [Decety et al., 1990; Ryding et al., 1993] structures. Recently, evidence that primary motor cortex is involved in motor imagery tasks has also emerged [Hallett et al., 1994; Beisteiner et al., 1995; Lang et al., 1996; Pfurtscheller & Neuper, 1997], raising questions as to whether it has a purely executive function.

Together these results suggest that the same timing mechanisms are in place for internally simulated and overt movement. However, correlates of mental 'switching' are unknown. Here we investigated 1) whether mental transitions from syncopated to synchronized timing occur when subjects imagine performing each pattern under increasing coordination rate, and 2) whether correlates of the timing pattern (either overtly performed or mentally simulated) can be found in the spatiotemporal dynamics of magnetoencephalographic (MEG) brain activity. Previous attempts to identify such correlates have shown that event-related fields associated with imagined sensorimotor coordination do not differ depending on the timing pattern [Fuchs, personal communication]. Here we show evidence that the neuromagnetic beta (15-30 Hz) rhythm is such a correlate.

4.2 Methods

4.21 Subjects

Four right-handed subjects (3 male, 1 female) participated. However, only data from three are reported here; MEG signals from one of the male subjects were corrupted due to heavy dental work. The experiment was approved by the Institutional Review Board and conformed to standards of ethics in human research outlined in the Declaration of Helsinki. Informed consent was obtained from all subjects prior to any MEG recording.

4.22 Task Conditions

The task in this experiment was to overtly or mentally coordinate peak flexion of the right index finger with an auditory metronome. Two timing relationships were

examined: synchronization (flex on the beat) and syncopation (flex in between consecutive beats). The four task conditions were collected in blocks. A block consisted of one run of each condition in the following order: 1) Synchronize, 2) Mental Synchronize, 3) Syncopate, and 4) Mental Syncopate. This order was chosen so that subjects performed each mental condition directly after its overt counterpart. 16 blocks were collected per subject.

The metronome rate was systematically increased from 1.0 to 2.75 Hz in 0.25 Hz steps after every 10 cycles (one plateau). This range of frequencies was chosen because syncopation is typically stable only for rates less than about 2 Hz, after which subjects spontaneously transition to synchronization in order to keep a 1:1 relation with the metronome. In contrast, most subjects are able to maintain a synchronized pattern throughout this entire frequency range. Subjects were instructed to coordinate in the manner prescribed by the task condition and further told not to consciously attempt to intervene if they felt themselves losing the correct timing relation. The main objective in each trial was to maintain a 1:1 stimulus/response ratio.

4.23 Experimental Procedure

Subjects participated in all conditions while seated inside a magnetically shielded room (Vacuum Schmelze, Hanau) with their heads firmly held within the helmet of the magnetometer. The metronome (1 kHz, 60 msec tones) was delivered binaurally through plastic headphones at a volume that the subjects reported to be comfortable. In the overt conditions, subjects responded by applying pressure against a sensitive air cushion placed just beneath the tip of their right index finger. Subjects were instructed not to move

during the mental conditions, and were asked to keep their finger on the air cushion so that the lack of movement could be established. Finally, subjects were asked to fixate at a point located approximately two meters in front of them and to confine all eye or extraneous body movements to rest breaks between blocks.

4.24 Data Acquisition

MEG activity during all four conditions was recorded using a full-head magnetoencephalograph (CTF Inc., Port Coquitlam, Canada) comprised of 143 SQuID (Superconducting Quantum Interference Device) sensors distributed homogeneously across the scalp. Conversion to third-order gradiometers was performed in firmware using a set of reference coils. MEG, metronome and response signals were bandpass (0.3-80 Hz) and notch filtered (50 and 100 Hz), and then digitized at a rate of 312.5 Hz. A coordinate system for each subject's head was defined with respect to three fiduciary points: the nasion, left, and right preauricular points (whose three-dimensional coordinates were measured prior to each experiment using a set of reference coils). Finally, sensor coordinates were projected into two dimensions for topographical mapping.

4.25 Behavioral Analysis

Metronome and response signals from the overt coordination conditions were compared on a cycle-by-cycle basis in order to determine the timing relationship. One cycle was defined as one period of the metronome, i.e. tone onset to following tone onset. There were 160 total cycles per plateau and condition. Relative phase values (calculated between tone onset and response peak) were used to classify each cycle as syncopation

(180° ± 60°), synchronization (0° ± 60°), or other. Cycles classified as 'other' (e.g., phase wrapping) were excluded from further analysis. Remaining cycles were then segregated by plateau frequency. For the Syncopate condition, a transition plateau was established by comparing the relative numbers of syncopate versus synchronize cycles. For pre-transition plateaus only syncopation cycles were kept whereas only synchronization cycles were kept for the post-transition plateaus. For the Synchronize condition, only cycles that met criteria for synchronization were kept for MEG analysis. Response signals from the mental conditions were examined only to confirm that subjects did not move overtly.

4.26 MEG Analysis

MEG signals were manually inspected for artifacts. If any portion of a cycle was contaminated, the entire cycle was discarded from further analysis. Before computing signal power, all raw cycles were preprocessed by first subtracting the event-related field for the corresponding condition/plateau (computed by ensemble averaging in the time domain all cycles within that group with respect to tone onset) in order to meet stationarity requirements for spectral estimation [see Bendat & Piersol, 1986 for discussion]. Each cycle was then multiplied by a ½ sine tapering window and transformed into the frequency domain by discrete Fourier transform (DFT). Finally, power spectra were averaged across cycles in each data group and banded by calculating the average of components in each of the following frequency bands: mu (8-12 Hz), low beta (15-20 Hz), high beta (20-30 Hz) and gamma (35-45 Hz).

MET

N

MN

P

MP
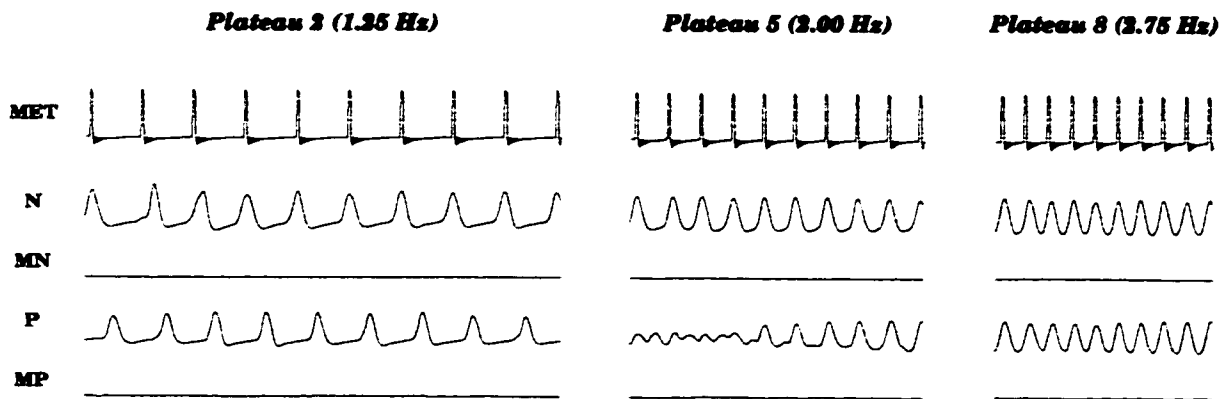
Figure 4.1: Sample of behavioral data from subject 1 for a low, middle and high frequency plateau. Plotted on top is the metronome signal. Below this are the response time series averaged across 16 runs from each of the 4 conditions: N (Synchronize), MN (Mental Synchronize), P (Syncopate), MP (Mental Syncopate). All response data is on the same scale. The lack of finger movement in the mental cases is evident. The transition in the Syncopate condition is reflected by the lack of a consistent response pattern (on average) in the beginning of plateau 5.

Figure 4.1

The following comparisons of resulting values were made by subtracting power in the second condition from that in the first (same plateau only):

- Synchronize – Syncopate
- Mental Synchronize – Mental Syncopate
- Syncopate – Mental Syncopate
- Synchronize – Mental Synchronize

Differences were then converted to z-scores to test for significant differences between the conditions. Significance levels were set to $p < 0.05$ after adjustment for multiple comparisons (143 channels) using a Bonferroni correction. Finally, the significant differences were topographically mapped. Values between sensor locations and at locations where the corresponding sensor was bad or noisy were interpolated using a spline of 3rd order. The color scale was set such that all sensors for which the z-score difference between conditions was not significant were black.

4.3 Results

4.31 Task Performance

As expected subjects were able to synchronize on all plateaus in the Synchronize condition. The average relative phase value for this condition (all plateaus across all subjects) was 6.7° (± 21.2°). Approximately 15% of cycles were excluded because they did not meet criteria for synchronized coordination. In contrast, none of the subjects were able to maintain syncopation throughout the entire run in the Syncopate condition. Subject 1 switched most often at plateau 5 (2.25 Hz) while the other two subjects switched one plateau later (2.5 Hz). After the transition points, all subjects showed synchronized behavior for the rest of each run. Grand average relative phase values before and after the transition were 172.9° (± 23.7°) and 12.7° (± 24.3°), respectively.

91

30% of the total number of cycles were discarded because they did not meet criteria for syncopation (pre-transition plateaus) or synchronization (post-transition plateaus).

Figure 4.1 shows sample behavioral data taken from subject 1 for all of the conditions. Averaged response time series from a low (1.25 Hz), middle (2.0 Hz) and high (2.75 Hz) frequency plateau are displayed in the last four rows (N: Synchronize condition, MN: Mental Synchronize condition, P: Syncopate condition, MP: Mental Syncopate condition). The timing transition in the Syncopate condition generally occurred on plateau 5 for this subject as is evident by the lack of a consistent response pattern (on average) (fig 4.1, row 4). After the transition, responses are synchronized with each metronome beat (compare rows 1 (MET) and 4).

Also evident in figure 4.1 is the lack of overt movement in either mental condition (conditions MN and MP). Subjects experienced no major problems in performing the Mental Synchronize task. However, on post-experiment interview all reported the perception of switching to synchronization in the Mental Syncopate condition, suggesting that off-the-beat timing relations become unstable at faster rates even when there is no overt movement.

4.31 MEG

Approximately 7% of cycles in each of the four conditions were excluded from subsequent power analyses because of movement artifacts.

4.321 Power Differences: Overt Conditions

We first compared the two overt movement conditions in order to find frequency bands that exhibited amplitude modulation as a function of timing relationship. Since all
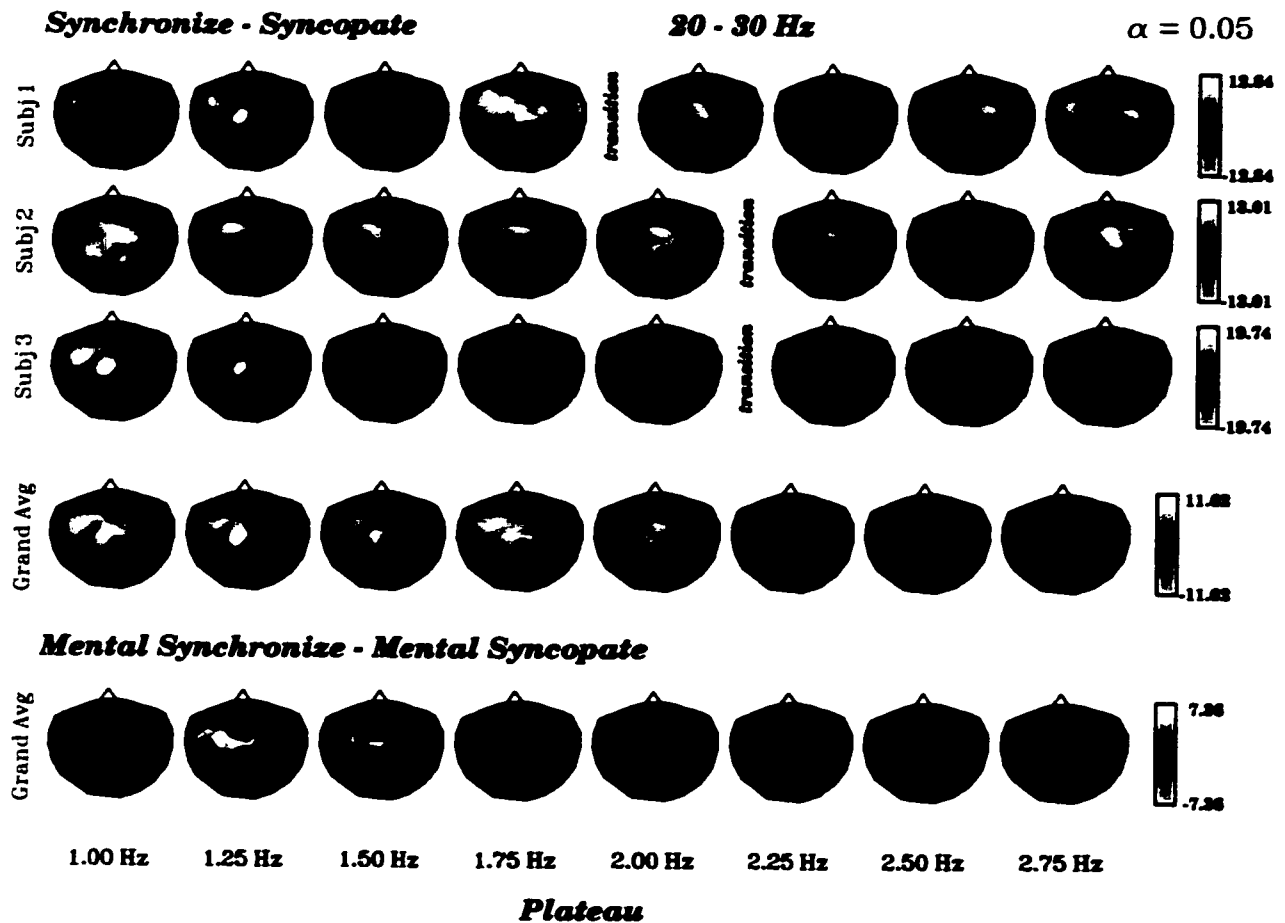
Figure 4.2: Topographic maps showing areas of significant differences in MEG signal power in the high beta (20-30 Hz) frequency range. Maps of the 15-20 Hz range were similar and are not shown. Difference values for each sensor were converted to z-scores before plotting; any score that did not exceed a confidence level of α=0.05 is shown as black. The first four rows show individual and grand-averaged maps that resulted when overt syncopation was subtracted from overt synchronization. The transition point in the Syncopate condition is indicated for each subject. The bottom row shows the grand-averaged maps from the comparison between mental conditions. Almost all differences are positive indicating higher power for a synchronized timing relation. The orientation of each map is from above with the nose on top.

Figure 4.2

subjects switched to synchronization at higher plateaus, only differences found for pre-transition plateaus can be attributed to off versus on-the-beat timing. Neither the mu (8-12 Hz) nor gamma (35-45 Hz) rhythms were consistently affected by the mode of coordination. More specifically, while there were a few significant differences between conditions in these frequency bands, their topographical location varied both across subjects and plateau rate. In contrast, both the low (15-20 Hz) and high (20-30 Hz) beta rhythms showed spatially consistent significant effects in all three subjects.

Figure 4.2 shows topographic maps of significant differences in the high beta range for each subject individually (rows 1-3) as well as their average (row 4). Results from the low beta range were almost identical and are not shown. Colored sensors are those for which the difference in beta power levels between the two conditions exceeded a significance level of $p < 0.05$. The color itself indicates the direction of difference with red/yellow corresponding to more power in the Synchronize condition and blue the reverse. The transition point for each subject in the Syncopate condition is indicated. Prior to this point, the maps reveal two main effects. First, the difference between the Synchronize and Syncopate conditions was always positive, indicating a lower amplitude of beta activity during syncopated coordination. Second, these differences were strongest over left central areas, consistent with the location of the contralateral sensorimotor cortex, though midline and bilateral central sensors also showed significant differences (e.g., see plateaus 4 (1.75 Hz) and 5 (2.00 Hz)). These maps imply that the neuromagnetic beta rhythm in motor-related cortical areas is affected by the temporal context of sensorimotor integration.

After the transition to synchronization there was a marked attenuation of the differences between conditions on average (figure 4.2, row 4). However, for subjects 2 and 3 there are still significant differences in bilateral central and precentral areas (rows 1 and 2). In other words, despite the fact that subjects were now synchronizing in both conditions, the beta rhythm was still significantly weaker in the Syncopate condition. Therefore, brain activity associated with synchronization at high rates depended on whether subjects were previously in a syncopated or synchronized coordinative pattern.

4.322 Power Differences: Overt versus Mental Conditions

To investigate the relation between the beta rhythm and the presence or absence of overt movement, we subtracted each mental condition from its overt counterpart. Shown in figure 4.3 are the results from the Syncopate – Mental Syncopate comparison. The transition points in the Syncopate condition are again indicated. The differences were topographically similar across subjects as well as movement rate. Significant differences were found in central and precentral areas of both hemispheres and across the midline, possibly reflecting differences in activation of premotor areas. In almost all cases, beta activity was stronger when subjects imagined doing the task suggesting that the neuromagnetic beta rhythm in these areas is suppressed by the presence of overt movement. Since we do not know exactly where subjects perceptually switched to synchronization in the Mental Syncopate condition, it is difficult to interpret changes in the intensity of these differences as a function of plateau rate. Nevertheless, it is clear from the maps that just prior to where the transition occurred in the Syncopate condition, these differences are much stronger (row 4, plateau 4 (1.75 Hz)). A lack of equally
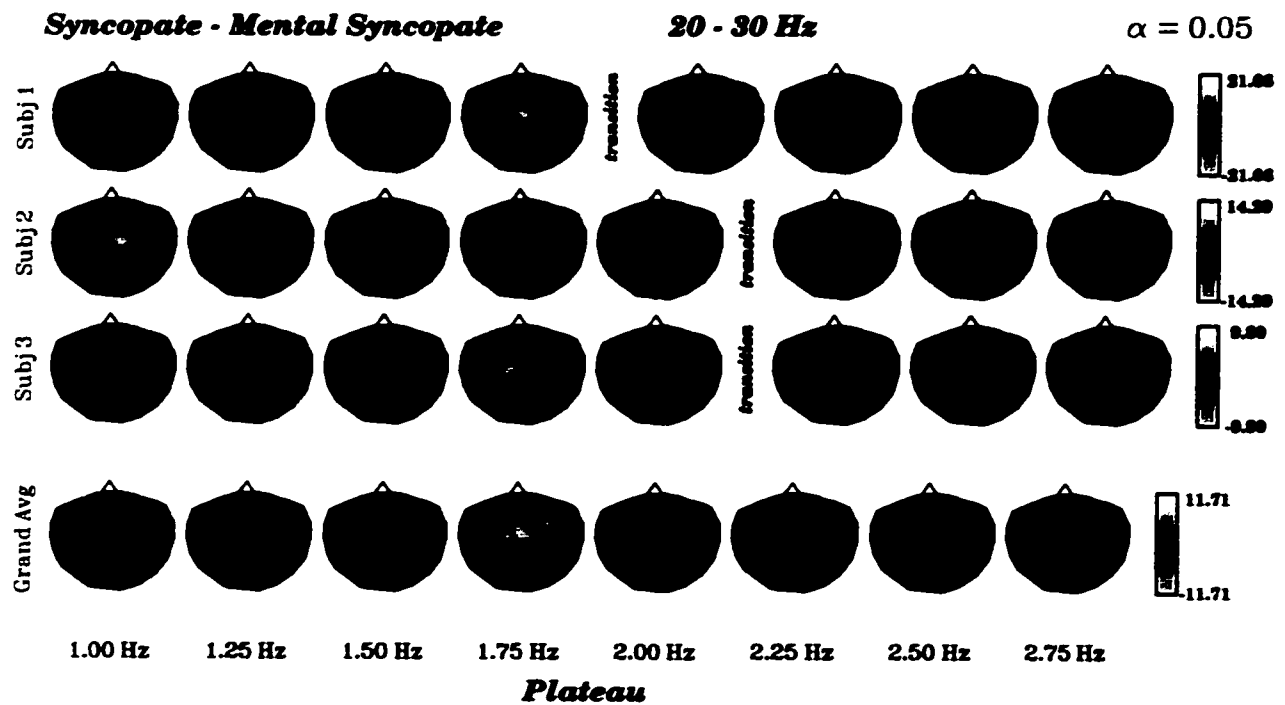
Figure 4.3: Individual and grand-averaged maps of significant differences between overt and mental syncopation. Differences were concentrated in bilateral and midline precentral areas and were almost all negative indicating a stronger beta rhythm during imagined syncopation. See also caption for figure 4.2.
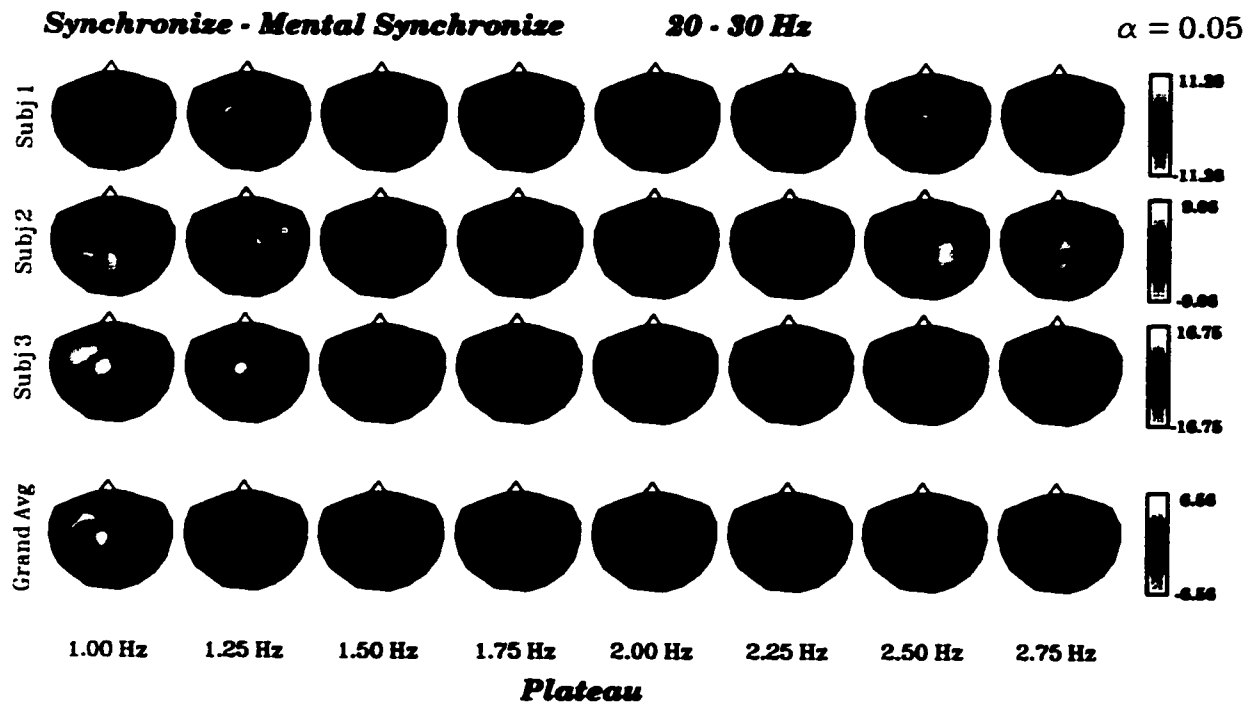
Figure 4.3

Figure 4.4: Individual and grand-averaged maps of significant differences between overt and mental synchronization. In contrast to figure 4.3, both the topography and direction of difference depend on the subject, resulting in non-significant differences on average (row 4). See also caption for figure 4.2.

Figure 4.4

strong differences at the lower plateaus suggests that the amount of beta power is not solely dependent upon the presence or absence of movement. The enhancement of differences in beta power near the transition point may, however, reflect the higher difficulty of the movement task as syncopated timing becomes increasingly unstable.

We further examined the relationship between beta rhythm amplitude and the presence or absence of movement by comparing the Synchronize and Mental Synchronize conditions. If the reduction of beta rhythm amplitude in bilateral central and precentral areas during overt as compared to imagined syncopation is the result of subjects actively moving in the former case then the same relation should exist when comparing the two synchronization conditions. As seen in figure 4.4, the results were quite different for two subjects (rows 2 and 3), resulting in little to no significant differences on average (row 4). In fact, these two subjects even showed greater suppression of beta activity during the overt situation on some plateaus (e.g. plateaus 1-3 for subject 3). These results support the conclusion that the neuromagnetic beta rhythm is sensitive to the temporal context in which a movement pattern is organized rather than to the presence or absence of movement itself.

Results for the low beta (15-20 Hz) frequency range were again very similar to figures 4.3 and 4.4. Differences associated with the mu (8-12) and gamma (35-45) bands were almost always negative suggesting that, in general, overt movement is associated with lower signal power in these frequency ranges. However, the topography was much more variable across subjects resulting in few significant differences on average.

The above comparisons suggest that the neuromagnetic beta rhythm distinguishes between syncopated and synchronized timing strategies independent of whether the task was overtly performed. If this hypothesis is true then one would expect to see differences in beta rhythm amplitude when imagined syncopation and synchronization are compared. The bottom row in figure 4.2 shows the grand-averaged maps that resulted when Mental Syncopation was subtracted from Mental Synchronization. Though the effects were not as strong as in the overt comparison it is clear that, on average, there are significant differences for plateaus 2 and 3 in the same direction and over the same cortical areas. This demonstrates that the beta rhythm in contralateral sensorimotor cortex is sensitive to the timing between sensory and motor events even when the movement is not actually executed. However, these differences are clearly weaker than in the previous comparison, which suggests that overt movement enhances this sensitivity. Furthermore, the lack of significant differences at higher plateaus indicates that historical context is less influential on current sensorimotor integration processes when the movement is only imagined.

4.4 Discussion

Our main finding is that the strength of the neuromagnetic beta (15-30 Hz) rhythm in sensorimotor and premotor areas during coordination depends on the timing between auditory and motor 'events'. Significantly weaker beta activity accompanied a syncopated (off-the-beat) as compared to synchronized (on-the-beat) relation. This was true for both overtly performed and imagined coordination though the difference was

enhanced by the presence of movement. Due to the ramping of the metronome rate, we were unable to isolate MEG activity at each plateau for comparison with a pre-movement baseline or rest period. Nevertheless, the relative suppression of beta power with syncopated patterns likely reflects the same mechanisms that underlie the phenomenon of event-related desynchronization (ERD) [see Pfurtscheller & Lopes da Silva, 1999 for discussion]. In other words, syncopated timing relations are associated with stronger beta ERD than synchronized ones.

ERD is thought to reflect focal activation of the underlying neural tissue [Pfurtscheller, 1992; Toro et al., 1994] and its occurrence in response to transient movement is well documented in the beta frequency range for both EEG [Pfurtscheller, 1981; Leocani et al., 1997; Stančák et al., 2000] and MEG [Salmelin & Hari, 1994; Feige et al., 1996]. A decrease of beta (15-20 Hz) power relative to rest has also been observed for rhythmic sequential movements paced by an external metronome at a rate of 2 Hz [Manganotti et al., 1998]. Other studies have implicated the beta rhythm in motor planning processes. There is some evidence, for example, that the neuromagnetic beta rhythm is associated with motor preparation for sensorimotor integration tasks [Kristeva-Feige et al., 1993]. Furthermore, beta ERD has been shown to accompany imagination of movement although this occurs for the mu rhythm as well [Pfurtscheller & Neuper, 1997]. Our results extend this earlier work and imply that neurons which contribute to oscillations in the beta range are more responsive (i.e. exhibit stronger *desynchronization*) to more difficult timing patterns.

Comparisons between overt and mental performance of the same timing relation revealed that, in general, there was a greater suppression of all rhythms when subjects actually moved. However, the beta band differences observed in bilateral pre-central areas between syncopation and mental syncopation were clearly *not* solely the result of having movement in the former condition. If this were the case, the same differences would be expected in the synchronize – mental synchronize comparison. This conclusion is further supported by the distribution of these differences over areas considered to be involved in motor planning rather than motor execution.

The fact that subjects report perceptual switches from syncopation to synchronization during the imagined coordination task supports the hypothesis that there is a central representation of behaviorally-relevant temporal information in the absence of performance. Moreover, the occurrence of mental transitions demonstrates that constraints on the brain's ability to temporally coordinate internally generated responses with the environment exist independent of whether the responses involve overt movement. We found a relative suppression of beta power in contralateral sensorimotor areas for mental syncopation versus mental synchronization that parallels the overt comparison. This suggests not only that primary sensorimotor areas play a functional role in the temporal organization of behavior but also that such temporal organization is reflected by the suppression/desynchronization of the neuromagnetic beta rhythm.

One alternative explanation is that the strength of beta oscillations depends not on the timing strategy, per se, but rather how difficult it is, i.e. how much effort it requires. Synchronization is relatively automatic as long as the metronome rate is within a

101

rhythmic range (such that accurate anticipation of upcoming beats is possible) without exceeding biomechanical limitations [Fraisse, 1982]. In contrast, syncopated timing patterns are clearly more difficult to perform and require more attention [Kelso, 1994; Carson et al., 1999; see also Temprado et al., 1999 for similar results with bimanual coordination]. This interpretation is supported by the finding of differences in beta power even when subjects were performing the same timing relation, e.g. post-transition plateaus (2.25-2.75 Hz) in figure 4.1. Specifically, synchronization at high rates was associated with a significantly stronger beta rhythm if subjects had been synchronizing throughout the entire run as compared to runs in which they transitioned from a syncopated mode of coordination. However, the effect of historical context on the temporal organization of behavior is not well understood and it is possible that the neural mechanisms that control synchronized timing are different in the two cases.

In addition we found an enhancement of power differences between overt and mental syncopation just prior to the overt transition plateau. Though the target timing relation was the same in both conditions, we have no direct measure of when subjects perceptually switched to synchronization in the mental case. It is possible that these enhanced differences correspond to plateaus for which subjects had already switched in the mental situation. This might be the case if, for example, actual performance of the coordinative movement stabilizes the timing relation by providing additional reafferent information not present during mental imagery alone. A stabilizing effect of additional information on coordination has been previously shown [Fink et al., in press]. On the other hand, the transitions could have occurred at the same plateau on average in both

conditions. In this case the stronger differences just prior to the transition could reflect higher attentional demands associated with maintaining overt syncopation as it becomes increasingly unstable.

It is worth mentioning, however, that in one of the few studies to look at the relation between required attentional focus and brain rhythms, Manganotti and colleagues (1998) observed an increase in the amount of mu ERD with movement sequences of increasing length but no such effects were observed for beta activity. Furthermore, though Nashmi et al. (1994) demonstrated a facilitating effect of attention and motor preparation on 'beta' activity, these oscillations were in a much higher frequency range (30-50 Hz).

The differences observed in the beta range were in contrast to MEG activity in the mu (8-12 Hz) or gamma (35-45 Hz) ranges, which did not differentiate between the two patterns in either the overt or imagined comparisons. These results support the conclusion that a distinct neuronal population generates the motor-related beta rhythm and are consistent with previous work which shows that the topography as well as timing of ERD/ERS events with respect to movement onset depend on the frequency range examined [Pfurtscheller & Neuper, 1992; Salmelin & Hari, 1994; Leocani et al., 1997].

Spatially, beta oscillations have been localized to anterior regions of sensorimotor cortex whereas mu rhythm changes are thought to arise in post-central cortex [Salmelin & Hari, 1994; Pfurtscheller et al., 1996; Hari et al, 1997; Pfurtscheller & Lopes da Silva, 1999]. Temporally, whereas both mu and beta rhythms desynchronize about 1.75-2 sec prior to movement onset, resynchronization of the beta rhythm is quicker [Pfurtscheller et

al., 1996; 1998; Leocani et al., 1997] and usually stronger, well exceeding pre-movement levels [Pfurtscheller et al., 1996; Hari et al., 1997]. Rebound of the beta rhythm has also been shown to depend on the muscle group activated [Hari et al., 1997; Pfurtscheller et al., 1998].

In summary, the occurrence of timing transitions in both overt and imagined coordination indicate that there are constraints on the brain's ability to organize movement with respect to an external periodic stimulus which are independent of whether the movement is actually carried out. We show evidence that the neuromagnetic beta (15-30 Hz) rhythm is a signature of processes in the brain that underlie the temporal integration of rhythmic sensory and motor-related events and furthermore transitions from one timing relation to another. The relative suppression of beta oscillations in sensorimotor and premotor areas during syncopation as compared to synchronization is observable not only for overtly executed but also for mentally simulated coordination. Moreover, the beta rhythm is sensitive to previously performed timing patterns. Finally, whereas overt syncopation results in a reduction of beta rhythm amplitude in bilateral central and precentral areas relative to mental syncopation, the same relation does not consistently exist for overt versus mental synchronization. Together these results suggest that the strength of the beta rhythm at least partially reflects activity in cortical populations that subserve the planning of movement in a given environmental context rather than motor execution.

5.0 Experiment 4: Neuromagnetic motor fields accompanying self-paced rhythmic finger movement of different rates

5.1 Introduction

This experiment investigates rate-dependent effects on movement-related patterns of neuromagnetic activity. Movement-related magnetic fields associated with non-rhythmic, transient voluntary movement have been well described over the last two decades. In general two types of fields have been distinguished: pre-movement and movement-evoked. Several studies have revealed slow magnetic field changes prior to movement [Deecke et al., 1982; Hari et al., 1983; Cheyne & Weinberg, 1989; Kristeva et al., 1991]. This readiness field begins approximately one second prior to movement and gradually builds to maximal amplitude near the point of movement onset. It is consistently recordable over sensorimotor areas in both hemispheres, though it tends to be stronger on the contralateral side [Deecke et al., 1982]. Moreover, this field is topographically dipolar on both sides of the head and has been approximated with bilateral current sources in the sensorimotor cortex directed anteriorly [Cheyne et al., 1995]. Unlike the readiness or Bereitschaftspotential measured with electroencephalography (EEG) [Kornhuber & Deecke, 1965], which is strongest over the midline, the readiness field is not thought to reflect activation of the supplementary motor area (SMA) along the mesial wall of the interhemispheric fissure. One hypothesis is that SMA activation, which EEG recordings indicate is bilateral prior to movement, may not

be measurable with MEG because of field cancellation [Cheyne & Weinberg, 1989; Kristeva et al., 1991; Cheyne et al., 1995]. This idea is supported by the finding of SMA activity in patients who have damage to one side of the interhemispheric wall [Lang et al., 1991]. However, recent work suggests that more complicated forms of movement are preceded by field activity that is localized to the SMA region [Erdler, 2000].

During movement three field components have been identified. These have been termed the movement-evoked fields I-III (MEFI-MEFIII) [Kristeva et al., 1991]. The MEFI typically occurs approximately 100 msec after EMG onset with the next two components occurring about 100 and 200 msec later, respectively. Of these three, the MEFI is the strongest and most stable. It is characterized by a large reversal of the readiness field observable over the contralateral sensorimotor area. MEFI has been localized to the posterior medial wall of the central sulcus using both dipole modeling [Cheyne & Weinberg, 1989] and registration of field activity with structural scans obtained via magnetic resonance imaging [Kristeva-Feige et al., 1994]. The latency of the MEFI is also known to be longer for foot versus finger movements, suggesting a dependence of this component on peripheral input [Kristeva-Feige et al., 1994]. This dependence was verified by Cheyne et al. (1997) who showed that slowing conduction times of the nerves of the hand by cooling the forearm also resulted in a delay of the MEFI. Finally, the blocking of cutaneous input with anesthetic does not eliminate the MEFI component [Kristeva-Feige et al., 1996]. Together, these results strongly suggest that the MEFI reflects reafferent information from muscle receptors in the periphery [Cheyne et al., 1997].

Though not observable in all subjects, the MEFII and MEFIII have also been localized to sensorimotor cortex. However, dipole analysis indicates a more anterior source for the MEFII whereas the MEFIII and MEFI appear to be generated by the same cortical population [Kristeva-Feige et al., 1994]. The timing and topographical focus of the MEFII raises the question of whether the MEFII corresponds to the motor command for extension (the return phase of the movement in the Kristeva-Feige et al. (1994) experiment).

Here we examine patterns of neuromagnetic activity associated with movement at 21 different rates systematically spanning the range typically considered rhythmic, ~0.6 to 3.0 Hz. None of the previous studies have examined the MEF complex over a broad parametric range. Of primary interest is how pre-movement and movement-evoked fields are affected by the length of time between successive movements. The choice of this range of rates is motivated by transition phenomena observed in the timing of rhythmic sensory-motor coordination [Kelso et al., 1990]. It is well established that the ability of subjects to coordinate finger movement with an external metronome in a 1:1 fashion critically depends on the rate of the metronome, and hence movement. For example, even when instructed to react to each metronome beat, subjects begin to show anticipatory timing at a rate of 1.0 Hz [Engström et al., 1996]. Transitions from syncopated (between successive beats) to synchronized (on each beat) patterns of coordination have also been observed for higher rates of movement [Kelso et al., 1990]. Whereas both modes of coordination are possible for rates below 2 Hz, beyond this frequency syncopation is generally unstable [Fraisse, 1982; Kelso et al., 1990]. If

subjects are asked to syncopate and the rate of coordination is systematically increased, they spontaneously switch to synchronization in order to keep a 1:1 stimulus/response relationship [Kelso et al., 1990]. No such transitions occur if subjects begin in a synchronized pattern, indicating that it is an inherently more stable timing relation.

Transitions from syncopation to synchronization are associated with changes at both behavioral [Kelso et al., 1991] and neural [Kelso et al., 1991, 1992; Fuchs et al., 1992, 2000c; Mayville et al., 1999] levels but the neural mechanisms responsible for such transitions are still unclear. However, recent work [Fuchs et al., 2000; Mayville et al., submitted] suggests that timing switches may result from rate-dependent effects on the brain's response to sensory and/or motor events that introduce dynamical changes in sensorimotor integration networks. By decomposing event-related fields associated with both modes of auditory-motor coordination, these studies showed that there was a significant decrease in the amplitude of auditory-related brain processes as the rate of the metronome was increased from 1.0 to 2.75 Hz. Motor-evoked activation patterns, on the other hand, showed little or no changes in amplitude as a function of coordination rate. In related work, timing of the MEF components were shown to be significantly correlated to movement velocity [Kelso et al., 1998]. This result revealed a tight coupling between behavior of the motor-evoked field and the response profile that is independent of the inter-response interval. However, it is not certain if these results hold for situations in which a metronome is not present, i.e. for self-paced movement. The presence of an external pacing stimulus, especially auditory, could affect the aggregate field signals detectable at the head surface. Such additional fields may, therefore, affect MEF

amplitudes. Moreover, they may swamp the presence of other, weaker motor-related fields.

Here we systematically investigate field activity associated with self-paced movement across a wide range of rates. We seek to confirm not only the tight coupling between the MEF and motor response but also a lack of dependence of MEF dynamics on movement rate. We further attempt to identify and describe other motor-related fields that accompany rhythmic movement. Our expectation is that there may be additional motor-related processes that do change as a function of movement rate and thus could contribute to instabilities that underlie transitions between different modes of coordination.

5.2 Methods

5.21 Subjects

Four right-handed subjects (3 males, 1 female) participated in this experiment. Prior to recording, the experimental protocols were approved by the Institutional Review Board and informed consent was obtained from all subjects.

5.22 Continuation Task

In order to systematically vary rhythmic movement rate we employed a continuation task that consisted of two phases. Each run began with a *pacing* phase during which subjects were instructed to synchronize movement of their right index finger with an auditory metronome. After 20 cycles (tones), the metronome was turned off and the subjects' task was to continue moving at the same rate until an "end of run" cue (1-sec tone) occurred. This cue was delivered after the amount of time corresponding

to an additional 20 metronome cycles had elapsed. This post-metronome portion is referred to as the *continuation* phase.

Twenty-one different metronome rates were used spanning the range 0.5 to 2.5 Hz in 0.1 Hz steps. One run contained a single rate and the presentation order of the rates was randomized across runs. 5-6 runs were collected per rate, per subject.

5.23 Experimental Procedure

Subjects participated in the experiment while seated inside a magnetically shielded room (Vacuum Schmelze, Hanau) with their heads firmly held within the helmet housing the dewar of the MEG apparatus. The metronome [1 kHz, 60 msec duration tones] was delivered binaurally through plastic headphones at a volume that the subjects reported to be comfortable. Subjects responded by pressing against a sensitive air pressure cushion connected to a pressure-voltage transducer located just outside the shielded room. Increases in pressure corresponded to finger flexion while a return of air pressure to baseline signified the extension (return) phase of each movement (figure 5.1A). Subjects were asked to fixate at a point located approximately two meters in front of them and to confine all eye or extraneous body movements to rest breaks between runs.

5.24 Data Acquisition

MEG activity was recorded using a full-head magnetoencephalograph (CTF Inc., Port Coquitlam, Canada) comprised of 143 SQuID (superconducting quantum interference device) sensors distributed homogeneously across the head surface. Conversion to third-order gradiometers was performed in firmware using a set of
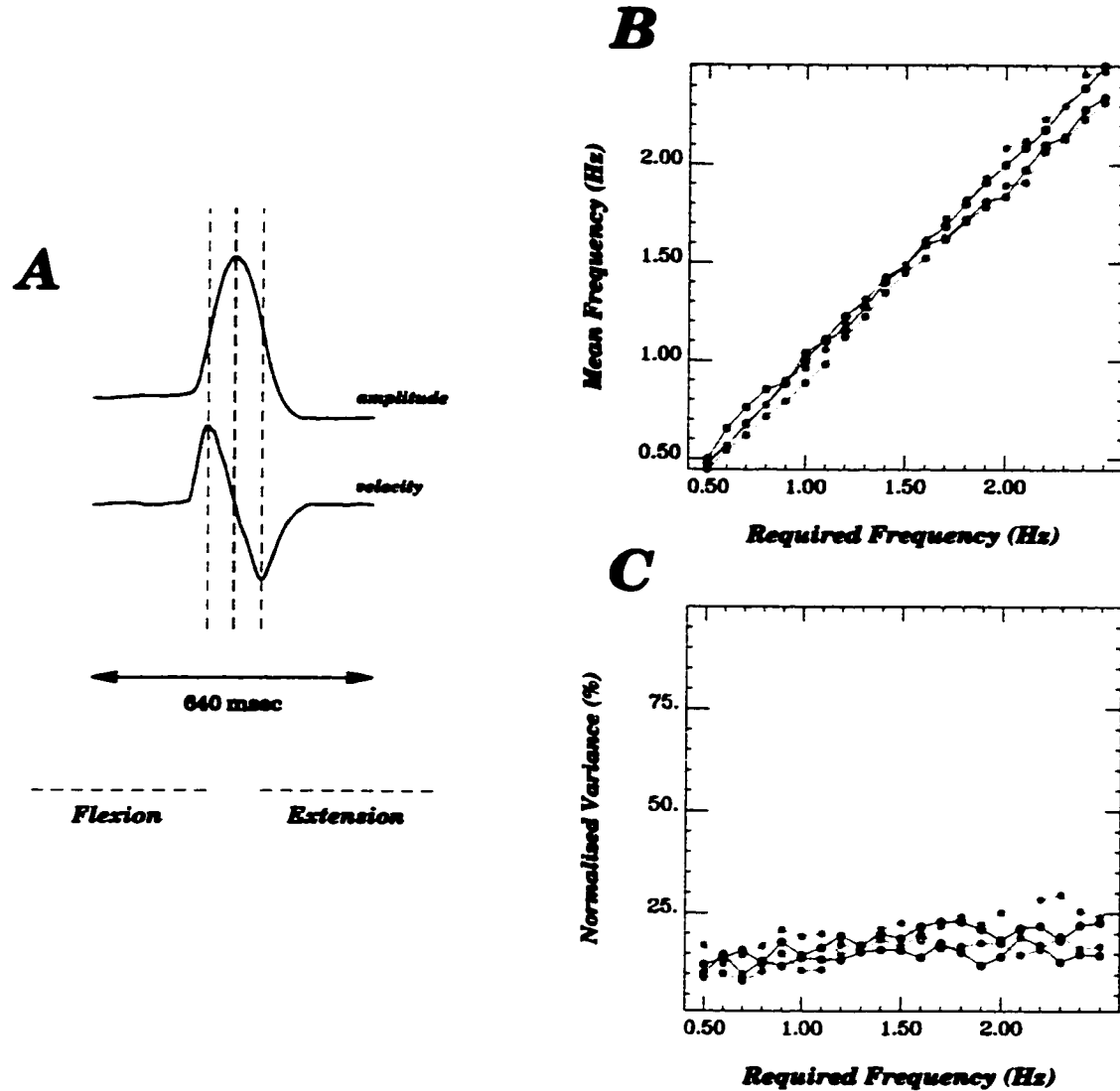
Figure 5.1: **A)** A typical response profile (top) and its derivative (bottom). Flexion and extension of the fingertip correspond to an upward and downward deflection, respectively. Points of maximal velocity in both directions are indicated by the red (flexion) and blue (extension) dashed lines. Peak flexion is at the black dashed line. The entire response (from onset of flexion to end of extension phase) is approximately 200 msec. **B)** Mean response frequency for continuation phase vs. condition (i.e. pacing) frequency. All four subjects (denoted by separate lines) were able to internally pace their movement at the 21 distinct rates. **C)** Variance of each subject's response rate expressed as a percentage of the required response rate. Subjects typically varied by about ¼ to ¼ of the required period at all frequency conditions.

Figure 5.1

reference coils. MEG, metronome and response signals were bandpass (0.3-80 Hz) and notch (50 and 100 Hz) filtered. Digitization was done at a rate of 312.5 Hz. A coordinate system for each subject's head was defined with respect to three fiduciary points: the nasion, left, and right preauricular points (whose three-dimensional coordinates were measured prior to each experiment using a set of reference coils). Finally, sensor coordinates were projected into two dimensions for topographical mapping.

5.25 Data Analysis

Only data from the continuation phase of each run were analyzed such that all included movements were self-paced. Prior to MEG signal processing, we examined the subjects' behavioral performance. First, the peak of each response (peak flexion) was marked. Distributions of inter-response intervals (IRIs) were then calculated separately for each pacing frequency condition in order to see whether subjects were successfully able to internally reproduce the metronome frequency. Response cycles for which the succeeding IRI was within ± 2 standard deviations of each distribution mean were kept for MEG signal analysis. This was done to exclude outlying (extremely slow or fast) responses.

After artifact rejection (performed via manual inspection), MEG signals associated with the retained responses were averaged to obtain event-related fields (ERFs) for each frequency condition. Averaging was performed on a 1-sec window centered at the peak of each response. All 21 ERFs were appended together (in order of increasing rate) and then subjected to a Karhunen-Loève decomposition or Principal

Components Analysis. Through this procedure we extracted the dominant spatial modes or field patterns and then examined the corresponding time-dependent amplitudes of each pattern. Similarity between patterns was assessed with a Pearson correlation.

For the movement-evoked field, the three strongest peaks in the time-dependent amplitudes were marked when possible. Latencies of these peaks were also calculated with respect to the point of maximal response velocity in both the flexion and extension directions (figure 5.1A) in order to examine further the relation between MEF dynamics and response profile. We then plotted both the amplitude and latency (with respect to the response peak) of these points as a function of frequency condition and performed a linear regression on each line to determine its slope. Finally, the dependence of peak latency and/or amplitude on rate was assessed by performing a one-sample t test to determine if each slope was significantly different from zero.

Peak-to-peak amplitudes of the second strongest field pattern were also examined as a function of rate. We then investigated the relation of this second field to the previously described readiness field by re-averaged MEG signals using a 2-sec window that extended from 1.5 sec prior to 0.5 sec after each response peak. These new averages were also decomposed using the Karhunen-Loève procedure to 1) ensure that the spatial pattern did not significantly change between the two average sets and 2) obtain the extended time-dependent amplitudes so that the behavior of this field pattern over the entire course of each response cycle could be described.

5.3 Results

5.31 Task Performance

Figure 5.1A shows a typical response measured with the pressure device. The responses were biphasic with flexion of the finger associated with an increase in pressure (i.e. upward deflection) and subsequent extension causing a decrease in pressure (i.e. downward deflection). The derivative of the response is plotted below to illustrate how the peak of the response (zero crossing) as well as the points of maximal velocity in the flexion (maximum) and extension (minimum) directions were marked. The right half of figure 5.1 shows the mean (5.1B) and variance (5.1C) of the IRI distributions (expressed in Hz) as a function of pacing frequency. On average, all subjects were successfully able to internally pace finger movement at the required frequency (figure 5.1B). The response rate for each subject never varied more than ¼ of a cycle period (figure 5.1C) for subjects 1-3 (red, green, blue lines) at any of the 21 frequencies. For subject 4 (pink line), the response variance only slightly exceeded 25% of the required response rate for movement frequencies 2.2-2.4 Hz. These results not only show that the rate manipulation was successful but also ensure that there was no significant temporal overlap between responses at a given rate.

5.32 MEG Signals

For the averaged signals, the strongest field components occurred during the behavioral response for all 21 rates, demonstrating the predominance of movement-evoked activity for rhythmic movement. Typically, two or three large peaks in the ERFs were evident in sensors over the central portion of the contralateral hemisphere (see

114

figure 5.2, highlighted boxes (top half) and time series (bottom half)). The field pattern sampled at each peak was strongly dipolar as indicated by a polarity reversal in the time series between lateral and medial sensor locations (compare left and right time series on the bottom of figure 5.2). Specifically, field lines either entered laterally and exited medially consistent with a postero-laterally directed current source (figure 5.2 top, -25.6 and 153.6 msec) or the reverse (figure 5.2 top, 76.8 msec). The dipolar structure, orientation, and location over the rolandic area of the contralateral hemisphere is consistent with the movement-evoked fields I-III (MEFI-III) observed for slow transient movements [Cheyne & Weinberg, 1989; Kristeva et al., 1991].

Given the similarity of the field patterns at each peak (irrespective of polarity) we collectively refer to this topographic pattern as the MEF. The MEF occurred in every frequency condition, thus emerging as the strongest spatial mode when a Karhunen-Loève decomposition was performed on all 21 ERFs appended together (figure 5.3, left column). For subjects 1 and 2, the amount of total signal variance accounted for by this pattern was 70.8% and 62.5%, respectively. In the remaining two subjects, the MEF was weaker and accounted for less than half of the ERF signal variance. The topography of the MEF was very similar across subjects as indicated by the high correlation values in table 5.1 (top).

Figure 5.2 (page 117): Event-related fields from subject 1 for the 1.0 Hz condition. The top half shows the ERFs topographically sampled every 25.6 msec. Topographic maps are viewed from above the head with the nose on top. Red/yellow indicate positive magnetic field and correspond to magnetic field lines exiting the head. Blue indicates negative magnetic field, i.e. field lines entering the head. The red line beneath each map indicates where the ERFs were sampled with respect to the averaged response. The strongest field pattern is clearly dipolar in nature with maximal amplitudes over left central sensors. Corresponding time series from these sensors are plotted in the bottom half. Three movement-evoked peaks are clearly visible in both the topographic maps (highlighted in yellow) and time series.

Event-Related Fields: Continuation at 1.0 Hz

117
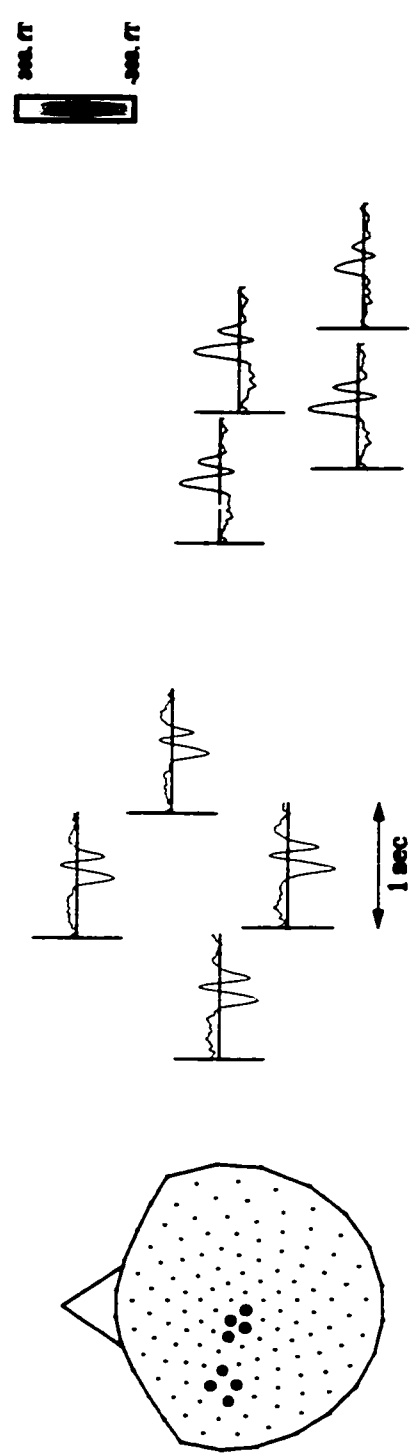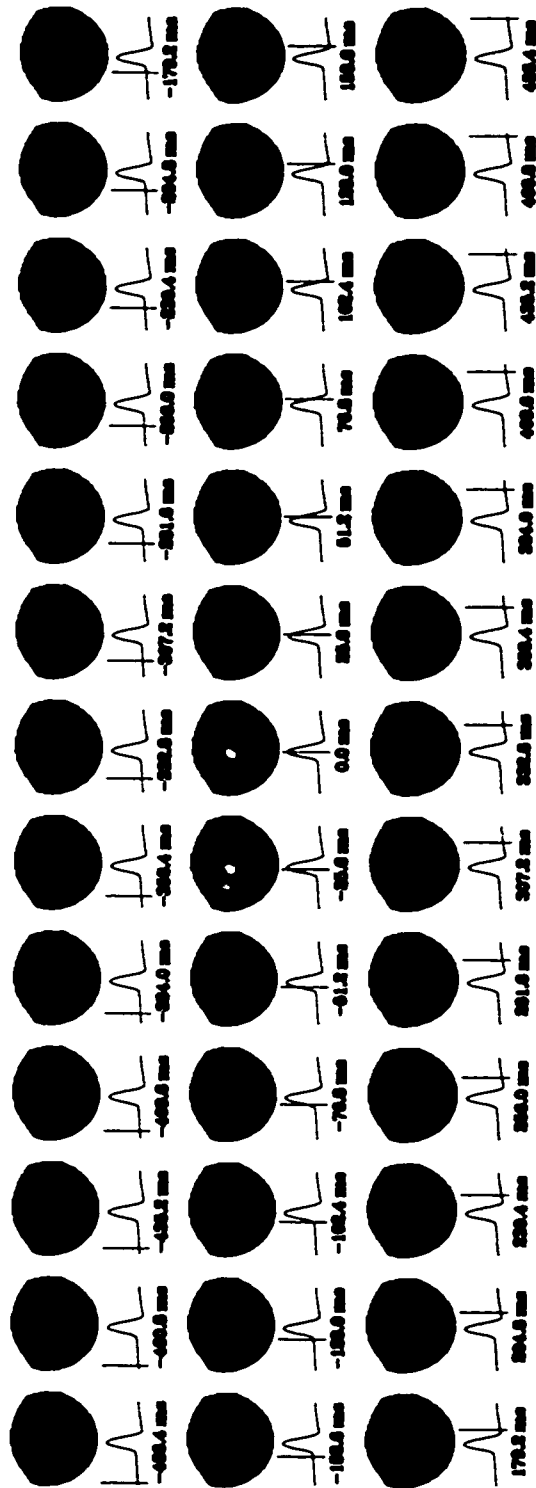
Figure 5.2

Dominant Spatial Patterns
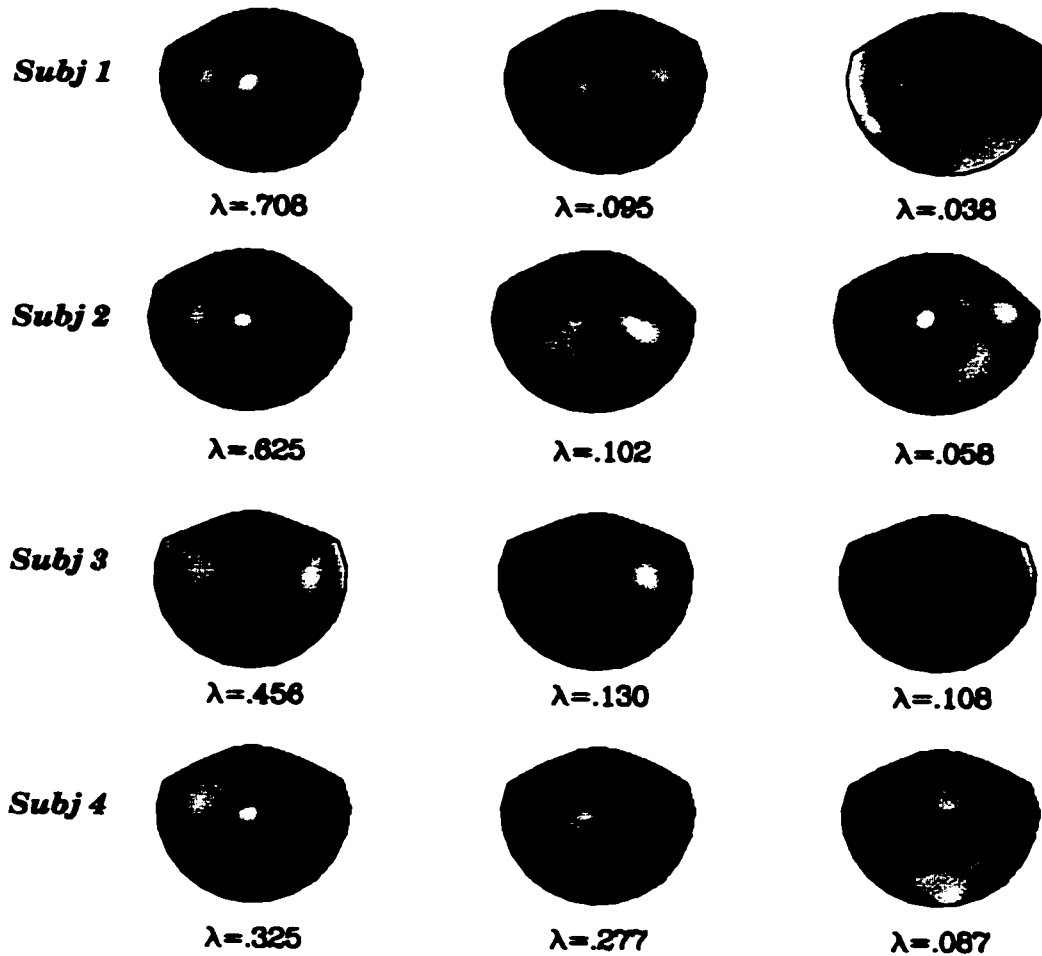
Figure 5.3: Spatial patterns accounting for most of the total ERF signal variance (i.e. all 21 ERFs appended together) as calculated with a Karhunen-Loève decomposition. The proportion of variance is indicated by the eigenvalue beneath each map. For all four subjects, a left central dipolar pattern was dominant though it was much stronger for subjects 1 and 2. The second strongest pattern was also similar across subjects and was characterized by a more centrally focused dipolar field.

Figure 5.3

Table 5.1: Correlation (r) values between decomposed patterns of individual subjects

		S1	S2	S3	S4
Pattern 1	S1	1.00	*	*	*
	S2	0.97	1.00	*	*
	S3	0.74	0.74	1.00	*
	S4	0.91	0.91	0.86	1.00

		S1	S2	S3	S4
Pattern 2	S1	1.00	*	*	*
	S2	0.85	1.00	*	*
	S3	0.55	0.70	1.00	*
	S4	0.90	0.89	0.60	1.00

		S1	S2	S3	S4
Pattern 3	S1	1.00	*	*	*
	S2	0.38	1.00	*	*
	S3	0.23	0.30	1.00	*
	S4	0.34	0.66	0.33	1.00

Our first question was whether or not the dynamics of the MEF changed as a function of movement rate. We investigated both the latency and amplitude of peaks in the MEF by examining its time-dependent amplitude from the Karhunen-Loève decomposition. The results are displayed in figure 5.4a-d for each of the subjects. Results from the first two subjects, for whom the MEF was very strong, are essentially identical. Three MEF peaks (marked with red, green and blue solid lines) were clearly visible for all 21 rates (figure 5.4a and 5.4b, top time series). The first peak occurred approximately 40 msec after maximal velocity in the flexion direction (compare red solid and dashed lines, bottom left of each figure) and approximately 15-20 msec prior to peak

flexion (corresponding to a latency of 0 msec). The second peak was opposite in polarity and reached maximal amplitude approximately 100 msec after the first, at the point of maximal velocity in the extension direction (compare green solid and blue dashed lines). Finally, a second field reversal resulted in a weaker third MEF component that occurred about 80 msec later. These temporal relations were the same across the entire range of movement rates as indicated by the slopes in the bottom left graphs of figures 5.4a-d, none of which were significantly different from zero (all $t(20)<0.1$, $p>0.05$). This indicates that the dynamics of both the MEF and response profile remained constant despite changes in rate.

For the remaining two subjects, who had a weaker MEF, only two peaks were identifiable at all frequencies (figure 5.4c and 5.4d). The timing and polarity of these peaks were similar to the first two peaks observed for subjects 1 and 2 with the exception that both occurred slightly later with respect to the behavioral response (approximately 20-30 msec delay). The first MEF component for these subjects coincided with the point of peak flexion rather than just after maximal velocity in the flexion direction. As with subjects 1 and 2, there was no change in peak latencies as a function of movement rate (no slopes significantly different from zero; $t(20)<0.1$, $p>0.05$).

Peak amplitudes also exhibited no significant dependence on movement rate for any of the four subjects (min t value = 0.01, max t value = -1.9, all $p>0.05$), again indicated by the relatively flat lines in the bottom right graphs of figures 5.4a-5.4d (note that the units of amplitude are arbitrary due to the Karhunen-Loève procedure and are not in femtoTesla). In general the strongest peak was the first evoked field (denoted by the

Figure 5.4 (pages 122-125): Temporal dynamics of the dominant field pattern for subjects 1-4. Vertical lines separate each frequency condition. The top time series is the time-dependent amplitude for the pattern shown on top. Below is the averaged behavioral response time series. Peaks in the time dependent amplitudes are marked separately for each frequency condition with red, green and blue lines. For subjects 1 and 2 (**5.4a** and **5.4b**), three peaks in the time-dependent amplitudes of the motor field were identifiable. In contrast, only two were distinctly visible at all 21 frequencies for subjects 3 and 4 (**5.4c** and **5.4d**). On the bottom left of each figure is a plot of latency (with respect to response peak) vs. frequency condition for each marked peak. Also plotted are the corresponding latencies for points of maximal velocity in the flexion (red dashed line) and extension (blue dashed line) directions. All four subjects show a tight coupling between finger movement and the dynamics of this field pattern that *did not* depend on the movement frequency. On the bottom right are the corresponding peak amplitudes (in arbitrary units) vs. frequency condition. There was no significant dependence of peak amplitudes on the movement frequency.

Pattern Dynamics   Subj 1

λ=.708

Figure 5.4a

122

Pattern Dynamics   Subj 2

λ=.622

123

Figure 5.4b

Pattern Dynamics   Subj 3

λ=.456

Figure 5.4c

124

Pattern Dynamics　　**Subj 4**

λ=320

1 sec

Required Frequency

Amplitude

200.　100.　0.　−100.　−200.

2.00　1.50　1.00　0.50

Required Frequency (Hz)

Latency (msec)

100.　0.　−100.

0.50　1.00　1.50　2.00

125
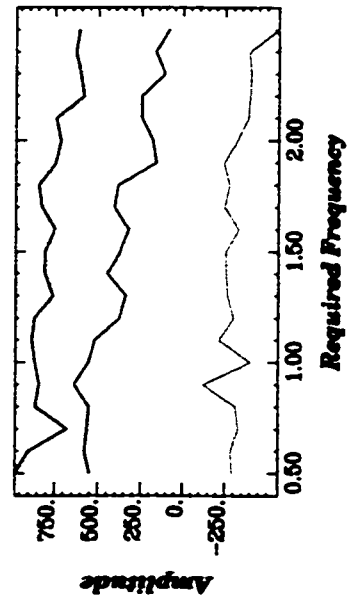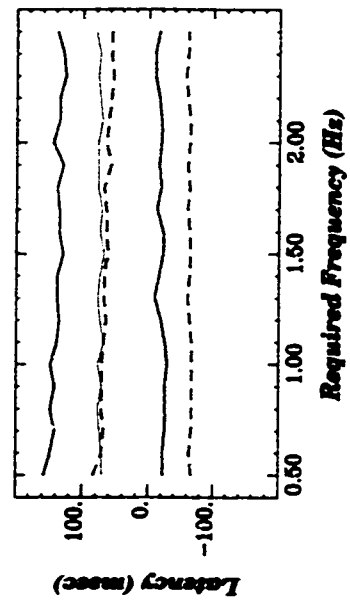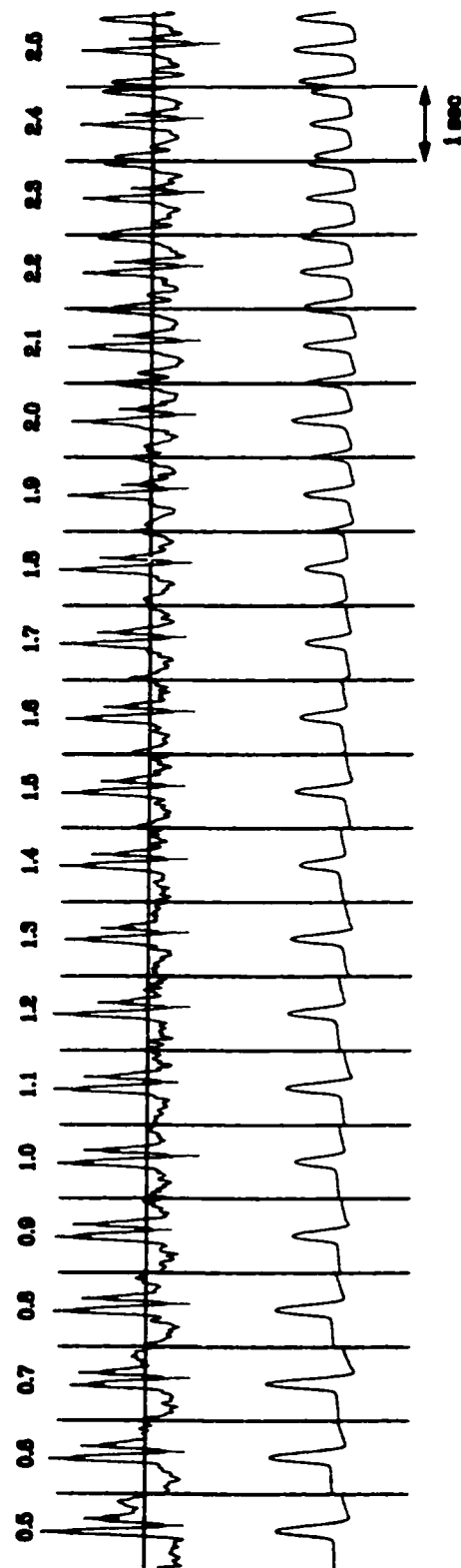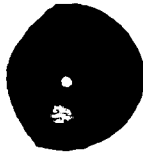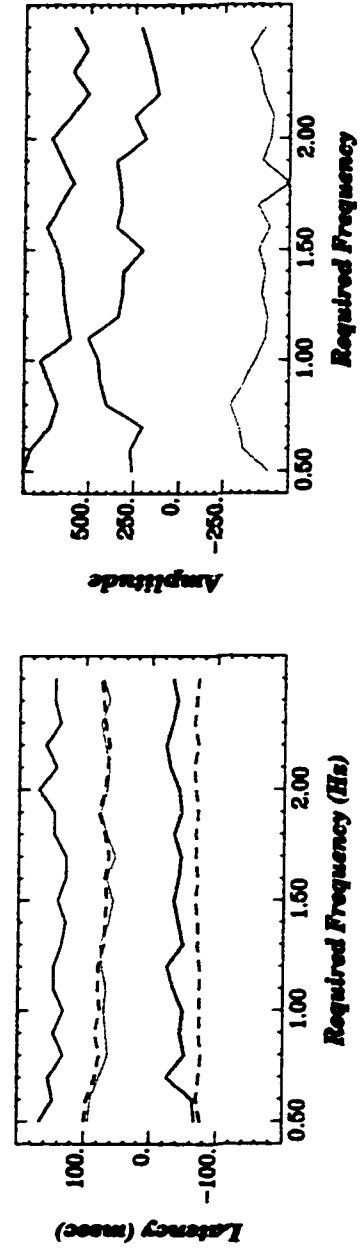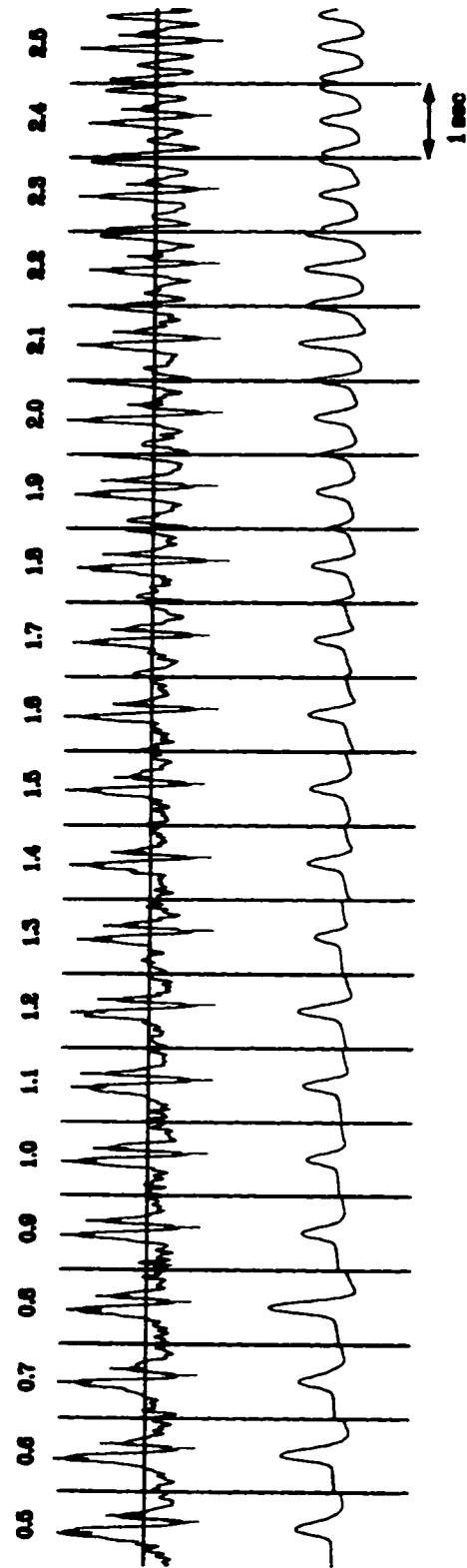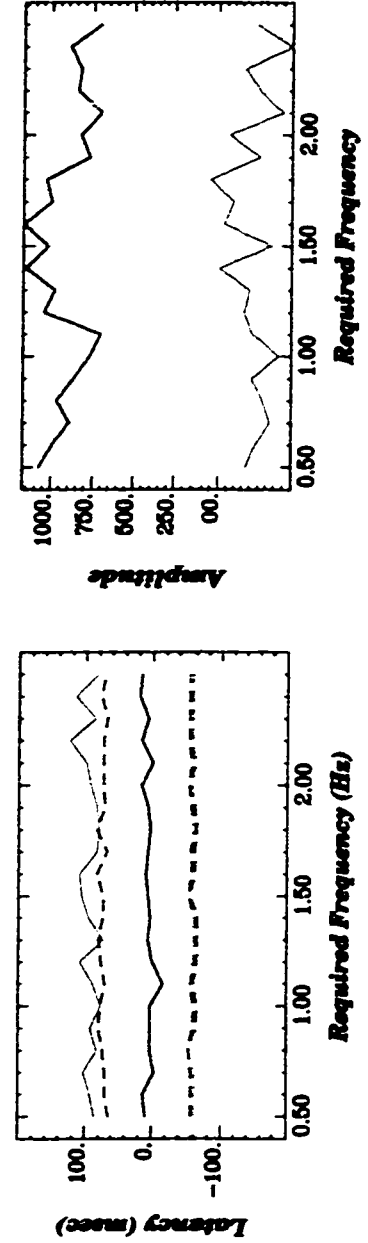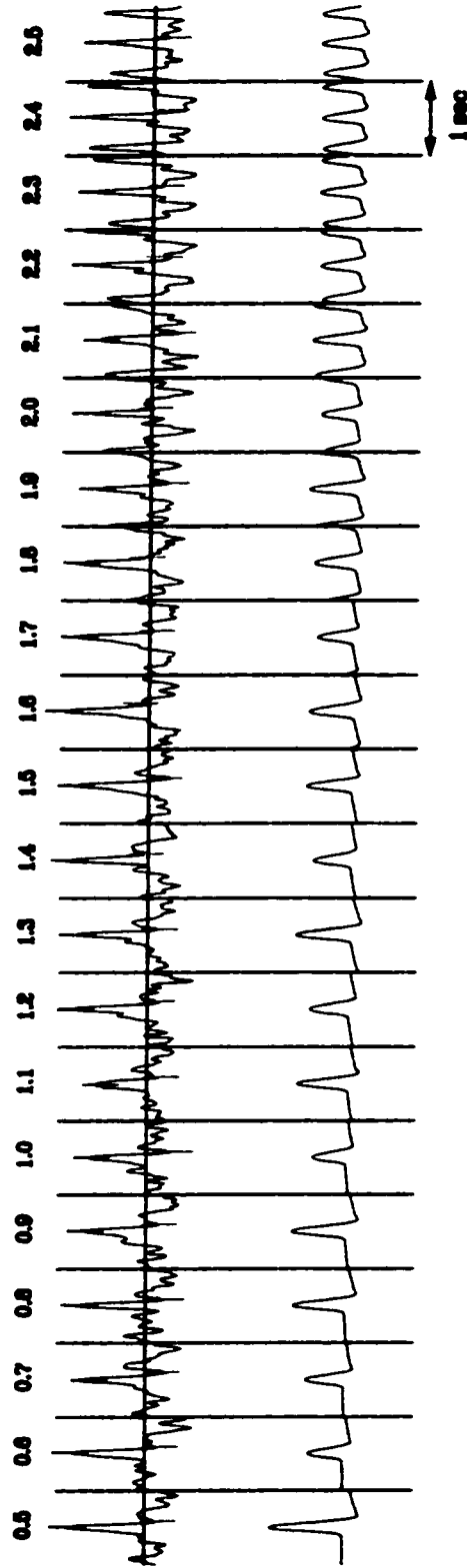
Figure 5.4d
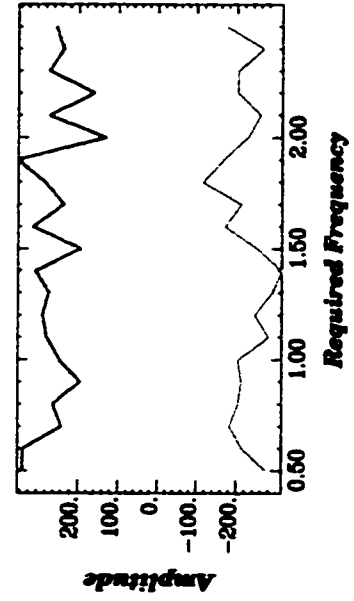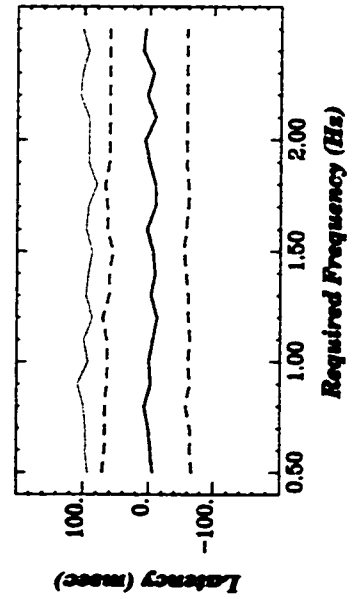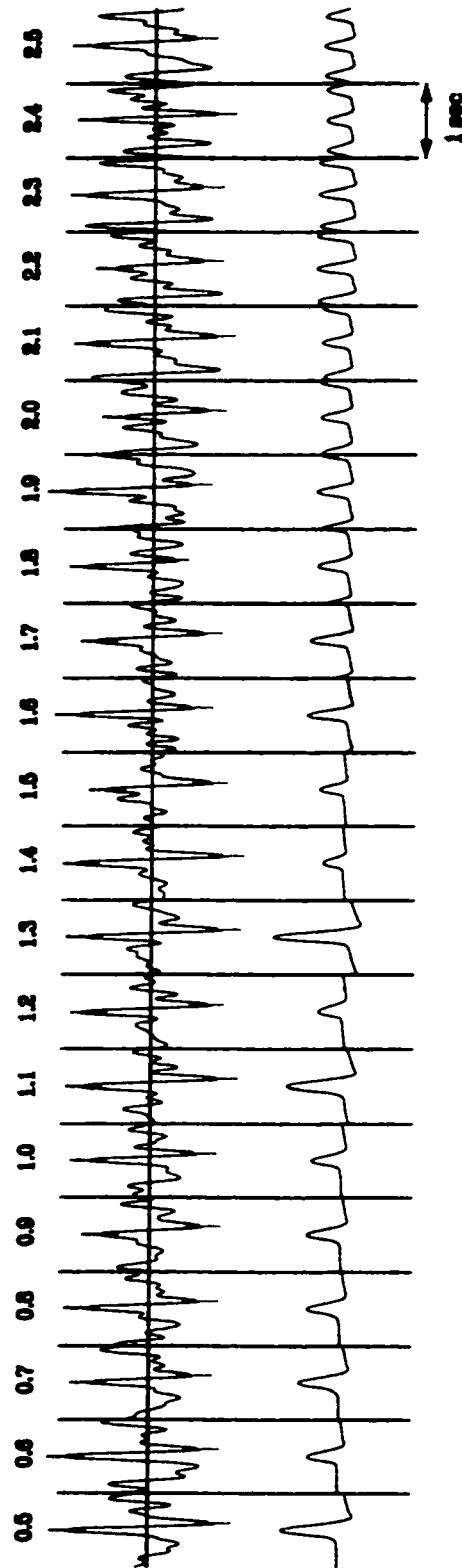
red solid line). For three of the subjects, this first MEF component was 2-3 times larger than the other two.

The latency of the first MEF peak is entirely consistent with the MEFI if extrapolated to the onset, rather than peak of the movement response. Likewise, the second and third peaks occur approximately 100 and 180 msec after this first peak which is consistent with the MEFII and the MEFIII. Also consistent are the polarity reversals characteristic of the latter two components. Together these results confirm the tight coupling between the emergence of the MEF pattern and the motor response during rhythmic movement [Kelso et al., 1998]. Furthermore, the timing of the MEF appears to depend on the biphasic response profile rather than response rate. In other words, its dynamics were unaffected by the length of time between successive responses for the entire range performed here (0.5-2.5 Hz). MEF amplitude also showed no dependence on response rate.

Figure 5.3 reveals that the second strongest field pattern was not only very coherent spatially but also topographically similar across subjects (see correlations in table 5.1, middle). This pattern was also central and dipolar but with the center of the dipole located approximately over the midline (figure 5.3, 2nd column). Though the proportion of ERF signal variance accounted for by this pattern was low for all subjects (ranging from 9.5 – 27.7%) we investigated its temporal dynamics to see whether it was affected by movement rate. Figure 5.5 shows the time-dependent amplitudes of this 2nd mode for all subjects (rows 1-4). Despite the noisier time series, two features are apparent. First, this pattern is strongest for slow movement rates. At approximately 1.0

126

Hz, the maximal peak-to-peak amplitude drops by more than half for all subjects and then plateaus for successive rate increases (figure 5.5, bottom). Second, at low movement rates there is a slow drift in the amplitude that is generally characterized by a strong polarity reversal near mid cycle (corresponding to the peak of the behavioral response).

In order to obtain a better description of the timing of this field pattern prior to each response, we reaveraged the data using a 2-sec window that extended from 1.5 sec before to 0.5 sec after the response peak. We then appended the ERFs from 0.5-1.0 Hz (where the amplitudes of this pattern were strongest) and did another KL-decomposition in order to extract the extended time-dependent amplitudes. Shown in figure 5.6 are the results from subject 4, for whom this field pattern accounted for the strongest proportion of total ERF signal variance (in fact this time it accounted for more than the MEF in this subject, again demonstrating its relative strength for slow movement frequencies). The time series in figure 5.6 were smoothed with a 60-msec moving window average in order to highlight the general amplitude trend. Red dashed lines demarcate the approximate point of movement onset. From the time series it is clear that this field pattern exhibited a gradual accumulation of amplitude until movement onset at which point there was a sharp and strong polarity reversal. As the interval between successive movements became smaller, the wave shapes became more oscillatory due to the alternating polarity reversals before/at and after each movement (figure 5.6). Beyond rates of 1.0 Hz no such slow oscillations were visible, reflecting the pattern's decreased amplitude.

Figure 5.5 (page 129): Temporal dynamics of the second strongest field pattern shown on the top for each of the four subjects. Rows 1-4 show the time-dependent amplitudes of this pattern for subjects 1-4, respectively. Vertical lines separate each frequency condition. Maximal absolute amplitude (normalized for each subject between 0 and 1) of the time-dependent amplitude is plotted as a function of required movement frequency on the bottom. The amplitude of this pattern was strongest for movement frequencies below 1.0 Hz.

Figure 5.6 (page 130): Time-dependent amplitudes of the second motor-related field pattern extended from 1.5 sec prior to 0.5 sec after the response peak. Below are the averaged response time series. Data shown are from subject 4 for whom this pattern was strongest. The red dashed line is provided as a visual guide to the approximate onset of movement. Amplitude is in arbitrary units although all six time series are plotted on the same amplitude scale.

Pattern Dynamics - 2nd KL Mode

Figure 5.5

Subj 4

$\lambda = .522$

0.5 Hz

0.6 Hz

0.7 Hz

0.8 Hz

0.9 Hz

1.0 Hz

2 sec
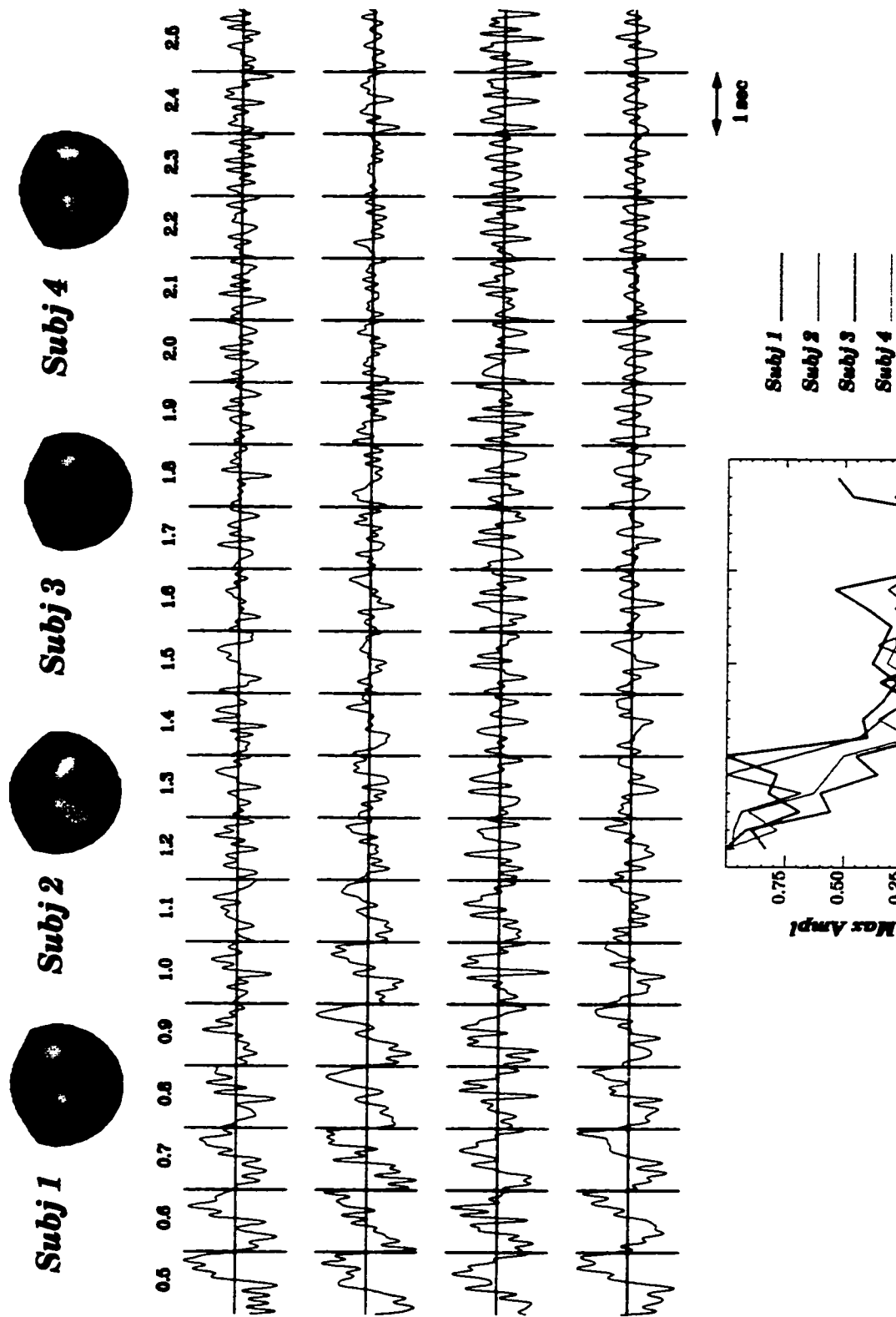
Figure 5.6
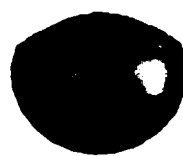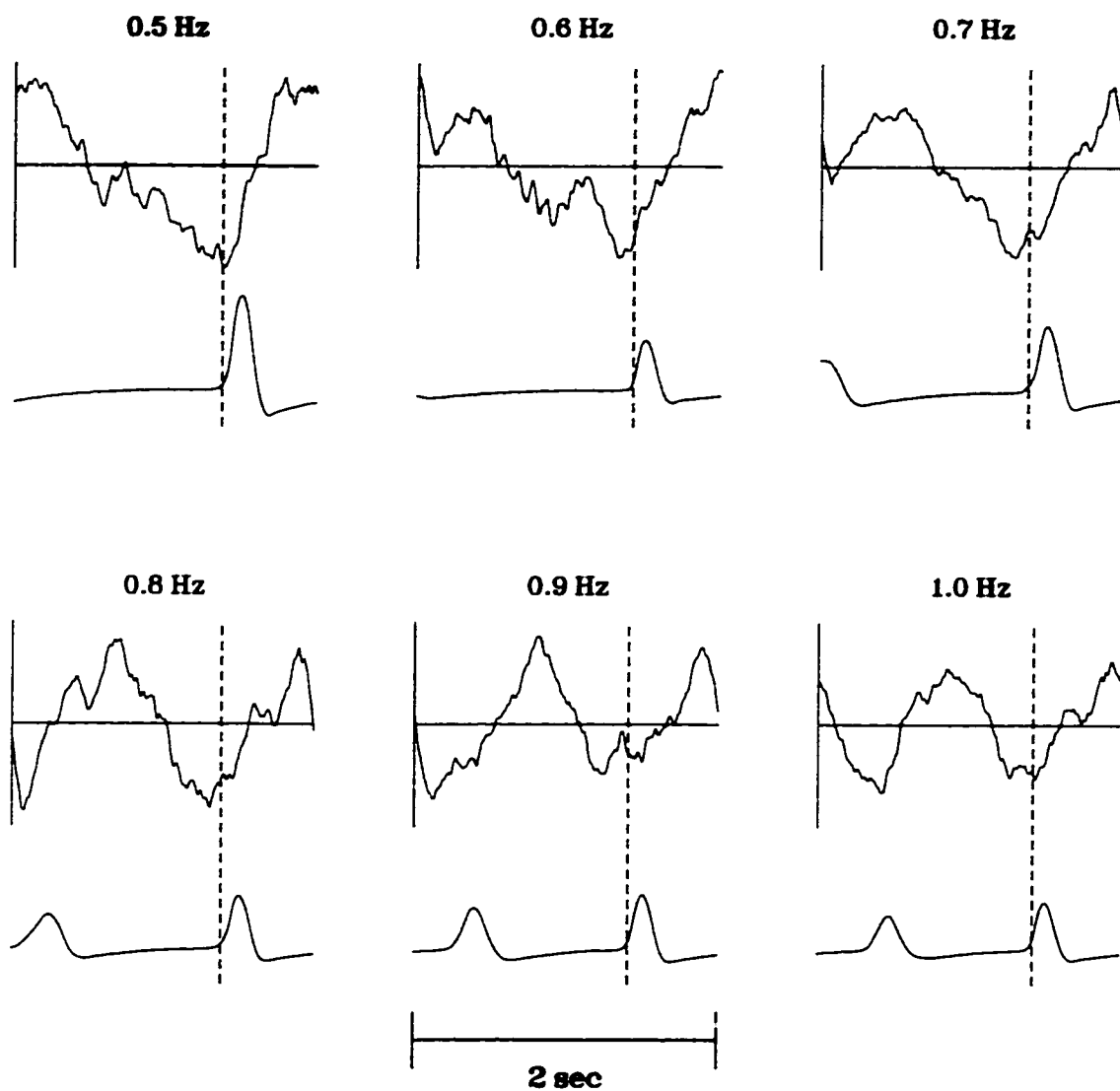
5.4 Discussion

This experiment demonstrates that the dominant neuromagnetic field pattern associated with rhythmic self-paced movement is a dipolar motor-evoked field restricted to the contralateral hemisphere and characterized by a reversal of field line direction in sensors located approximately over sensorimotor cortex. This field first emerges during the flexion phase of the movement and subsequently exhibits one or two changes in polarity depending on the subject. The initial field orientation is consistent with current flow pointing postero-laterally with a reversal in polarity originating from a net current in the opposite direction. The topography and temporal sequence of field reversals suggest they correspond to the movement-evoked fields, MEFI-MEFIII described previously for non-rhythmic, transient voluntary movements [Cheyne & Weinberg, 1989; Kristeva et al., 1991]. Also consistent with previous observations, the strongest component of the MEF observed here is the first peak to occur after movement onset. The later two components were weaker with two of the four subjects failing to show a second field reversal (the MEFIII).

Our main question concerned whether the dynamics of the MEF exhibited changes as a function of movement rate. The results clearly indicate that there is no rate-dependence for the MEF in terms of either peak latencies or amplitudes, at least for the broad range of frequencies tested here (0.5-2.5 Hz). Furthermore, our findings confirm a tight coupling between dynamics of the MEF and behavioral response as has been previously reported [Kelso et al., 1998] and theoretically modeled [Fuchs et al., 2000b]. Attempts to localize the MEF components using dipole estimates [Cheyne & Weinberg,

131

1989; Kristeva et al. 1991] and coregistration of field activity with MRI [Kristeva-Feige et al., 1994] suggest that the MEFI and III are generated in the post-central gyrus. A contribution of peripheral reafferent input to the generation of the MEFI has also been demonstrated [Kristeva-Feige et al., 1996; Cheyne et al., 1997]. In our study the MEFI and III occur shortly after maximal velocity in the flexion and extension directions, respectively. Together, these results suggest that it is reafferent information from these two muscle groups that generates the MEFI and III. A recent study by Holroyd et al. (1999) supports this conclusion. The latter work highlights the importance of a biphasic response for the generation of a second MEF field reversal (MEFIII) by showing its absence in situations where subjects flex and extend on alternating beats of a metronome.

In contrast to the MEFI and MEFIII, the first field reversal of the MEF (MEFII) has not been as successfully localized. Though MEFII appears to be confined to sources within the contralateral sensorimotor area, the primary input to such sources is not yet known. The timing relation between the MEFII and the response profile in this experiment suggests that it is does not reflect a motor command to the extensor muscles since in all four subjects the MEFII occurs simultaneously with or after maximal velocity in the extension direction and thus clearly after the onset of the extension phase of movement.

Interestingly, the temporal relation between the MEF complex and the response, though constant across movement rate, differed depending on subject. For the first two subjects, the MEFI occurred just after maximal velocity in the flexion direction whereas for the last two it occurred approximately 50 msec later coinciding with the point of peak

flexion (i.e. peak of the response). Similarly, whereas the MEFII emerged simultaneously with maximal velocity in the extension direction for subjects 1 and 2, it was delayed by approximately 20-30 msec in subjects 3 and 4. The two subject pairs also differed in the strength of the MEF, which was weaker in the latter two subjects (accounting for 45.6 and 32.0% of the total signal variance as compared to 70.8 and 62.2% for subjects 1 and 2). Moreover, whereas all three MEF components were identifiable for subjects 1 and 2, subjects 3 and 4 only showed two. Individual differences in cortical morphology (e.g. dipole orientation) could account for the relative attenuation of the MEF complex in subjects 3 and 4 but it is unclear how such differences could lead to temporal delays in observable MEF components. Another possibility that cannot be ruled out is that the control of rhythmic movement is handled differently by the nervous system in the two pairs of subjects, e.g. coordinating motor trajectories with respect to movement speed versus movement amplitude. Even under the assumption that the MEFI reflects reafferent information from the periphery [Kristeva-Feige et al., 1994; Cheyne et al., 1997], such information may be used differently in the ongoing modulation of motor behavior for different subjects.

A second question addressed by this experiment was whether other motor-related fields associated with rhythmic movement can be detected when no external pacing stimulus is present. Here we found a second weaker field not previously observed in studies on rhythmic sensori-motor coordination [e.g. Kelso et al., 1998; Fuchs et al., 2000c; Mayville et al., submitted] that was very coherent spatially and similar in topography across subjects. The time dependent amplitudes of this field were also

similar across subjects for movement rates below 1.1 Hz and can be described as a slow modulation of amplitude that becomes increasingly oscillatory as the interval between successive responses gets smaller. Both the topography and temporal dynamics of the second field suggest that it corresponds to the readiness field which occurs in the foreperiod of non-rhythmic voluntary movements separated by long intervals (>3 sec) [Deecke et al., 1982, 1983; Hari et al., 1983, Cheyne & Weinberg, 1989].

Spatially this second field was characterized by maximal field lines entering in the central portion of one hemisphere and exiting in the other. Specifically, prior to movement, field lines entered on the right side and exited on the left (indicated by the negative time dependent amplitudes in figure 5.5). After movement onset, the directions reversed. If the opposing field line directions in the two hemispheres are assumed to be the center of a single dipole then these time-dependent polarity changes are consistent with an anteriorly directed current source prior to movement and a posteriorly directed current source after. Moreover, the lateral separation of the opposing field lines on the head surface suggests that such a source would be relatively deep. In a recent MEG study, Erdler et al. (2000) report that there is an early readiness or Bereitschaftsfeld (BF 1) preceding the onset of a complex movement sequence which is approximated by a single anteriorly directed dipole located in the SMA. They hypothesize that this may actually reflect two slightly antiparallel, bilateral SMA sources whose fields are partially cancelled because the sources are in close proximity to one another (e.g. on immediately opposing surfaces of the interhemispheric fissure). The authors also suggest that the detection of pre-movement SMA activity in MEG may require a motor task that is

sufficiently complex. The paradigm used in the present experiment is arguably more complex than simple finger flexion separated by long intervals (>3 sec) which is not typically associated with pre-movement magnetic fields generated within the SMA. First, subjects moved rhythmically and second, they were attempting to maintain a given rate of movement as required by the task condition.

Alternatively, the second field observed in this experiment could relate to the readiness field originally reported for simple, transient finger flexion [Deecke et al., 1982, 1983; Cheyne & Weinberg, 1989; Kristeva et al., 1991]. This readiness field (termed the BF 2 by Erdler et al., 2000) is distinguished from the BF 1 in both its onset (which is approximately 1 sec prior to movement onset as opposed to about 2 sec for the BF 1) and estimated source locations which are the bilateral sensorimotor cortices and not the SMA. Indeed, the topographic patterns for subjects 2 and 3 does suggest that there may actually be two more laterally located dipoles, one in each hemisphere, although a comparison of columns 1 and 2 in figure 5.3 reveals that these are not in the same location as the MEF which presumably originates in contralateral sensorimotor cortex.

It was difficult to quantitatively characterize the temporal dynamics of the second field because of its relatively low signal-to-noise ratio, possibly due to the hi-pass filter setting used (0.3 Hz) which is higher than typically used for recording slow changes in brain/cortical activity. Furthermore, given the rhythmic nature of the movement in this task, it is not possible to separate pre- from post-movement periods since post-response periods are obviously also pre-response periods for the succeeding movement.

135

Nevertheless the gradual accumulation of field amplitude prior to movements separated by 2.0 sec (see figure 5.6, 0.5 Hz movement rate) is consistent with the readiness field that occurs prior to simple, voluntary movements separated by long intervals (>3 sec). The latter has been shown to start building up approximately one second prior to the onset of movement [Deecke et al., 1982, 1983; Cheyne & Weinberg, 1989; Kristeva et al., 1991].

In our experiment the amplitude of this second field pattern drops sharply once the movement rate exceeds about 1.0 Hz thus constraining the duration between successive movements below one second. If the second motor field we observe does reflect planning/preparatory processes associated with rhythmic movement, an interesting question is whether or not its rate-dependent amplitude decrease has any functional consequences for the organization of motor behavior. This might be expected if the sources which generate it are part of motor planning and/or initiation mechanisms as has been proposed for the readiness potential preceding voluntary movement in EEG [Kornhuber & Deecke, 1965; Barrett et al., 1986; Kornhuber et al., 1989]. While there were no observable consequences in this experiment (i.e. subjects were able to internally pace their movements equally well across all 21 rates), it is well known that the ability to coordinate finger movement with an external metronome depends crucially on rate. For example, Engström et al. (1996) observed that, for metronome rates exceeding 1.0 Hz, subjects switched from a reactive coordinative pattern to an anticipatory one in which their responses preceded each metronome beat. This occurred despite the fact that subjects were specifically instructed only to react to each metronome beat. Likewise

between-beat timing patterns are also typically only stable if the rate of coordination is below about 2 Hz, beyond which subjects switch to synchronization [Kelso et al., 1990]. It is possible, therefore, that changes in the strength of this field reflect underlying rate-dependent changes in motor planning mechanisms that play a role in known transitions in sensory-motor coordination.

In conclusion, we found that rhythmic self-paced finger movement is associated with a pair of neuromagnetic field patterns. The first and strongest of the two is consistent with the MEF previously observed for voluntary movement. The temporal dynamics of the MEF components depend solely on the response profile and *not* the interval between successive movements (for movement rates between 0.5 and 2.5 Hz). In contrast, the amplitude of the second field pattern drops by more than half when the movement rate exceeds 1.0 Hz (inter-response intervals < 1 sec). At lower rates the amplitude of this pattern exhibits a slow gradual accumulation suggestive fields previously associated with motor preparation. This decrease may signify changes in the degree of planning necessary to move rhythmically at faster and faster rates. The striking similarity of the two principal field patterns and their corresponding time-dependent amplitudes across subjects illustrates the robustness of the spatiotemporal dynamics of MEG activity associated with rhythmic self-paced movement.

6.0 Experiment 5: Differences in cortical and subcortical networks associated with syncopated versus synchronized coordinative timing patterns as revealed with fMRI

6.1 Introduction

A key aspect of any motor control task is timing. This experiment examined human brain activation associated with two distinct timing relations in sensorimotor coordination. Specifically we used functional magnetic resonance imaging (fMRI) to investigate the BOLD (blood oxygen level dependent contrast) effect associated with both syncopated (off-the-beat) and synchronized (on-the-beat) modes of sensorimotor coordination. Whereas a synchronized mode of coordination is typically established very rapidly if the metronome frequency is within a range that one would normally call rhythmic (~0.6-4.0 Hz), syncopated patterns are much more difficult and can typically only be performed successfully for lower rhythmic rates (<2.0 Hz) [Fraisse, 1982; Kelso et al., 1990].

Recent investigations with both electroencephalography (EEG) and magnetoencephalography (MEG) have addressed the issue of whether differences between the two timing strategies translate into distinct patterns of neural activity. Mayville et al. (1999) showed that event-related potentials recorded from sites approximately overlying contralateral sensorimotor cortex were significantly stronger during performance of syncopated versus synchronized auditory-motor coordination.

Differences in sensorimotor cortex are also suggested by investigations of neuromagnetic brain rhythms. MEG signal power in the beta (15-30 Hz) frequency range was shown to be significantly weaker in contralateral central sensors, indicating a relative suppression of the sensorimotor beta rhythm for syncopated movement [Mayville et al., submitted]. Interestingly, the same effect was observed when subjects only imagined syncopating and synchronizing with an auditory metronome [Mayville et al., in preparation] suggesting that the underlying neural mechanism is dependent upon the timing strategy itself and not the execution of movement. Furthermore, comparison between overt and imagined syncopation revealed consistently significant differences in the neuromagnetic beta rhythm in lateral and medial precentral sensors of both hemispheres. In contrast, the same comparison for synchronization revealed similar effects in only one of the subjects, raising the question of whether premotor areas are also differentially involved in on versus off-the-beat coordination [Mayville et al., in preparation].

A long line of research associates premotor function with preparatory as opposed to executive motor processes [e.g. Kornhuber & Deecke, 1965; Roland et al., 1980; Deecke et al., 1985; Barrett et al., 1986; Lang et al., 1989]. One hypothesis is that the relative difficulty of off-the-beat timing patterns places additional demands on motor planning mechanisms. If this is true one might expect to see enhanced activation of premotor areas during the performance of syncopated relative to synchronized sensory-motor coordination.

The dependence of activity in subcortical brain areas on the timing relation between stimulus and response in rhythmic coordination is not known. Previous studies

employing visual and auditory metronomes indicate that the ipsilateral cerebellum is required to synchronize one's movement to external pacing stimuli [Larsson et al., 1996; Lejeune et al., 1997; Rao et al., 1997; Penhune et al., 1998]. The latter study also found activation in the basal ganglia. This is not surprising given the large body of literature which implicates both of these structures in timing processes on motor and perceptual levels [e.g. Ivry et al., 1988; Ivry & Keele, 1989; Harrington et al., 1998; Malapani et al., 1998; Penhune et al., 1998; Harrington & Haaland, 1999; Schubotz et al., 2000]. An interesting question is whether or not placing one's movement in between successive stimuli involves these areas to a different degree. Preliminary work in our lab using fMRI to investigate cerebellar function in syncopation and synchronization timing tasks indeed suggests that the cerebellum is more active when subjects move off the beat [Fuchs et al., 1999]. However, this study only examined four to eight coronal slices primarily covering the cerebellum and not extending far enough in the anterior direction to encompass the basal ganglia or frontal cortical areas (including premotor cortex). In the present experiment we sampled the entire brain volume using 20 axial slices that covered the entire superior-inferior and anterior-posterior range of cortical and subcortical tissue.

6.2 Methods

6.21 Subjects

9 subjects (5 male, 4 female) participated in this experiment. Subjects' ages ranged from 20-41. All subjects were right-handed according to self-report. Informed

consent was obtained from each subject prior to any data collection. This experiment conformed to all ethical standards regarding research with human subjects.

6.22 Task Conditions

Subjects performed a rhythmic coordination task that involved squeezing a pillow between their right index finger and thumb in time with an auditory metronome at 1.25 Hz. Two different timing relations were examined: syncopation (between successive beats) and synchronization (on each beat). In addition, there were two control conditions, an auditory control in which subjects only listened to the metronome and a self-paced motor control in which they attempted to squeeze the pillow at a rate of 1.25 Hz in the absence of the metronome.

Each condition was collected as a block of 4 contiguous trials where one trial consisted of 30 seconds of rest (**OFF** period) followed by 30 seconds of task performance (**ON** period) (figure 6.1). In the coordination and auditory-only conditions, subjects were cued to begin the **ON** period simply by the onset of the metronome. Likewise, the start of each **OFF** period was signaled by the stop of the metronome. For the motor-only control, the experimenter cued subjects from the control room with the words "move" and "rest" for the **ON** and **OFF** periods, respectively.

All subjects performed the control conditions first. The auditory preceded the motor control so that subjects would know from the auditory condition how fast to pace their movement. The order of the coordination conditions was balanced across subjects such that half performed the syncopation task first and the other half did synchronization first. Subjects were given breaks between each condition as needed.

6.23 Task Instructions

For the coordination conditions, subjects were instructed to perform the timing relation prescribed by the task condition as best they could when the metronome was on. They were further told to try and maintain the target timing relation *at all times*; if they felt themselves losing the correct pattern they should try to regain it rather than adopt a different mode of timing. Finally they were instructed not to think about the task at all during each **OFF** period (e.g. worry about how well they did) and to avoid preparing for the next **ON** period (e.g. by readjusting their grip on the pillow). The latter instruction was given prior to each motor control as well. In the auditory control, subjects were told to think of it as an exercise in selective attention and to do their best to attend to the sound of the metronome over the background magnet noise.

6.24 Experimental Procedure

Subjects performed each task condition with their eyes closed. All subjects were given earplugs in order to minimize interference from the scanner noise. The metronome was delivered via plastic headphones designed for use with MRI (Avotec Inc., Stuart, FL). The volume of the metronome was maximal for all subjects in order to be clearly distinguishable from the magnet – none of the subjects reported this to be uncomfortable. Response signals were measured as changes in air pressure in the pillow that were subsequently transduced into a voltage signal and then recorded with a computer located outside the scanner room. The metronome signal was simultaneously recorded so that subjects' success at performing the different timing relations could be assessed. Both metronome and response signals were sampled at a rate of 500 Hz.

6.25 Image Acquisition

Structural and functional MR images were acquired using a 1.5 Tesla MR scanner (General Electric, Milwaukee, WI) equipped with real-time image processing capability. Full-head 3D anatomical scans were collected at the beginning of each session. These were 256×256 T1-weighted axial images collected with a gradient echo SPGR pulse sequence. Sequence parameters were TE=5.0 msec, TR=34 msec, flip angle=45°, bandwidth=15.63 Hz. The field of view and total number of slices (2.0 mm thick) was adjusted for each subject. High-resolution 256×256 background images were then collected for 20 axial slices (5.0 mm thick, 2.5 mm apart) placed so as to cover the entire brain volume, including the cerebellum. These were collected using a 2D gradient echo SPGR pulse sequence with the parameters TE=in phase, TR=325 msec, flip angle=90°, bandwidth=15.63 Hz. These background images were used for real-time display of fMRI data during collection and then later in order to coregister fMRI images to each subjects' full-head structural scan. During the experiment, fMRI images were acquired at the same 20 slice locations with the following gradient echo EPI sequence: TE= 60 msec, TR=3 sec, flip angle=90°, bandwidth=62.5 Hz. The field of view for both background and fMRI images was 240 mm. The resolution of each fMRI image was 64×64 yielding a voxel dimension of 3.75mm × 3.75mm × 7.5mm. Each fMRI series began with 4 baseline images (12 sec) to obtain signal equilibrium and an initial baseline state, followed by 80 images per slice location corresponding to 10 images for each OFF and ON period.

6.26 Image Analysis

The first stage of image analysis was to coregister the high-resolution background images to the 3D full head scan using SPM99 [Friston et al., 1995]. The resulting transformation matrix was applied when fMRI data was imported into the AFNI (Analysis of Functional Neuroimages; Cox, 1996; Cox & Hyde, 1997) analysis package through which all subsequent analyses were carried out.

Prior to analyzing fMRI time series, the full-head scan was transformed into Talairach space [Talairach & Tournoux, 1988] and interpolated to 1 mm cubic voxels. The analysis of each fMRI data set proceeded as follows. First, each set was corrected for head motion. Graphs of head motion were inspected by eye prior to correction to ensure that it never exceeded 2 mm. Second, we assessed task-related activity on a voxel by voxel basis by correlating each voxel time series with a square wave representing the sequence of task periods (figure 6.1, bottom time series). To minimize effects of the hemodynamic response rise/fall time only the final 8 images within each OFF or ON period were included. All voxels for which the correlation coefficient was greater than 0.5 were defined as task-dependent (see also caption, figure 6.1). Third, the correlated data sets were transformed into Talairach space (again yielding 1 mm cubic voxels). Finally each of the functional volumes was blurred (FWHM=4 mm) and clustered (minimum 2 mm radius, 1000 μl volume).

A within-subjects ANOVA was performed on each voxel in the full three-dimensional volume to determine significant differences between conditions. The dependent variable for each voxel was an intensity measure that was proportional to the

Figure 6.1 (page 146): Measuring task-related activity with fMRI. The top two rows illustrate the design of a typical block fMRI experiment which is composed of alternating periods of rest (**OFF**) and task performance (**ON**), each period lasting 30 seconds (total time per condition = 4 minutes). Shown in the second row is a typical sample of behavioral performance in the Syncopate task at 1.25 Hz: the black line shows the auditory metronome and the blue line the subject's response. In the third row is an example of a time series from a single voxel that showed task-related amplitude modulation. The degree of task-related activity was assessed by correlating each voxel time series with a square wave (row 4) that corresponds to the sequence of **OFF** and **ON** periods. Green dots indicate which of the sampled images were included in the correlation; the first two in each period were excluded to account for the hemodynamic rise/fall time. On the bottom is a typical activation pattern for right-hand finger movement. Plotted in red/yellow are voxels for which the correlation coefficient exceeded 0.5 (thus indicating task-related activation). The strength of activation was defined as the amount of total signal variance accounted for by the task-related square wave (regression coefficient) and corresponds to the exact color plotted with yellow indicating a higher degree of task-related amplitude modulation.

Ant

Right   Left

146

Figure 6.1
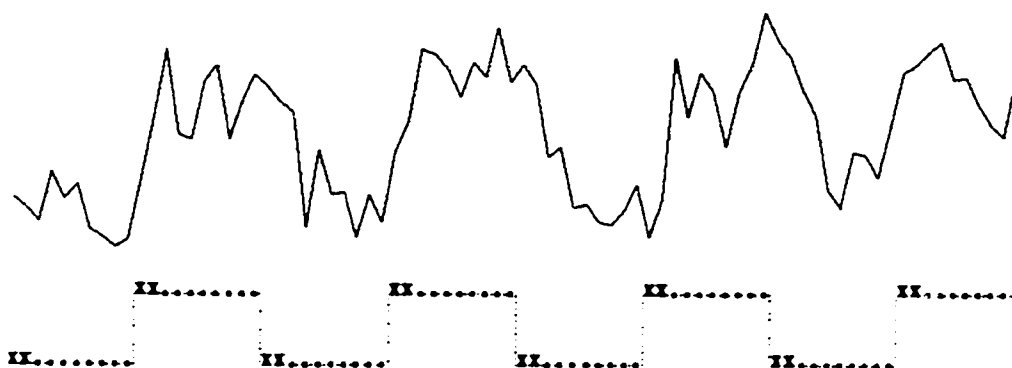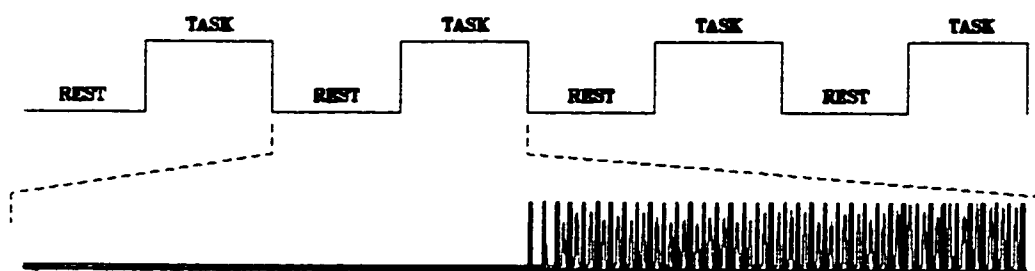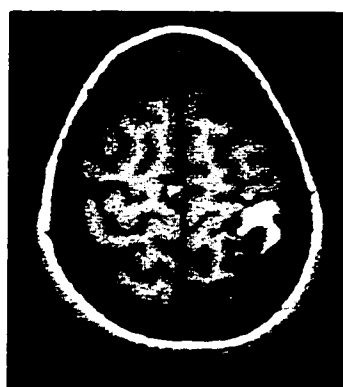
amplitude difference between **OFF** and **ON** periods (see AFNI manual for details). For all voxels that were not defined as task-dependent this value was set to zero. Differences between pairs of conditions (normalized by the pooled error variance from the overall ANOVA) were then examined post-hoc. Such differences fall off with the Student's t-distribution (see AFNI manual for details). Therefore, where shown, difference maps contain t-values that indicate how significantly a given voxel's activation differed between the two conditions. The threshold significance level was set to 0.01 for all parametric maps (i.e. all colored voxels exceeded this level).

6.3 Results

6.31 Task Performance

Subjects' performance in the coordination conditions was assessed on a cycle-by-cycle basis by calculating the relative phase between each response peak (defined as the point of maximal pressure) and the onset of the preceding metronome beat. All subjects were successfully able to both syncopate (180° phase) and synchronize (0° phase) with the auditory metronome (figure 6.2, top). Grand average relative phase values were 176.3° ± 35.2° and 10.3° ± 32.8° for the Syncopate and Synchronize conditions, respectively.

6.32 Syncopated vs. Synchronized Coordination

6.321 Areas of Primary Interest

The main goal of this experiment was to investigate whether a different array of brain areas are involved when subjects perform off-the-beat as opposed to synchronized coordinative timing patterns. Our initial focus was on cortical and subcortical areas that
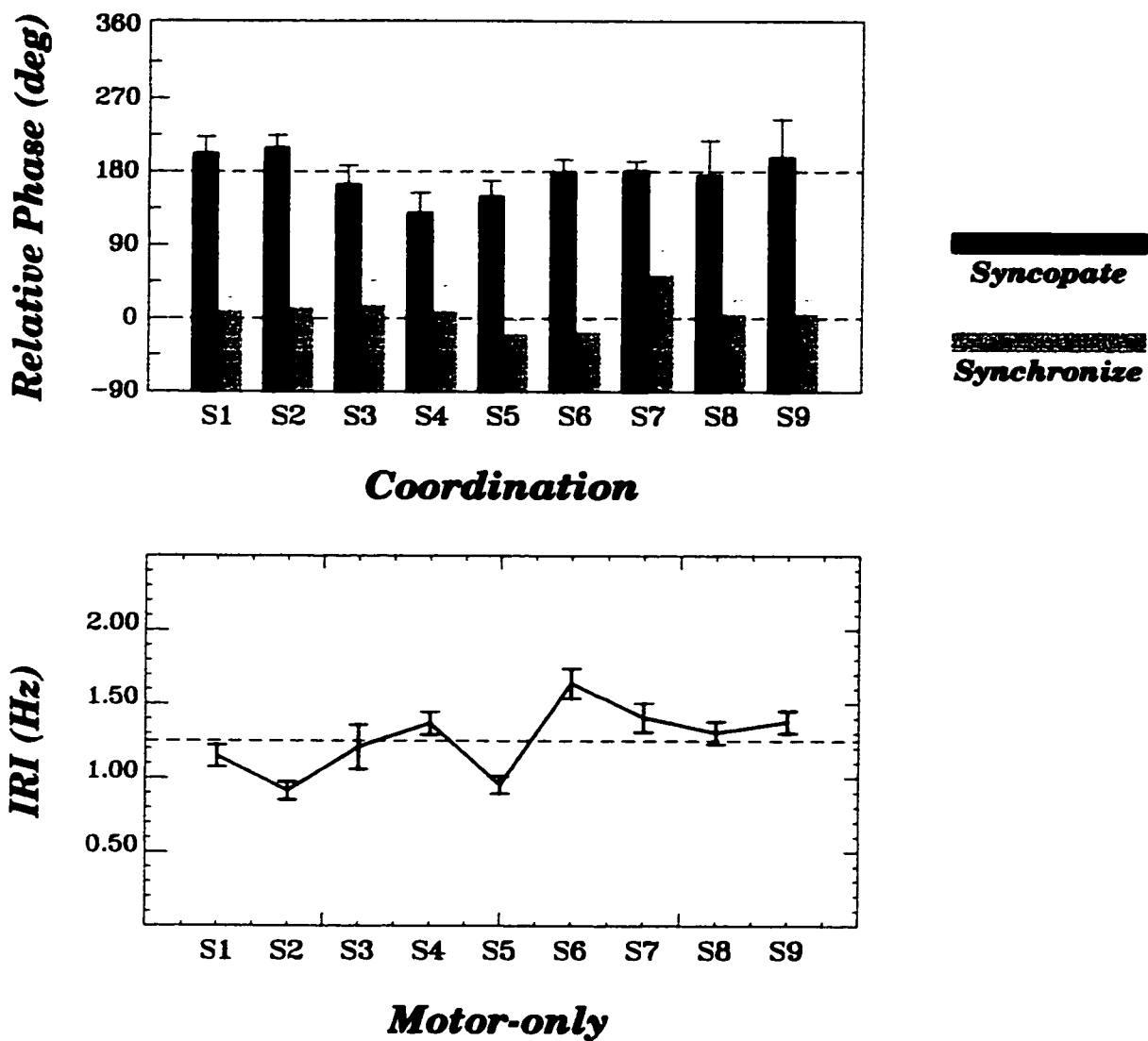
Figure 6.2: Individual subject performance on the coordination (top) and motor-only tasks (bottom). For the coordination conditions, bars indicate the mean relative phase between the peak of the response (maximal pressure) and onset of each metronome beat; lines indicate one standard deviation. For the motor-only task, the mean inter-response interval (IRI), expressed in Hz, is shown across subjects; again vertical lines represent one standard deviation.

Figure 6.2

are known to be crucial for motor control and/or timing. In the neocortex these include sensorimotor cortex as well as premotor areas (dorsolateral premotor cortex and the SMA). Subcortically there are the basal ganglia, cerebellum, and thalamic nuclei to which they are interconnected. With the exception of sensorimotor cortex, all of these areas were found to have stronger activation during syncopated as compared to synchronized coordination (figures 6.3a-c and table 6.1). No areas showed differences in the opposite direction (i.e. more active during synchronization). Talairach coordinates for all regions discussed below are contained in table 6.1.

Starting at the superior surface, both left and right dorsolateral premotor cortices (middle frontal gyrus – Brodmann's area 6) showed regions of significantly increased activation during syncopated coordination (figure 6.3a, yellow arrows). A single region in the left SMA (superior frontal gyrus, Brodmann's area 6) was also identified (figure 6.3a, blue arrows). It was unclear if these premotor areas were recruited only for syncopation or whether they were involved in both timing patterns but more strongly during syncopation. In order to answer this question we examined maps of activation for both coordination conditions independently for each subject. Only four of the nine subjects showed task-related signal modulation in either dorsolateral premotor cortex when performing the synchronization task (table 6.3) in contrast to eight subjects for syncopation. Furthermore, though synchronization was associated with activation of the SMA, this activity was localized to more posterior areas (difference in y direction=21 mm) whereas syncopated movement involved these same regions and an additional

Figure 6.3 (pages 151-153): Significant differences between the Syncopate and Synchronize conditions in the principal brain areas concerned with motor-control and or timing (see also tables 6.1 and 6.3). Colored voxels represent those for which the two conditions differed with a confidence level of $\alpha=.01$. All differences were positive (red/orange) corresponding to stronger task-related signals during the Syncopate condition. **6.3a**: Premotor areas, including dorsolateral premotor cortex (Brodmann's area 6) and SMA. Note the lack of differences in the primary sensorimotor areas. **6.3b**: Basal ganglia (striatum) and thalamus (ventral anterior nucleus). **6.3c**: Cerebellum. Bd: Brodmann's area. Orientation for axial or coronal slices: left side – right hemisphere, right side – left hemisphere; slice location along the superior-inferior or anterior-posterior axis is indicated below. For sagittal slices: left side – anterior, right side – posterior; slice location along the right-left axis is indicated below.

Premotor / SMA

Dorsolateral premotor (Bd 6) → 52 S ← Dorsolateral premotor (Bd 6)

SMA (Bd 6)

-6 A
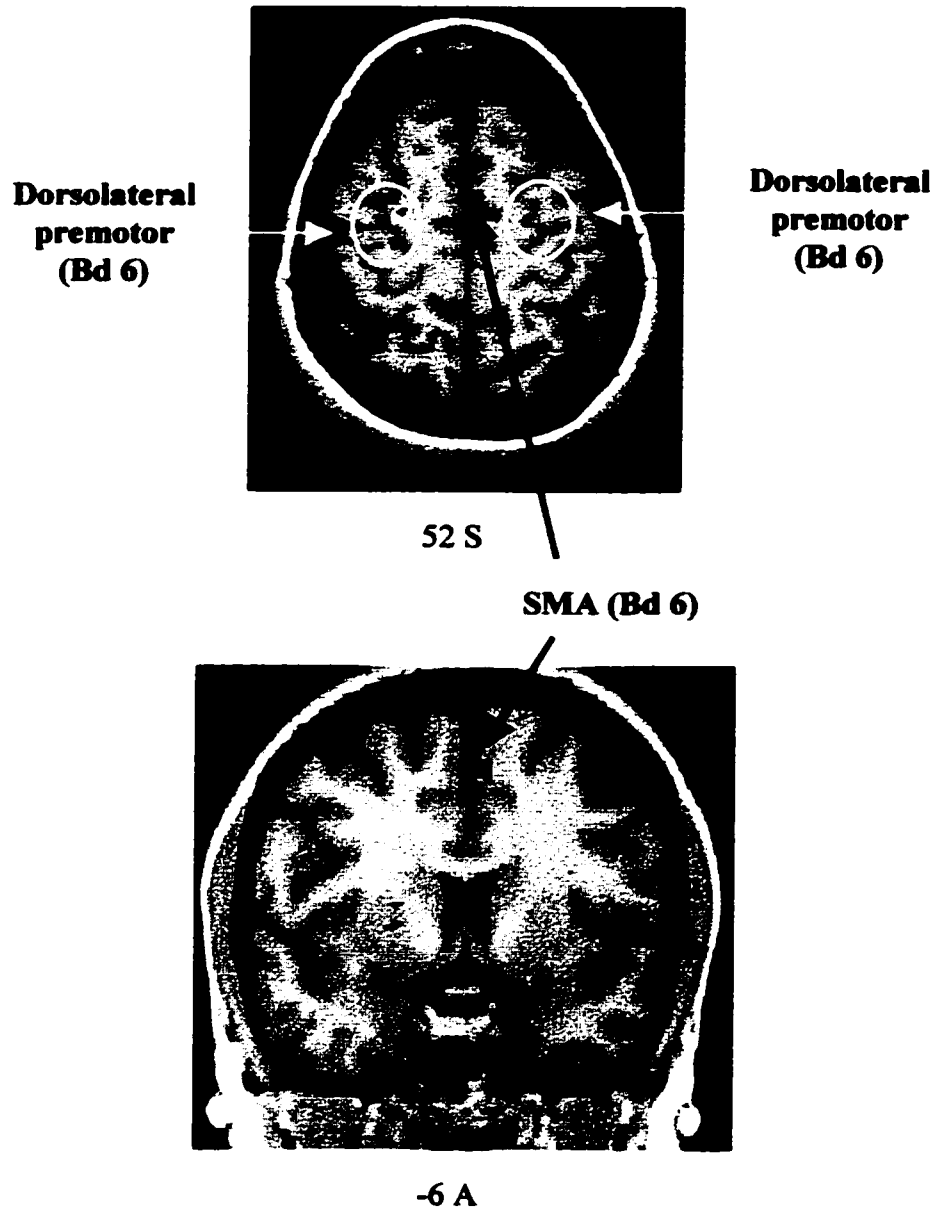
Figure 6.3a

Basal Ganglia / Thalamus

Caudate N

Caudate N

Caudate N

Putamen

Ventral
Ant N

9 S

11 S

Putamen

Caudate N

-16 R

Figure 6.3b

Cerebellum

Ant Lobe
Culmen

-20 I

Post Lobe
Tonsil

-34 I

-47 I

-51 I

153
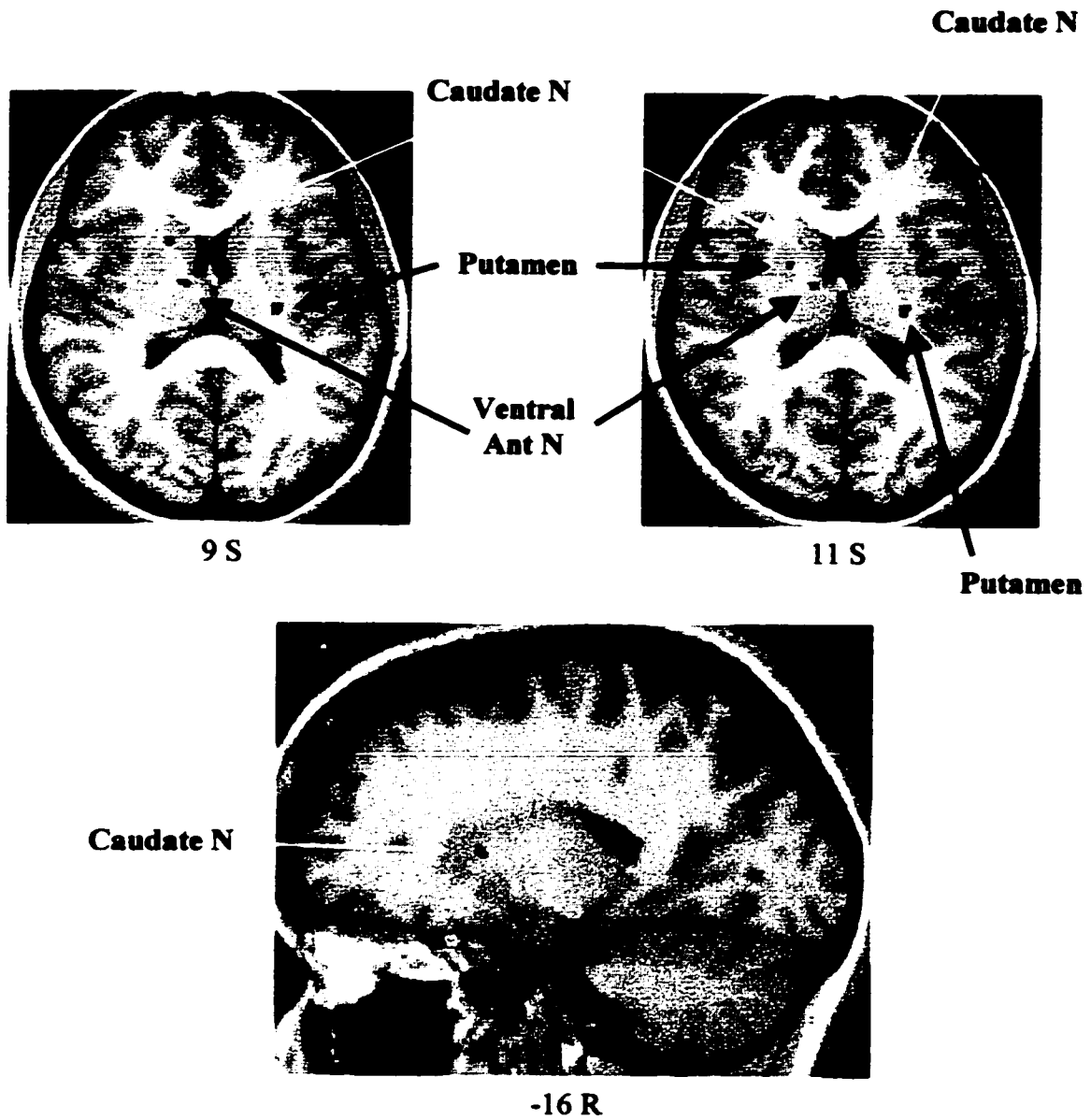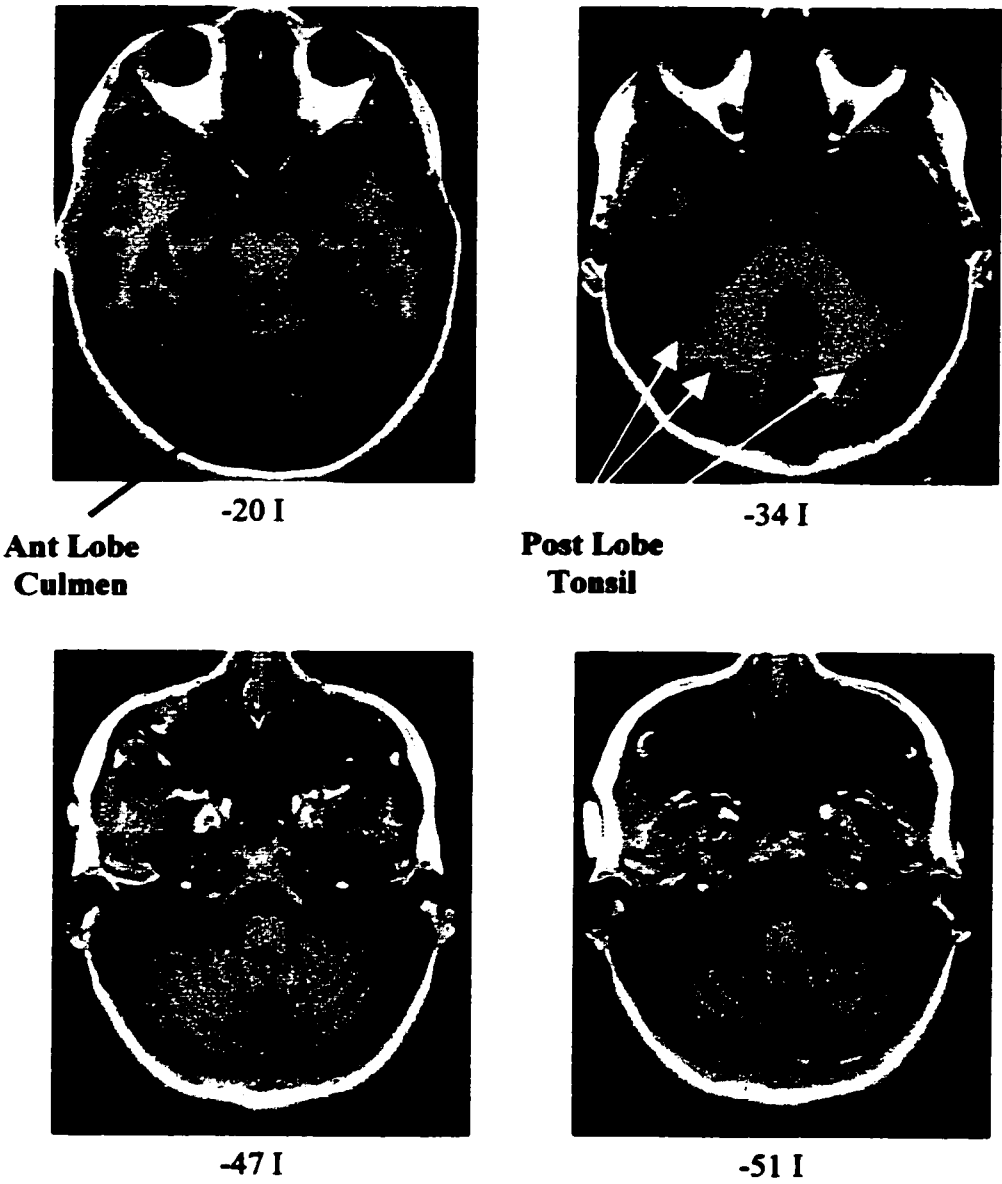
Figure 6.3c

region in the left anterior SMA. Together these results indicate that, on average, syncopation requires additional premotor areas.

Table 6.1: *Areas of Primary Interest*

	Left	*Right*
Sensorimotor Cortex (Bd 1-4)	*None*	*None*
Premotor Cortex (Bd 6)		
Middle Frontal Gyrus	-25L -1P 52S -29L -7P 52S	26R -13P 52S 30R -4P 52S 23R 0 52S
Superior Frontal Gyrus (SMA)	-4L 6A 52S	*None*
Basal Ganglia		
Caudate Nucleus	-13L 18A 11S	16R 15A 10S
Putamen	-27L -14P 9S	21R 6A 5S
Thalamus		
Ventral Anterior Nucleus	*None*	11R -4P 8S
Cerebellum		
Anterior Lobe – Culmen	-22L -57P -20I	*None*
Posterior Lobe – Tonsil	-30L -62P -34I	39R -45P -34I 20R -59P -34I
Deep	*None*	35R -43P -47I 5R -68P -47I 35R -43P -51I 18R -49P -51I 18R -60P -51I

Within the basal ganglia, bilateral differences were observed in the striatum. Voxel clusters in both the caudate nucleus and putamen (figure 6.3b, blue and yellow arrows, respectively) showed increases in activation during syncopation. In addition, we identified a region in the right ventral anterior nucleus of the thalamus (figure 6.3b, green

arrows). This area receives major projections from the basal ganglia and projects to motor and premotor areas of the neocortex [Alexander et al., 1986]. As with the areas identified within the dorsolateral premotor cortex, these nuclei showed task-related activation during the Synchronize condition for three subjects only as compared to 8 for the Syncopate condition, indicating that they are more strongly involved during performance of a syncopated timing pattern.

The last area of primary interest was the cerebellum. Shown in figure 6.3c are the corresponding difference maps for four separate axial slices encompassing the cerebellar lobes. Syncopation was associated with clusters of increased activation distributed throughout the entire inferior-superior extent of the cerebellum. These clusters were primarily localized to the right (ipsilateral) hemisphere (figure 6.3c, top right and bottom two panels) although a few contralateral clusters were also observed in the more superior slices (top two panels). The corresponding anatomical location of the most inferior cerebellar clusters (bottom two panels) could not be identified due to limitations of the Talairach atlas. Superiorly, significant clusters were located within the posterior lobe (tonsil) and anterior lobe (culmen). The latter were restricted to the contralateral hemisphere. Further examination revealed that cerebellar activity was present for both the Syncopate and Synchronize conditions (table 6.3). However, during synchronization it was generally restricted to only a few clusters in the contralateral hemisphere whereas syncopated coordination resulted in relatively larger and more numerous areas of cerebellar activation in both hemispheres.

6.322 Other Areas of Interest

In addition to the areas of primary interest discussed above, we observed rather large clusters of voxels in several other frontal and temporal areas that also showed significantly stronger activation during syncopation (table 6.2). Prefrontally, syncopation was associated with activity in Brodmann's area 10, both in the left superior (figure 6.4a, yellow arrows) and right middle (figure 6.4a, green arrows) gyri. In addition, a cluster in Brodmann's area 46 in the left middle frontal gyrus (figure 6.4a, blue arrow) was found. Other frontal areas that were involved in syncopated coordination include the left insula (figure 6.4b, yellow arrows) and the right inferior frontal cortex (Brodmann's area 47, figure 6.4b, pink arrow). Within the temporal lobes several clusters were localized to the anterior part of Brodmann's area 22 in the left superior temporal gyrus (figure 6.4b, blue arrow). A second region in the right posterior middle temporal gyrus was also identified as Brodmann's area 22 (figure 6.4b, green arrow). None of these frontal or temporal areas showed task-related activation in the synchronize condition. Talairach coordinates corresponding to the approximate center of each cluster are listed in table 6.2.

Figure 6.4 (pages 158-159): Same as figure 6.3 but for other areas which were significantly affected by the mode of coordination (see also table 6.2). 6.4a: Prefrontal areas. 6.4b: Other frontal and temporal areas, including the insula, inferior frontal gyrus (Brodmann's area 47), superior temporal gyrus (Brodmann's area 22), and the middle temporal gyrus. Again, all areas showed increased activation during syncopation. Bd: Brodmann's area. Orientation for axial or coronal slices: left side – right hemisphere, right side – left hemisphere; slice location along the superior-inferior or anterior-posterior axis is indicated below. For sagittal slices: left side – anterior, right side – posterior; slice location along the right-left axis is indicated below.

Prefrontal

Sup Frontal
Gyrus
(Bd 10)

Mid Frontal
Gyrus
(Bd 46)

24 S

Mid Frontal
Gyrus
(Bd 10)

34 S

Sup Frontal
Gyrus
(Bd 10)

-42 A

Figure 6.4a
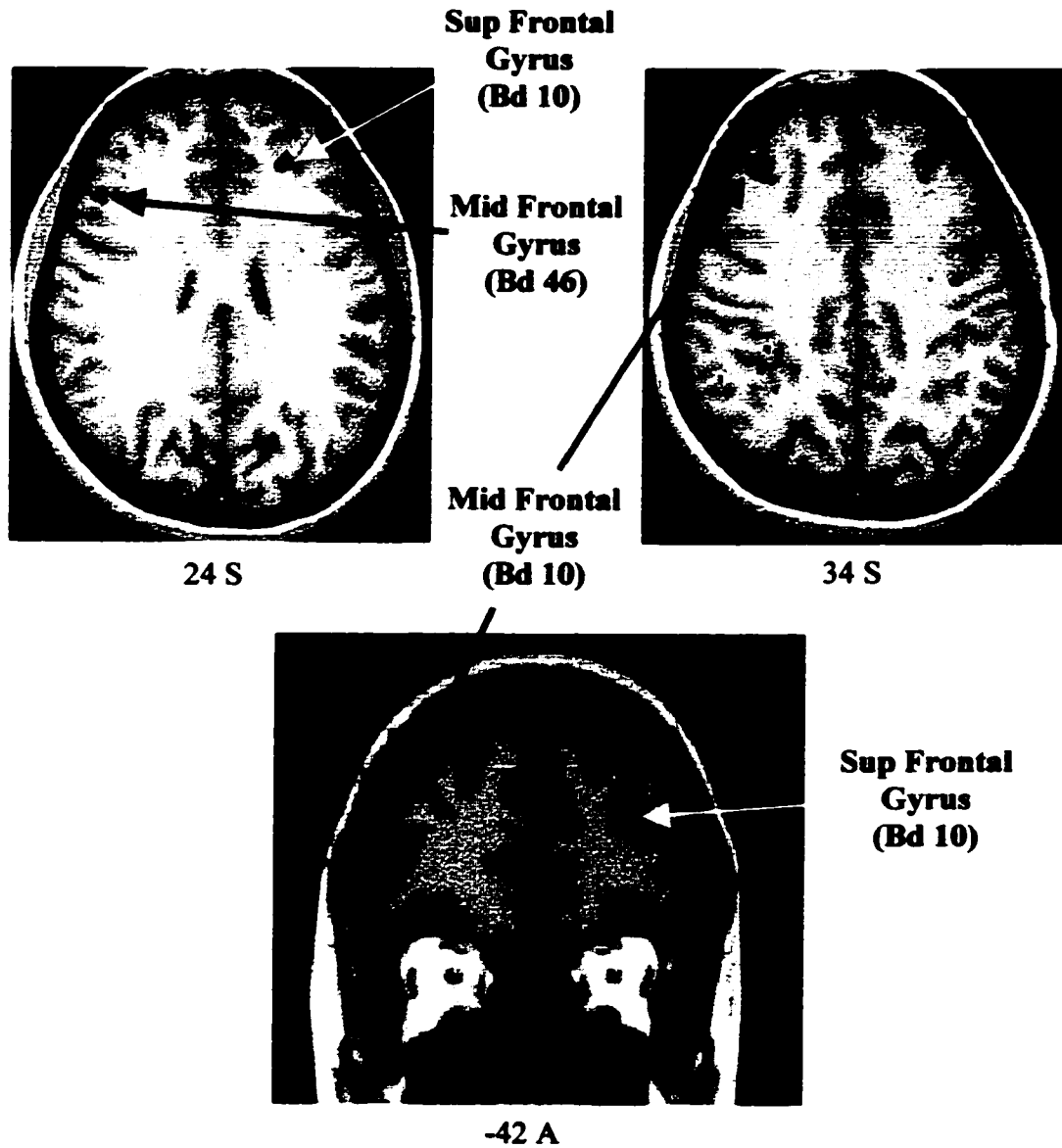
Other Frontal / Temporal

Insula
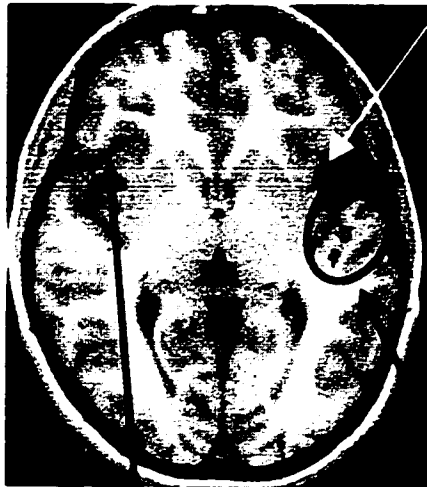
1 S

Inf Frontal
Gyrus (Bd 47)

Sup Temporal
Gyrus (Bd 22)

40 L

Mid Temporal
Gyrus (Bd 22)

5 S

-53 R

Figure 6.4b
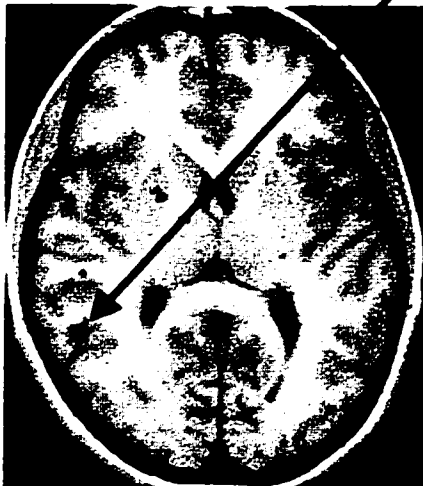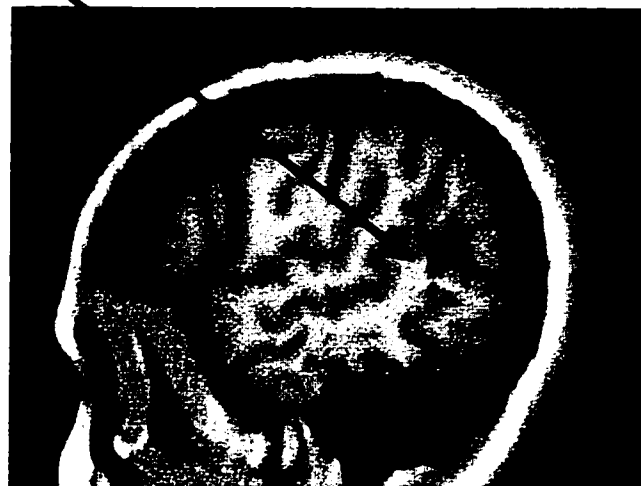
Table 6.2: *Other Areas of Interest*

	Left	Right
Frontal Cortex		
Superior Frontal Gyrus (Bd 10)	-25L 45A 24S	*None*
Middle Frontal Gyrus (Bd 10) (Bd 46)	*None*	 40R 43A 34S 46R 28A 24S
Insula	-40L 12A 1S	*None*
Inferior Frontal Cortex (Bd 47)	*None*	38R 25A 1S
Temporal Cortex		
Superior Temporal Gyrus (Bd 22)	-50L 3A 1S -49L -11P 1S -45L -19P 1S	*None*
Middle Temporal Gyrus (Bd 22)	*None*	51R -49P 5S

6.33 Coordination vs. Control Conditions

Another question of interest was whether the coupling of auditory and motor events in coordination involved a greater amount of activation in cortical areas that respond to auditory or motor events alone. Figure 6.5 (top half, 1st row) shows active clusters during the Auditory only control (grand-averaged maps). Only one cluster within primary auditory cortex was found. It was located in Brodmann's area 41 in the left superior temporal gyrus (right panel; table 6.4a). The small degree of primary auditory cortex activity is likely due to the loud volume of the background scanner noise. In addition, listening to the metronome resulted in a couple of active voxel clusters in the right middle temporal gyrus (Brodmann's area 21, left panel; table 6.4a).

Table 6.3: Individual Subject Data

		SM1		Premotor		SMA	Basal Gang.		Cereb.	
		Left	Right	Left	Right		Left	Right	Left	Right
Syncopate	S1	*		*	*	*	*	*	*	*
	S2	*		*	*	*	*	*	*	*
	S3	*		*	*	*	*	*	*	*
	S4	*		*	*	*	*	*	* -	*
	S5	*				*		*	*	*
	S6	*		*	*	*	*	*	*	*
	S7	*		*		*				
	S8	*	*	*	*	*	*	*	*	*
	S9	*	*	*	*	*	*	*	*	*
Synchronize	S1	*		*	*	*				*
	S2	*		*	*	*				*
	S3	*		*		*				*
	S4	*		*	*	*				*
	S5	*					*	*	*	*
	S6	*				*			*	*
	S7	*							*	*
	S8	*				*	*	*	*	*
	S9	*				*	*	*		*

Neither of these temporal areas showed significant differences in activity when the Auditory only control was compared to either coordination condition. However, subtracting the Auditory only control from the Syncopate condition yielded several significant clusters in Brodmann's area 22 of both temporal lobes (figure 6.5, 2nd row, left panel; table 6.4a). Consistent with the comparison between coordination conditions, all were more active during syncopated coordination than during listening alone. In contrast,

there were no differences between the Auditory only control and Synchronize condition in either temporal lobe (figure 6.5, 2nd row, right panel; table 6.4a).

Table 6.4a: Coordination vs. Auditory Control – Temporal Lobe activity

	Left	Right
Auditory only		
Primary Auditory Cortex (Bd 41)	-47L -26P 8S	*None*
(Bd 21)	*None*	67R -13P -1I
		64R -25P -1I
Syncopate - Auditory only		
(Bd 22)	-47L -12P 5S	53R -24P 5S
	-43L -21P 5S	51R -49P 5S
Synchronize - Auditory only	*None*	*None*

The grand average activation patterns for the Motor only control are shown in the bottom half of figure 6.5 (1st row). Self-paced movement resulted in large regions of activity in the contralateral sensorimotor area, SMA, and both ipsilateral and contralateral cerebellar lobes (though the activity was much stronger and more widespread ipsilaterally). As known from the comparison between the coordination conditions, Syncopated coordination resulted in an additional active cluster located in the anterior left SMA. On the other hand, neither coordination condition was associated with differences in the regions of sensorimotor cortex or the SMA that were activated by self-paced movement (figure 6.5, bottom half, compare 1st panels in each row; table 6.4b). As for the cerebellum, there were small regions in both the contralateral and ipsilateral cerebellum that showed stronger activation during syncopated coordination than during

Figure 6.5 (page 164): A comparison of the coordination and control conditions (see also table 6.4). **Auditory** (top half): Listening to the metronome was associated with activation of the left primary auditory cortex (Brodmann's area 41) in the superior temporal gyrus and right temporal association cortex (Brodmann's area 21) in the middle temporal gyrus (1st row). Within the temporal lobes, syncopation resulted in additional bilateral activation of Brodmann's area 22 (2nd row, left panel). No differences between the Synchronize and Auditory control conditions were found in either temporal lobe (2nd row, right panel). **Motor** (bottom half): Large task-related clusters in the contralateral sensorimotor cortex, SMA and ipsilateral cerebellum were found for self-paced movement (1st row). Neither cortical region showed significant changes in activation levels during coordination (2nd and 3rd rows, 1st panel). Relative to self-paced movement, cerebellar activation increased for syncopation (2nd row, right 2 panels) but decreased for synchronization (3rd row, 3rd panel). All slices are axial: left side – right hemisphere, right side – left hemisphere; slice location along the superior-inferior axis is indicated below.

Coordination vs. Controls

Figure 6.5

164
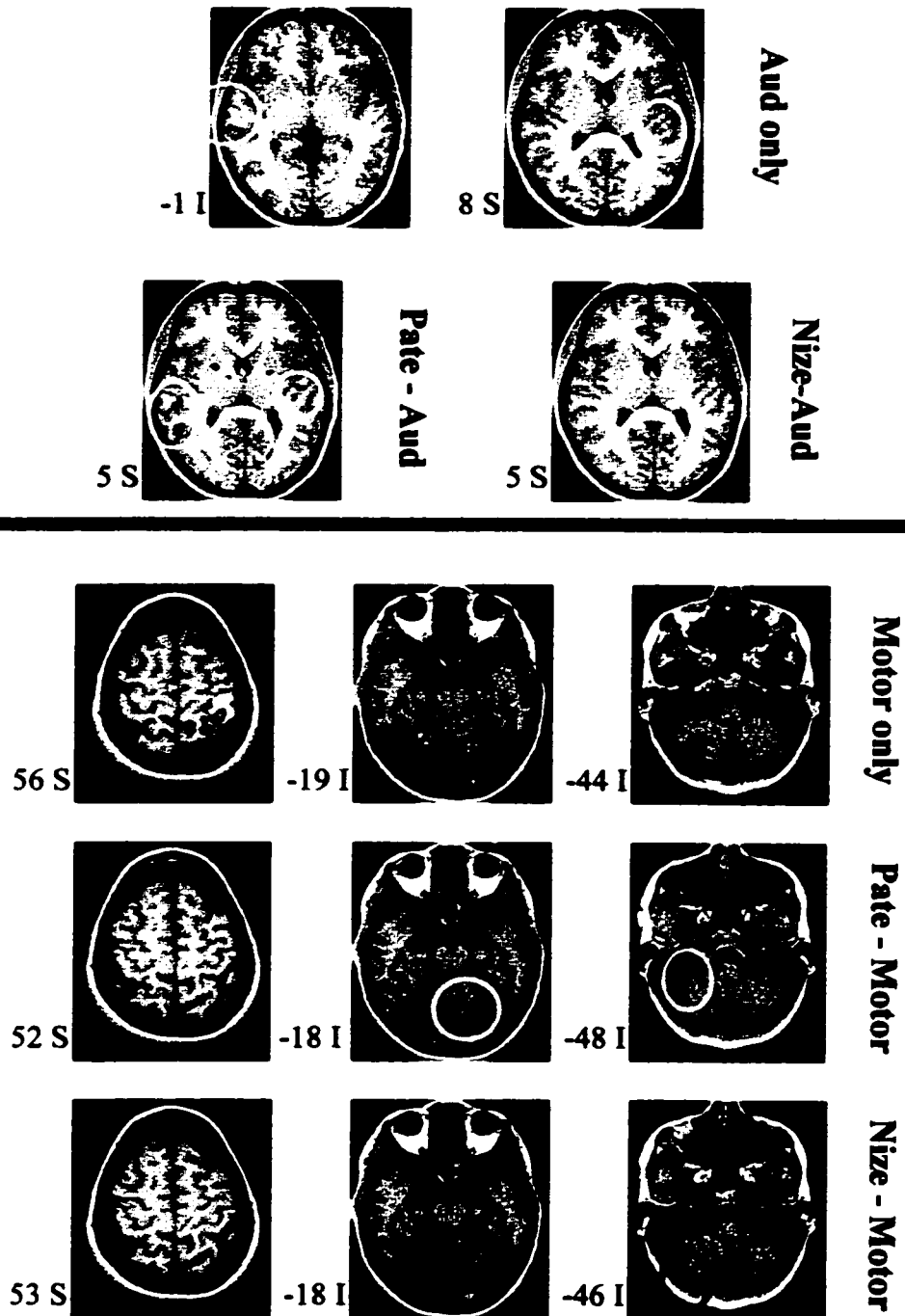
self-paced movement (middle row, 2nd and 3rd panels; table 6.4b). In contrast, negative differences were found for several bilateral cerebellar clusters when the Motor only control was subtracted from the Synchronize condition, thus indicating that these areas were more activated by self-paced as opposed to synchronized movement (3rd row, 3rd panel; table 6.4b).

Table 6.4b: Coordination vs. Motor Control

	Left	Right
Motor only		
Sensorimotor cortex (Bd 1-4)	-39L -28P 56S	*None*
Medial Frontal Gyrus (Bd 6-SMA)	0 -12P 56S	0 -12P 56S
Cerebellum	-15L -50P -44I	22R -52P -19I 28R -63P -44I
Syncopate - Motor only		
Sensorimotor cortex (Bd 1-4)	*None*	*None*
Medial Frontal Gyrus (Bd 6-SMA)	*None*	*None*
Cerebellum	-22L -59P -18I -5L -74P -18I	35R -43P -48I
Synchronize - Motor only		
Sensorimotor cortex (Bd 1-4)	*None*	*None*
Medial Frontal Gyrus (Bd 6-SMA)	*None*	*None*
Cerebellum**	-30L -51P -46I	29R -68P -46I 30R -74P -46I

** stronger activation during Motor only condition

6.4 Discussion

This experiment provides, for the first time, evidence that syncopated and synchronized timing patterns of auditory-motor integration involve distinct networks of cortical and subcortical brain areas. Specifically, syncopation appears to require the recruitment of additional neuronal populations within premotor cortex, the basal ganglia and cerebellum.

6.41 Premotor Areas

Within premotor cortex, both lateral and mesial regions showed significantly stronger activation during syncopated as compared to synchronized timed movements. Given the higher degree of difficulty associated with syncopated patterns, this result may reflect an increase in the amount of motor planning required to move off-the-beat. A relation between premotor activity and motor planning/preparation processes is well established. Several experiments have shown changes in neurophysiological activity in premotor areas, especially the SMA, prior to movement [e.g., Kornhuber & Deecke, 1965; Deecke et al., 1969; Deecke & Kornhuber, 1978; Barrett et al., 1986; Erdler et al., 2000]. Moreover, activation of premotor areas correlates with movement complexity [Orgogozo & Larsen, 1979; Lang et al., 1989, 1990; Simonetta et al., 1991; Rao et al., 1993; Shibasaki et al., 1993]. In fact, Gerloff et al. (1997) showed that transcranial magnetic stimulation of the SMA disrupts performance of complex sequential movements.

In this study, differences between syncopated and synchronized timing strategies were found in the anterior part of the SMA, whereas both modes of coordination involved

the more caudal SMA regions. Previous neuroimaging [Deiber et al., 1996; Boecker et al., 1998; Jenkins et al., 2000] and single cell recordings [Mushiake et al., 1991; Halsband et al., 1994] also indicate a functional distinction between anterior and posterior portions of the SMA. These studies implicate caudal SMA regions in processes related to motor execution whereas the anterior SMA appears to be more involved in motor planning mechanisms, especially regarding the initiation of movement onset. Comparisons of self versus externally paced movements support the hypothesis that premotor areas, especially the SMA, are necessary for the internal initiation of movement. Using PET, Larsson et al. (1996) observed stronger activity in both lateral premotor cortex and the SMA when externally triggered movements were subtracted from self-paced ones, though the relative increases were stronger for the SMA. Similar results have also been found by others [Kermadi et al., 1997; Wessel et al., 1997; Gerloff et al., 1998; Jenkins et al., 2000]. Finally, though patients with lesions of the dorsolateral premotor cortex and supplementary motor area can reproduce rhythms with external pacing, their ability to do so without such pacing is impaired [Halsband et al., 1993].

In light of this previous work, our results suggest that the performance of more difficult syncopated timing patterns necessitates the activation of premotor areas not involved during synchronization because of increased motor planning demands. The increased preparation needed to syncopate with a metronome may result from the fact that syncopation entails a sufficient separation of response from nearby metronome beats. Therefore, though the rate of movement is constrained by the metronome, responses are not triggered by it.

6.42 Basal Ganglia

A role of the basal ganglia in timing has been largely motivated by studies of patients with Parkinson's disease, in whom dopaminergic levels within these nuclei are known to be severely depleted. Parkinson's patients show deficits on their performance of a wide variety of rhythmic movements. Though Parkinson's patients are generally able to accurately reproduce a given temporal interval on average, their variability is significantly enhanced. This phenomenon has been observed for finger tapping [Wing et al., 1984; O'Boyle et al., 1996; Harrington et al., 1998], wrist movements [Pastor et al., 1992a] and gait patterns constrained by an external metronome [Ebersbach et al., 1999].

In much of this work, results have been interpreted with respect to Wing and Kristofferson's (1973) timing model, which is based on the assumption that there is an internal clock whose variance is independent of that associated with motor implementation processes. Within the framework of this model, many of these studies show that the increased response variability exhibited by Parkinson's patients is attributable to increased variance of an internal clock and *not* production of the motor response itself [see Ivry & Keele, 1989 for conflicting results]. This has led to the conclusion that the basal ganglia act a clock for these types of movements [see Harrington & Haaland, 1999 for review]. However, there are often violations of the two-timing model. The independence of clock and motor variance was partially based on the observation that the temporal sequence of inter-response intervals exhibited a −1 lag correlation [Wing & Kristofferson, 1973]. Since their study, however, both self-paced [Gilden et al., 1995] and synchronized/syncopated [Chen et al., 1997, submitted]

movements have been shown to exhibit correlations over multiple time scales, suggesting that the −1 lag correlation measured by Wing and Kristofferson may have been due to the relatively short amount of data examined (~20 as compared to ~1000 responses). While such findings do not necessarily negate the existence of an internal clock they suggest that conclusions based on Wing and Kristofferson's model should be interpreted with caution, especially since there is no way to measure the 'clock' component of the variance independently (i.e. it is based only on the measured response variance).

On the other hand, other converging lines of evidence also implicate the basal ganglia in internal timing processes. For example, Parkinson's patients exhibit diminished time perception abilities [Artieda et al., 1992; Harrington et al., 1998; Pastor et al., 1992b; see Ivry & Keele, 1989 for exception] which supports the conclusion that their motor-related deficits may be the result of timing rather than response implementation problems. Consistent with these results are recent findings that the processing of intervals in the millisecond range is dependent upon the level of dopaminergic activity in the basal ganglia [Rammsayer, 1999]. Further evidence is provided by several functional neuroimaging studies that show increases in both PET and fMRI signals in response to perceptual and/or motor tasks that involve temporal processing [see Harrington & Haaland, 1999 for review].

If the basal ganglia do serve as a clock for movement then there should be a relation between the firing patterns of its movement-related cells and the timing of motor output. Single cell recordings in animals during reactive movements have shown that the majority of basal ganglia neurons actually fire *after* movement onset in contrast to cells

within the motor cortex that fire before [see Rothwell, 1994 for discussion]. This suggests that the basal ganglia do not have a major role in the initiation of reactive movements. In more complex tasks, however, changes in basal ganglia activity have been observed to occur during periods of motor preparation [e.g. Alexander & Crutcher, 1990; Jaeger et al., 1993]. Moreover, in tasks where a sequence of movements are involved, firing bursts have been found to precede the onset of subsequent movements by ~100-200 msec when the subsequent movements are predictable in time [Brotchie et al., 1991]. A special role of the basal ganglia in sequential movement is also suggested by a PET study by Boecker et al. (1998). They observed regional cerebral blood flow increases in the SMA and associated pallido-thalamic loop as subjects performed increasingly complex (and overlearned) sequences of finger movements. Together, these results suggest the hypothesis that the basal ganglia provide timing information when upcoming movements are expected and predictable in time. Our results are consistent with this hypothesis and suggest that more a complicated syncopated pattern of coordination involves additional basal ganglia resources.

One possibility is that separation of the response from surrounding metronome beats places additional demands on movement initiation mechanisms that involve the basal ganglia. A couple of recent findings are particularly relevant for this conclusion. Johnson et al. (1998) examined in-phase and anti-phase patterns of bimanual coordination, which have many parallels with synchronized and syncopated modes of unimanual coordination, respectively. For example under conditions of increasing movement rate, anti-phase patterns become unstable and subjects switch to an in-phase

pattern [Kelso, 1984] similar to the rate-dependent transitions from syncopation to synchronization [Kelso et al., 1990]. In the Johnson et al. study (1998) it was found that Parkinson's patients were unable to perform anti-phase patterns of bimanual movement both when the movements were self and externally-paced, consistent with the idea that the basal ganglia are preferentially involved in more complicated forms of sequential movement. A second finding was that their performance of in-phase movements was significantly worse in the absence of external cues. This latter finding highlights the likely role of the basal ganglia in movements which are internally determined [see also Georgiou et al., 1993, 1994; Jackson et al., 1995]. Given these results, one interpretation of our findings is that syncopation is associated with significantly more basal ganglia activity because it is a more complicated form of sequential movement that, although externally paced, entails initiating movement at appropriate delays with respect to surrounding pacing cues.

6.43 Cerebellum

Our results demonstrate that the cerebellum is required for the performance of both syncopated and synchronized coordination tasks. For both modes of coordination, almost all subjects showed activity in the right cerebellar hemisphere as expected since this was the side ipsilateral to movement. However, several ipsilateral regions (both medially and laterally located) had significantly higher signal intensities for an off-the-beat timing pattern, suggesting that the cerebellum's functional role may be different in the two cases. Support for this hypothesis also comes from the observation that 8 out of 9

subjects showed contralateral cerebellar activation during syncopation whereas only 4 out of 9 did when synchronizing.

Several converging lines of evidence support a role for the cerebellum in timing processes. First, patients with lesions of the cerebellar lobes are deficient in rhythmic tapping tasks. Ivry et al. (1988) asked patients with lesions to either the lateral or medial cerebellum to perform a continuation task in which they first synchronized with an auditory metronome (2 Hz rate) and then continued to move at the same rate after the metronome was removed. All of the patients (n=7) showed an increase in response variability associated with self-paced tapping when responding with either a finger or the foot ipsilateral to the side of the lesion. Using Wing & Kristofferson's (1973) timing model, Ivry et al. concluded that the poor performance of patients with lateral cerebellar lesions was due to deficits in a central timing process. On the other hand, whereas patients with medially located cerebellar lesions knew when to respond, they were unable to implement the motor act itself. Increased variability on a rhythmic tapping task in cerebellar patients was also shown in a separate study [Ivry & Keele, 1989].

Consistent with these results, Rao et al. (1997) showed cerebellar changes in fMRI signal intensity when subjects performed rhythmic movements. They found ipsilateral increases in activity both when subjects synchronized finger movement with an auditory metronome and when they continued to move at the same rate in the absence of the metronome. Using PET, Catalan et al. (1998) also demonstrated ipsilateral cerebellar activity during externally paced sequential finger movements. Moreover, they showed that sequential movements of greater complexity were associated with further increases

172

in cerebellar rCBF. Increased cerebellar activation with rhythmic movements of increasing complexity was also found by Penhune et al. (1998).

Despite a long association of cerebellar function with motor behavior, it has become increasingly clear in the past few decades that the cerebellum is also involved in other perceptual and cognitive activities. For example, the ability to accurately and consistently judge temporal durations is impaired in patients with cerebellar damage [Ivry & Keele, 1989; Malapani et al., 1998]. In addition, Schubotz et al. (2000) identified bilateral regions of cerebellar activation when subjects monitored both visual and auditory rhythms for timing deviations. Allen et al. (1997) also reported Cerebellar activation with selective attention to visual shapes.

Perhaps the most intriguing results, however, come from a recent study by Tesche and Karhu (2000) in which they measured the effect of different temporal patterns of somatosensory stimulation on the amplitude of neuromagnetic rhythms generated by neuronal populations within the cerebellum. Their results showed prominent cerebellar activation not only immediately prior to the delivery of an anticipated stimulus but also when the stimulus was omitted. This anticipatory response was also shown to be much stronger for the first stimulus following an omitted stimulus than for an included one. Moreover, the cerebellar activity associated with deviation from the established temporal pattern was enhanced by attention to the stimuli (as opposed to reading a book during the stimulation).

The finding of cerebellar activation in such a wide range of motor and non-motor tasks has led to the hypothesis that its primary function is actually the acquisition and

processing of sensory information which then allows it to provide highly accurate temporal information for situations that require it [Ivry, 1996, 1997, 2000]. From this perspective, the deficits observed in many motor behaviors could be the result of a disruption of this internal temporal representation as opposed to problems with motor control systems [Bower, 1997; Gao et al., 1996; Ivry, 2000]. Our finding of increased cerebellar activity during syncopation may thus reflect the fact that off-the-beat timing relationships require a higher degree of temporal acuity than do synchronized ones, since in the former case one must predict not only the onset of the next metronome beat but also the point in time between successive beats.

6.44 Other Frontal and Temporal Areas

Syncopation was also associated with significantly more activation of several regions distributed throughout the frontal and temporal lobes. Frontally, we found clusters in anterior regions of the superior and middle frontal gyri (Brodmann's areas 10 and 46). A role of prefrontal cortex in the organization of motor behavior is generally thought to relate to attention and/or working memory rather than the direct temporal control of movement [see Harrington & Haaland, 1999 for discussion]. Activation of prefrontal areas is especially prominent during learning of new motor tasks, e.g. finger sequences, but is reduced or absent if such sequences are overlearned [Jueptner et al., 1997, Boecker, 1998]. Significant increases in rCBF to the middle frontal gyrus have also been observed during learning of a difficult inverted visuomotor coordination task [Lang et al., 1988]. These increases were correlated with rCBF changes in the basal ganglia, supporting the idea that these cortical regions comprise part of a broad motor

timing network. With regard to working memory, experimental data obtained from monkeys implicate prefrontal neurons in sensory-motor coupling, especially when there are temporal delays [Quintana et al., 1988; Fuster, 1989; see also Goldman-Rakic, 1987]. Increased prefrontal activation during syncopation as compared to synchronization may therefore reflect not only the fact that syncopated patterns are associated with a higher attentional load [Kelso, 1994; Carson et al., 1999; see also Temprado et al., 1999] but also that they require a delay between response and metronome.

In temporal cortex, syncopation resulted in activation of several regions within Brodmann's area 22 that were not associated with synchronization. In the left hemisphere, there were several rather large clusters in the most anterior portion of the temporal lobe. A single cluster within the right hemisphere was also identified but this was located more posterior. A similar pattern of activation in Brodmann's area 22 was observed by Platel et al. (1997) in a study that examined music perception. Specifically, these areas were shown to be involved in a familiarity task in which subjects were asked whether or not they recognized a given piece of music. The authors point out that this task required subjects to attend to both the pitch and rhythm of the tone sequence. Our results suggest that, rather than familiarity, such areas may be involved in the integration of rhythmic sensory information. The predominance of temporal activity in the left hemisphere could correspond to a specialization of this hemisphere for the processing and production of sensory and motor events occurring in rapid procession as has been proposed in speech research [Tallal et al., 1993].

6.45 Sensorimotor Cortex

Sensorimotor cortex was the only area of primary interest whose activation showed no significant dependence on the timing pattern performed. The absence of effects in sensorimotor cortex is in contrast to previous work which demonstrated significant differences in the amplitude of neuroelectric [Mayville et al., 1999] and neuromagnetic [Mayville et al., submitted, in preparation] signals recorded from sites overlying the contralateral sensorimotor area. One possible reason for this discrepancy concerns the temporal dynamics of neural activity. Since the BOLD effect is dependent on the hemodynamic response, it is insensitive to fine timing differences in the activation of neuronal populations. Such differences in the temporal sequence of depolarization/hyperpolarization in a given cell population could, on the other hand, significantly affect the summation of electrical currents which would directly affect the amplitude of electric potentials and/or magnetic fields detectable at the scalp. Alternately, the sensorimotor amplitude differences detected by these earlier studies may simply reflect differences in the number of neurons that are simultaneously involved in performing the task (larger population for syncopation versus synchronization) but the numbers are not different enough to affect the local hemodynamic response.

6.46 Conclusions

In conclusion, the distribution of cortical and subcortical areas involved in coordinating one's movement with an external metronome depends on the timing pattern employed. Both synchronized and syncopated patterns require activation of contralateral

sensorimotor and caudal supplementary motor cortices as well as the (primarily ipsilateral) cerebellum. Moving off the beat, however, requires not only additional activation of the cerebellum but also the recruitment of another network comprised of the basal ganglia, dorsolateral premotor, rostral supplementary motor, prefrontal, and temporal association cortices. This finding indicates that separation of one's response from surrounding metronome beats places additional demands on motor planning, attentional and sensorimotor integration processes. One interpretation is that syncopated movements, though externally paced by definition, are not externally triggered and thus necessitate a separate mechanism for the initiation of movement not required for synchronized timing patterns. The basal ganglia and premotor cortices are both likely to participate in such a mechanism. In addition, the temporal delay between the motor response and stimulus could tap working memory and integration resources located in prefrontal and temporal association areas. It would therefore be of some interest to investigate how learning to syncopate may alter, even disengage, some of these neural structures as the task becomes more automated.

7.0 General Discussion

The experiments presented in this thesis demonstrate that spatiotemporal patterns of brain activity, as measured by three separate macroscopic neuroimaging techniques, significantly depend on the timing relation between rhythmic sensory and motor events as well as their rate. By having subjects perform both syncopated and synchronized movements at the same rate, we were able to identify features of brain activity that reflect the temporal pattern of sensorimotor coordination. In addition, by systematically varying an external control parameter, the metronome frequency, we show not only that the ability to integrate rhythmic sensory and motor events with a given timing relation is constrained by the rate at which they occur but also that these constraints exist even when responses are not overtly executed. Moreover, we show evidence that both sensory and motor-related neural processes exhibit a dependence on rhythmic rate that may relate to these timing constraints.

7.1 Differences in Brain Activity Related to Timing

First we treat features of brain activity that were found to uniquely relate to the mode of coordination, independent of coordination frequency. Results from Experiments 1-3 and 5 show that the amplitude of brain activity differs in its topography when subjects syncopate versus synchronize with an external auditory metronome. Experiment 1 indicates that the strength of event-related potentials, as indexed by power of the EEG

signal at the dominant coordination frequency component, is significantly higher during syncopated movements. The confinement of these differences to left central recording sites suggests that neural activity in contralateral sensorimotor areas varies depending on the mode of coordination. In contrast, there were no significant amplitude differences in event-related field activity across the entire head surface (Experiment 2) that distinguished between syncopation and synchronization when performed at the same rate. One explanation for this discrepancy between EEG and MEG is that at low movement rates where syncopation is possible, the event-related fields are dominated by an auditory-related pattern that overlaps topographically at the head surface with contralateral sensorimotor areas (It is worth noting that additional investigation, not presented herein, revealed that this dominance was not an artifact of averaging MEG activity with respect to auditory and not motor events).

On the other hand, by averaging MEG signals across trials in the frequency domain, we confirmed the existence of significant differences between the two timing patterns in the amplitude of brain activity recorded over left central regions of the head. Specifically, in Experiments 2 and 3 the strength of the neuromagnetic beta rhythm (15-30 Hz) was suppressed in these areas during syncopation relative to synchronization. In light of previous work [Pfurtscheller et al., 1989, 1992, 1996, 1998; Kristeva-Feige et al., 1993; Salmelin & Hari, 1994; Hari et al., 1997; Leocani et al., 1997] this result may be interpreted as a stronger desynchronization of ongoing oscillations in the beta range during syncopated movement. This phenomenon, known as event-related

desynchronization (ERD) is thought to signify a shift from an 'idling' state to task-related activation [Pfurtscheller et al., 1996; Pfurtscheller & Lopes da Silva, 1999].

An important result found in Experiment 3 was that the neuromagnetic beta rhythm in contralateral sensorimotor areas distinguishes between syncopated and synchronized patterns of coordination even when they are mentally simulated. This finding has two implications. First, it indicates that the function of neuronal populations within sensorimotor cortex is not restricted to the processing of efferent or reafferent information related to movement execution. This is consistent with a growing body of work in which activation of the primary sensorimotor area has been observed during motor imagery [e.g. Hallett et al., 1994; Beisteiner et al., 1995; Lang et al., 1996; Pfurtscheller & Neuper, 1997]. Second, it suggests that neurons that contribute to oscillations in the beta range are involved in motor planning processes associated with the temporal organization of behavior.

As discussed in Chapter 4, it is unclear whether the beta rhythm is a correlate of the timing relation, per se. Support for the hypothesis that strength of the neuromagnetic beta rhythm is not directly determined by the temporal delay between sensory and motor 'events' comes from the observation of significant differences in signal power in this frequency range even when the mode of coordination was the same across the conditions compared. For example, in Experiments 2 and 3 overtly synchronizing at high rates was associated with a stronger beta rhythm if subjects had been synchronizing throughout the entire run as compared to runs in which they switched from a syncopated mode of coordination. In addition, in Experiment 3 differences in the amount of beta power were

found when mental syncopation or synchronization was subtracted from its overt counterpart. However, the topographic distribution and direction of these differences across subjects were only consistent for the syncopate comparison, thus indicating that the differences are not attributable simply to the presence or absence of overt movement either. An alternative explanation is that the neuromagnetic beta rhythm reflects the amount of effort associated with maintaining a given mode of coordination. Syncopated timing patterns are clearly more difficult and have been shown to require more attention when overtly performed [Kelso, 1994; Carson et al., 1999; see also Temprado et al., 1999].

The EEG and MEG results discussed so far are consistent in the sense that they both indicate that interactions among neuronal populations within contralateral sensorimotor cortex are affected by the temporal organization of behavior with respect to the environment. At the same time they conflict with respect to whether syncopated patterns are associated with an increase or decrease of the amplitude of brain activity. This contradiction cannot be resolved completely because it is unknown whether the same neuronal populations which generate spontaneous fast oscillations in the brain (that are not phase-locked to the given task event across trials) contribute to the EEG or MEG signal that defines the event-related potential or field (i.e. signal components that are phase-locked to the given task event across trials). One hypothesis is that event-related potentials and/or fields reflect the response of cortical neurons to afferent activity whereas ERD/ERS correspond to changes in the local interactions between neurons and interneurons that determine the frequency of faster oscillations [Pfurtscheller & Lopes da

Silva, 1999]. Nevertheless, both the EEG and MEG results from Experiments 1 and 2 indicate that syncopated coordination is associated with a greater degree of task-related activation in contralateral sensorimotor areas.

Interestingly, sensorimotor cortex was the lone area of primary interest in Experiment 5 whose fMRI activation showed no significant dependence on the timing pattern performed. Since it is dependent on the hemodynamic response, the BOLD effect is insensitive to fine timing differences in the activation of neuronal populations that may affect the summation of currents which underlie electric potentials and/or magnetic fields. Alternately, amplitude differences in the EEG and MEG signals may simply be the result of the sheer size of the neuronal population in sensorimotor cortex that is involved in syncopated versus synchronized coordination. Given that the mechanism which couples neuronal activity to the BOLD effect is not completely understood, it is possible that changes in BOLD contrast are nonlinearly related to changes in neuronal activation such that increasing/decreasing the degree of local synchrony among neurons does not necessarily translate into differences in the hemodynamic response or oxygen extraction rate.

On the other hand, Experiment 5 revealed syncopation to be accompanied by significantly increased activity in several other brain areas. Cortically, these included a cluster in the anterior portion of the supplementary motor area (SMA) as well as several clusters in both left and right dorsolateral premotor cortices. These regions comprise Brodmann's cytoarchitectonic area 6 and participate in motor planning. No significant differences were found in electrode sites over these areas in the EEG experiment though

the beta rhythm differences reported in Experiments 2 and 3 do appear to extend bilaterally over precentral areas and across the midline. It is perhaps surprising that neither dorsolateral region emerged in the EEG or MEG studies but the lack of SMA activity in EEG and MEG is not hard to explain. The SMA is located on the mesial surface of the interhemispheric wall just anterior to the vertex. Unfortunately, the auditory response in EEG is maximal at the vertex and thus may mask SMA activity associated with auditory-motor coordination. In the case of MEG, it is generally thought that since the SMA is bilaterally active prior to movement the fields from each hemisphere cancel due to their close proximity to one another [e.g. Cheyne & Weinberg, 1989; Kristeva et al., 1991; Cheyne et al., 1995]. This idea is supported by the finding of SMA activity in patients who have damage to one side of the interhemispheric wall [Lang et al., 1991]. However, recent MEG work suggests that more complicated forms of movement are preceded by field activity that is localized to the SMA region [Erdler, 2000]. Experiment 4 in this thesis also presents evidence that neuromagnetic activity consistent with a SMA source is ongoing during a sequence of rhythmic movements, but this field was much weaker compared to the evoked fields that occur during each response profile.

Other cortical areas that were associated with significantly stronger fMRI activation during syncopated as compared to synchronized coordination were bilateral prefrontal cortex (Brodmann's areas 10 and 46), the right inferior frontal gyrus (Brodmann's area 47), the left insula and anterior regions of the left superior temporal gyrus (Brodmann's area 22), and finally, a posterior region of the right superior temporal

gyrus (also Brodmann's area 22). Subcortically, both the basal ganglia and cerebellum showed differences as a function of coordination mode. The cerebellum was involved in both syncopation and synchronization, but in the former case activity was stronger and covered a broader portion of the cerebellar lobes, including the contralateral hemisphere. In contrast, activation of the striatum (caudate nucleus and putamen) was generally observed for syncopation only.

The results from Experiment 5 provide convincing evidence that a more extensive cortical and subcortical network is required to integrate rhythmic sensory and motor events in a syncopated compared to synchronized fashion. Whereas synchronization was primarily associated with activity in the contralateral sensorimotor cortex, caudal SMA and ipsilateral cerebellum, syncopation appears to involve these areas in addition to several others that have been implicated in many functions involved in motor planning and the organization of behavior within a given environmental context. Among these are timing, movement initiation, anticipation, working memory and/or attention, and the processing of sensory and motor events that occur in rapid succession [see Harrington & Haaland, 1999 for review; see also Fuster, 1989; Platel et al., 1997]

7.2 Rate-Dependent Changes in Brain Activity

In Experiment 2 we investigated the dependence of neuromagnetic activity associated with the brain's response to auditory and motor events on the rate at which they occur. This was done by decomposing the event-related fields associated with both modes of coordination into auditory and motor components and then examining the contribution of each component to the whole signal across increasing plateau frequencies.

We found that the amplitude of the auditory component decreased as the movement rate became faster whereas the motor component remained approximately constant. The brain's response to auditory stimulation at different rates has been well studied in both EEG [see Näätänen & Picton, 1987 for review] and MEG [Hari et al., 1982; Liu et al., 1998]. However, much of this has focused on slower, transient evoked responses (ISI > 2 sec) or much faster steady-state responses (40 Hz) [see Lins & Picton, 1995 for review]. The range that affords syncopated or synchronized coordination is in the middle; it must be fast enough to allow anticipation of the next stimulus but still remain within the limits of biomechanical operation [see, e.g. Engström et al., 1996].

Preliminary work [Carver et al., 1999] that has systematically investigated the rhythmic ISI range used here suggests that there is a significant drop in the amplitude of the brain's neuromagnetic response to auditory stimulation that is due primarily to an attenuation of the N1m component. This component typically occurs about 100 msec after the occurrence of an auditory stimulus and is thought to be generated by sources within primary auditory cortex in the superior temporal gyrus [see Näätänen & Picton, 1987 for review]. A drop in N1m amplitude across the rhythmic range associated with syncopation/synchronization is consistent with the earlier MEG work that investigated much slower rates of stimulation [Hari et al., 1982; Liu et al., 1998]. It is also consistent with the results from Experiment 2 since the field pattern which defined the auditory component in the decomposition was taken from a transient control condition in which subjects passively listened to auditory tones delivered at random intervals every 2-3 sec. The preliminary work by Carver et al. (1999) also indicates that, in addition to an

attenuation of the N1m component, increasing the rate of auditory stimulation leads to the emergence of a variety of additional field components which have yet to be localized. Moreover, the dynamical behavior of these components becomes increasingly oscillatory, which suggests that the range of rates that afford rhythmic sensorimotor coordination may be associated with a transition from transient to steady-state auditory brain responses. One hypothesis is that these features of the neuromagnetic signal signify reorganization in the processing of auditory information that may directly or indirectly affect sensorimotor integration networks. It is possible, even likely that responses become synchronized at higher frequencies because the motor response becomes entrained to the increasingly predictable series of tones.

The decomposition analysis in Experiment 2 revealed no dependence of motor response amplitude on rate. As with the auditory component, this response reflected the contribution of the dominant spatial pattern obtained from a transient motor control condition (inter-response intervals from 2-3 sec), which corresponded to a classic motor-evoked field [Cheyne & Weinberg, 1989; Kristeva et al., 1991]. In Experiment 4 we verified that the MEF amplitude does not depend on the length of the interval between successive responses across a wide range of rhythmic rates. We further showed that the latencies of the MEFI-MEFIII components, though tightly coupled to the biphasic response profile [see also Kelso et al., 1998; Holroyd et al., 1999], were not affected by movement rate either. However, a second weaker field pattern did exhibit a drop in amplitude at higher rates. It can be inferred from both the topography and dynamics of this second pattern that it corresponds to the Bereitschaftsmagnetfeld or readiness field

that prior research has shown to precede the onset of movement [Deecke et al., 1982; Hari et al., 1983; Cheyne & Weinberg, 1989; Kristeva et al., 1991; Erdler et al., 2000]. Our results imply not only that this readiness field can be observed during a sequence of rhythmic movements (in the Erdler et al., 2000 study it was only observed prior to the *beginning* of a rhythmic sequence) but also that there is a qualitative change in the underlying neural processes it reflects once the inter-response intervals get shorter than about one second.

The readiness field, as with the readiness potential [Kornhuber & Deecke, 1965; Deecke et al., 1976] is so named because it is presumed to represent a priming or preparation of the motor system for action. Both have been associated with a generator in the SMA [Deecke & Kornhuber, 1978; Deecke, 1987; Lang et al., 1990; Praamstra et al., 1996; Erdler et al., 2000]. This is consistent with a large number of studies which implicate this area in the temporal organization of movement [e.g. Orgogozo & Larsen, 1979; Roland et al., 1980; Dick et al., 1986; Tanji & Shima, 1994; Larsson et al., 1996; Gerloff et al., 1997; Rao et al., 1997; Penhune et al., 1998]. Given these results, the amplitude decrease in the second field pattern observed in Experiment 4 may indicate a reduced need for motor planning mechanisms involving the SMA at higher rhythmic movement rates.

7.3 A Possible Physiological Interpretation for Why Transitions from Syncopation to Synchronization Occur

In principle, the performance of both syncopated and synchronized patterns of movement requires that one generate a rhythmic sequence of responses at the correct rate and then shift the onset times appropriately so that the peak of each response has the

correct phase relation/temporal delay within each cycle. In practice, shifting a sequence of movements by ½ cycle is difficult to do even at low frequencies. Constraints on the ability to do this may arise from the fact that one has to predict not only when the next metronome beat will occur but also the point in time that separates successive metronome beats. Subjects who are successful at syncopating often report the use of a cognitive strategy to predict the latter, i.e. perceptually doubling the metronome. In the absence of such a strategy, however, subjects may produce a series of syncopated movements on a cycle-by-cycle basis rather than by organizing them as a continuous sequence.

One hypothesis is that treating each perception-action cycle individually requires the planning of each movement separately whereas organizing a continuous sequence of movements only requires planning in the beginning and then minimal modification or monitoring of movement once the sequence has begun. In this case the former situation can be expected to require additional neural resources in areas that participate in the preparation of movement. This may explain why we found significantly increased activation in, for example, the basal ganglia and premotor areas during syncopated movement. It may also explain why the neuromagnetic beta rhythm in central and precentral areas distinguishes between syncopated and synchronized patterns of coordination even when they are only imagined.

So why transitions? We still do not know the exact cause but one possibility is that motor planning mechanisms require a certain amount of time to operate. This idea is supported by the fact that neural activity in sensorimotor and premotor areas in the foreperiod of voluntary movement is characterized by a slow, gradual accumulation of

amplitude that can begin as early as 3 seconds prior to movement onset [e.g. Kornhuber & Deecke, 1965; Deecke et al., 1976]. The contingent negative variation [Walter et al., 1964] is another, possibly related, slow cortical wave occurring over seconds that is associated with the expectancy of stimuli that require a response. Increasing the rate of coordination may therefore leave too little time for the neural networks that these gradual amplitude changes reflect to function properly. Indeed our results from Experiment 4 show that the 'readiness' field accompanying rhythmic self-paced movement is strongly attenuated once the inter-response interval drops below one second. The consequence is that the nervous system switches from planning each movement separately to a more automatic form of motor control in which responses are organized as a rhythmic sequence and the external metronome is adopted as a pacing cue for movement execution. This scenario implies that the major task constraint that causes transitions from syncopation to synchronization is the 1:1 stimulus/response requirement. In other words, subjects cannot syncopate at faster rates because there is not enough time to prepare a movement for each cycle and they switch to synchronization because this is the only way to maintain the correct movement rate.

In conclusion, future work is needed to clarify the neural mechanisms that underlie transitions from syncopation to synchronization. The work contained in this thesis provides evidence that there is a reorganization of the interaction between neuronal populations distributed across several cortical and subcortical areas. Moreover, there are rate dependent changes in neural activity associated with both the processing of auditory stimuli and motor preparation that are likely to play a role in such transitions.

NOTE TO USERS

Page(s) missing in number only; text follows.
Microfilmed as received.

190

This reproduction is the best copy available.

UMI

8.0 References

Alexander GE, Crutcher MD (1990) Preparation for movement: neural representations of intended direction in three motor areas of the monkey. *J Neurophysiol* 64:133-178.

Alexander GE, DeLong MR, Strick PL (1986) Parallel organization of functionally segregated circuits linking basal ganglia and cortex. In: Cowan WM (ed.) *Annual Review of Neuroscience, vol. 9*, Society for Neuroscience, Washington, DC, pp 357-381.

Allen G, Buxton RB, Wong EC, Courchesne E (1997) Attentional activation of the cerebellum independent of motor involvement. *Science* 275:1940-1943.

Arbib MA (1985) Schemas for the temporal organization of behaviour. *Human Neurobiol* 4:63-72.

Artieda J, Pastor MA, Lacruz F, Obeso JA (1992) Temporal discrimination is abnormal in Parkinson's disease. *Brain* 115:119-210.

Barrett G, Shibasaki N, Neshige R (1986) Cortical potentials preceding voluntary movement: Evidence for three periods of preparation in man. *Electroencephalogr Clin Neurophysiol* 63:327-339.

Beisteiner R, Höllinger P, Lindinger G, Lang W, Berthoz A (1995) Mental representations of movements. Brain potentials associated with imagination of hand movements. *Electroencephalogr Clin Neurophysiol* 96:183-193.

Bendat JS, Piersol AG (1986) *Random Data: Analysis and Measurement Procedures* (2nd Ed). Wiley & Sons, New York.

Binder JR, Rao SM, Hammeke TA, Frost JA, Bandettini PA, Hyde JS (1994) Effects of stimulus rate on signal response during functional magnetic resonance imaging of auditory cortex. *Cog Brain Res* 2:31-38.

Boecker H, Dagher A, Ceballos-Baumann AO, Passingham RE, Samuel M, Friston KJ, Poline J-B, Dettmers C, Conrad B, Brooks DJ (1998) Role of the human rostral supplementary motor area and the basal ganglia in motor sequence control: investigations with H$_2$ ^{15}O PET. *J Neurophysiol* 79:1070-1080.

Bower JM (1997) Control of sensory data acquisition. *Int Rev Neurobiol* 41:489-513.

Bressler SL, Wallenstein GV, Kelso JAS (1996) Frontal lobe involvement in the spontaneous emergence of anticipatory visuomotor behavior. *Soc Neurosci Abstr* 22:1451.

Brotchie P, Ianseck R, Horne MK (1991) Motor function of the monkey globus pallidus, Papers 1 and 2. *Brain* 114:1667-1702.

Carson RG, Chua R, Byblow WD, Poon P, Smethurst CJ (1999) Changes in posture alter the attentional demands of voluntary movement. *Proc R Soc Lond B* 266:853-857.

Catalan MJ, Honda M, Weeks RA, Cohen LG, Hallett M (1998) The functional neuroanatomy of simple and complex sequential finger movements: a PET study. *Brain* 121:253-264.

Chen R, Gerloff C, Hallett M, Cohen LG (1997) Involvement of the ipsilateral motor cortex in finger movements of different complexities. *Ann Neurol* 41:247-254.

Chen Y, Ding M, Kelso JAS (1997) Long memory processes (1/f^α type) in human coordination. *Phys Rev Lett* 79(22):4501-4504.

Chen Y, Ding M, Kelso JAS (submitted) Origins of timing errors in human sensorimotor coordination. *Submitted to Journal of Human Motor Behavior.*

Cheyne D, Weinberg H (1989) Neuromagnetic fields accompanying unilateral finger movements: pre-movement and movement-evoked fields. *Experimental Brain Research* 78:604-612.

Cheyne D, Weinberg H, Gaetz W, Jantzen KJ (1995) Motor cortex activity and predicting side of movement: neural network and dipole analysis of pre-movement magnetic fields. *Neuroscience Letters* 188:81-84.

Cheyne D, Endo H, Takeda T, Weinberg H (1997) Sensory feedback contributes to early movement-evoked fields during voluntary finger movements in humans. *Brain Research* 771:196-202.

Classen J, Gerloff C, Honda M, Hallett M (1998) Integrative visumotor behavior is associated with interregionally coherent oscillations in the human brain. *J Neurophysiol* 79:1567-1573.

Cohen JD, Noll DC, Schneider W (1993) Functional magnetic resonance imaging: Overview and methods for psychological research. *Behavioral Research Methods, Instruments, & Computers* 25(2):101-113.

Cox RW (1996) AFNI: Software for analysis and visualization of functional magnetic resonance neuroimages. *Computers and Biomedical Research* 29: 162-173.

Cox RW, Hyde JS (1997) Software tools for analysis and visualization of fMRI data. *NMR in Biomedicine* 10: 171-178.

Daffertshofer A, Peper CE, Beek PJ (2000) Spectral analyses of event-related encephalographic signals. *Phys Lett A* 266:290-302.

Decety J (1996) Do imagined and executed actions share the same neural substrate? *Cog Brain Res* 3:87-93.

Decety J, Ingvar DH (1990) Brain structures participating in mental simulation of motor behavior: a neuropsychological interpretation. *Acta Psychologica* 73: 13-34.

Decety J, Sjöholm H, Ryding E, Stenberg G, Ingvar DH (1990) The cerebellum participates in mental activity: Tomographic measurements of regional cerebral blood flow. *Brain Res* 535:313-317.

Decety J, Perani D, Jeannerod M, Bettinardi V, Tadary B, Woods R, Mazziotta JC, Fazio F (1994) Mapping motor representations with positron emission tomography. *Nature* 371:600-602.

Deecke L (1987) Bereitschaftspotential as an indicator of movement preparation in supplementary motor area and motor cortex. In: Porter R (ed.) *Motor Areas of the Cerebral Cortex*. Wiley, Chichester, pp 231-250.

Deecke L, Kornhuber HH (1978) An electrical sign of participation of the mesial "supplementary" motor cortex in human voluntary finger movements. *Brain Res* 159:473-376.

Deecke L, Scheid P, Kornhuber HH (1969) Distribution of readiness potential: pre-motion positivity and motor potentials of the human cerebral cortex preceding voluntary finger movements. *Exp Brain Res* 7:158-168.

Deecke L, Grözinger B, Kornhuber HH (1976) Voluntary finger movement in man: cerebral potentials and theory. *Biol Cybern* 23:99-119.

Deecke L, Weinberg H, Brickett P (1982) Magnetic fields of the human brain accompanying voluntary movement: Bereitschaftsmagnetfeld. *Experimental Brain Research* 48:144-148.

Deecke L, Boschert J, Brickett P, Weinberg H (1983) Magnetoencephalographic evidence for possible supplementary motor area participation in human voluntary movement. In: Weinberg H, Stroink G, Kaila T (eds.) *Biomagnetism: applications and theory.* Pergamon Press, New York, pp. 369-372.

Deecke L, Kornhuber HH, Lang W, Lang M, Schreiber H (1985) Timing function of the frontal cortex in sequential motor and learning tasks. *Human Neurobiol* 4:143-154

Deiber MP, Ibanez V, Sadato N, Hallett M (1996) Cerebral structures participating in motor preparation in humans – a positron emission tomography study. *J Neurophysiol* 75:233-247.

DeYoe EA, Bandettini P, Neitz J, Miller D, Winans P (1994) Functional magnetic resonance imaging (FMRI) of the human brain. *J Neurosci Meth* 54:171-187.

Dick JPR, Benecke R, Rothwell JC, Day BL, Marsden CD (1986) Simple and complex movements in a patient with infarction of the right supplementary motor area. *Movement Disord* 1:255-266.

Ebersbach G, Heijmenberg M, Kindermann L, Trottenberg T, Wissel J, Poewe W (1999) Interference of rhythmic constraint on gait in healthy subjects and patients with early Parkinson's disease: Evidence for impaired locomotor pattern generation in early Parkinson's disease. *Movement Disorders* 14(4):619-625.

Engström DA, Kelso JAS, Holroyd T (1996) Reaction-anticipation transitions in human perception-action patterns. *Hum Mov Sci* 15:809-832.

Erdler M, Beisteiner R, Mayer D, Kaindl T, Edward V, Windischberger C, Lindinger G, Deecke L (2000) Supplementary motor area activation preceding voluntary movement is detectable with a whole-scalp magnetoencephalography system. *Neuroimage* 11:697-707.

Feige B, Kristeva-Feiga R, Rossi S, Pizzella V, Rossini P-M (1996) Neuromagnetic study of movement-related changes in rhythmic brain activity. *Brain Res* 734:252-260.

Fink PW, Foo P, Jirsa VK, Kelso JAS (in press) Local and global stabilization of coordination by sensory information. *Exp Brain Res.*

Fraisse P (1982) Rhythm and tempo. In: Deutsch D (ed.) *The Psychology of Music.* Academic Press, New York, pp 149-180.

Friedrich R, Uhl C (1996) Spatiotemporal analysis of human electroencephalograms: Petit-Mal epilepsy. *Physica D* 98:180.

Friston KJ, Ashburner J, Poline JB, Frith CD, Heather JD, Frackowiack RSJ (1995) Spatial realignment and normalization of images. *Human Brain Mapping* 2: 165-189.

Fuchs A, Kelso JAS, Haken H (1992) Phase transitions in the human brain: spatial mode dynamics. *Int J Bif Chaos* 2:917-939.

Fuchs A, Purcott KL, Nair DG, Mayville JM, Owens S, Steinberg F, Kelso JAS (1999) Brain activity in perception-motor coordination revealed by functional fMRI. *Dynamical Neuroscience VII, Integration Across Multiple Imaging Modalities*, Delray Beach, FL.

Fuchs A, Deecke L, Kelso JAS (2000a) Phase transitions in the human brain revealed by large SQuID arrays: Response to Daffertshofer, Peper and Beek. *Phys Lett A* 266:303-308.

Fuchs A, Jirsa VK, Kelso JAS (2000b) Theory of the relation between human brain activity (MEG) and hand movements. *Neuroimage* 11(5):359-369.

Fuchs A, Mayville JM, Cheyne D, Weinberg H, Deecke L, Kelso JAS (2000c) Spatiotemporal analysis of neuromagnetic events underlying the emergence of coordinative instabilities. *Neuroimage* 12(1):71-84.

Fuster JM (1989) *The prefrontal cortex. Anatomy, physiology and neuropsychology of the frontal lobe.* Raven press, New York.

Gao JH, Parsons LM, Bower JM, Xiong J, Li J, Fox PT (1996) Cerebellum implicated in sensory acquisition and discrimination rather than motor control. *Science* 272:545-547.

Georgiou N, Iansek R, Bradshaw JL, Phillips JG, Mattingley JB, Bradshaw JA (1993) An evaluation of the role of internal cues in the pathogenesis of parkinsonian hypokinesia. *Brain* 116:1575-87.

Georgiou N, Bradshaw JL, Iansek R, Phillips JG, Mattingley JB, Bradshaw JA (1994) Reduction in external cues and movement sequencing in Parkinson's disease. *J Neurol Neurosurg Psychiatry* 57:368-370.

Georgopoulos AP, Massey JT (1987) Cognitive spatial-motor processes. *Exp Brain Res* 65:361-370.

Gerloff C, Corwell B, Chen R, Hallett M, Cohen L (1997) Stimulation over the human supplementary motor area interferes with the organization of future elements in complex motor sequences. *Brain* 120:1587-1602.

Gerloff C, Richard J, Hadley J, Schulman AE, Honda M, Hallett M (1998) Functional coupling and regional activation of human cortical motor areas during simple, internally paced and externally paced finger movements. *Brain* 121:1513-1531.

Gilden DL, Thornton T, Mallon MW (1995) 1/f noise in human cognition. *Science* 267:1837-1839.

Goldman-Rakic PS (1987) Circuitry of primate prefrontal cortex and regulation of behavior by representational memory. In: Mountcastle V, Plum F (eds.) *The Nervous System, Higher Functions of the Brain, Vol. 5., Handbook of Physiology.* American Physiological Society, Washington, DC, pp 373-417.

Gray CM, König P, Engel AK, Singer W (1989) Oscillatory responses in cat visual cortex exhibit inter-columnar synchronization which reflects global stimulus properties. *Nature* 338:334-337.

Haken H (1977) *Synergetics: an Introduction* (3rd Ed, 1983). Springer, Berlin.

Haken H (1983) *Advanced Synergetics* (2nd Ed, 1987). Springer, Berlin.

Haken H (1996) *Principles of brain functioning.* Springer, Berlin.

Haken H, Kelso JAS, Bunz H (1985) A theoretical model of phase transitions in human hand movements. *Biol Cybern* 51:347-356.

Hallett M, Fieldman J, Cohen LG, Sadato N, Pascual-Leone A (1994) Involvement of primary motor cortex in motor imagery and mental practice. *Behav Brain Sci* 17:210.

Halsband U, Ito N, Tanji J, Freund H-J (1993) The role of premotor cortex and the supplementary motor area in the temporal control of movement in man. *Brain* 116:243-266.

Halsband U, Matsuzaka Y, Tanji J (1994) Neuronal activity in the primate supplementary, pre-supplementary and premotor cortex during externally and internally instructed sequential movements. *Neurosci Res* 20:149-155.

Hari R, Kaila K, Katila T, Tuomisto T, Varpula T (1982) Interstimulus interval dependence of the auditory vertex response and its magnetic counterpart:

implications for their neural generation. *Electroencephalogr Clin Neurophysiol* 54:561-569.

Hari R, Antervo A, Katila T, Poutanen T, Seppänen M, Tuomisto T, Varpula T (1983) Cerebral magnetic fields associated with voluntary limb movements. *Nuova Cimento* 2D:484-494.

Hari R, Salmelin R, Mäkelä JP, Salenius S, Helle M (1997) Magnetoencephalographic cortical rhythms. *Int J Psychophysiol* 26:51-62.

Hämäläinen M, Hari R, Ilmoniemi J, Knuutila J, Lounasmaa OV (1993) Magnetoencephalography-theory, instrumentation, and applications to noninvasive studies of the working human brain. *Rev Mod Phys* 65(2):413-497.

Harrington DL, Haaland KY (1998) Sequencing and timing operations of the basal ganglia. In: Rosenbaum DA, Collyer CE (eds) *Timing of Behavior: Neural, Psycholgical and Computational Perspectives*. MIT Press, Cambridge MA, pp 35-61.

Harrington DL, Haaland KY (1999) Neural underpinnings of temporal processing: a review of focal lesion, pharmacological, and functional imaging research. *Reviews in the Neurosciences* 10(2):91-116.

Harrington DL, Haaland KY, Hermanowicz N (1998) Temporal processing in the basal ganglia. *Neuropsychology* 12(1):3-12.

Holroyd T, Endo H, Kelso JAS, Takeda T (1999) Dynamics of the MEG recorded during rhythmic index-finger extension and flexion. In: Yoshimoto T, Kotani M, Kuriki S, Nakasato N, Karibe H (eds.) *Recent Advances in Biomagnetism: Proceedings of the 11th International Conference on Biomagnetism*. Tohoko University Press, Sendai, Japan, pp 446-449.

Ivry RB (1996) The representation of temporal information in perception and motor control. *Curr Opin Neurobiol* 6:851-857.

Ivry RB (1997) Cerebellar timing systems. *Int Rev Neurobiol* 41:555-573.

Ivry RB (2000) Exploring the role of the cerebellum in sensory anticipation and timing: commentary on Tesche and Karhu. *Human Brain Mapping* 9:115-118.

Ivry RB, Keele SW (1989) Timing functions of the cerebellum. *J Cog Neurosci* 1(2):136-152.

197

Ivry RB, Keele SW, Diener HC (1988) Dissociation of the lateral and medial cerebellum in movement timing and movement execution. *Exp Brain Res* 73:167-180.

Jackson SR, Jackson GM, Harrison J, Henderson L, Kennard C (1995) The internal control of action and Parkinson's disease: a kinematic analysis of visually-guided and memory-guided prehension movements. *Exp Brain Res* 105:147-162.

Jaeger D, Gilman S, Aldridge JW (1993) Primate basal ganglia activity in a precued reaching task – preparation for movement. *Exp Brain Res* 95(1):51-64.

Jenkins IH, Passingham RE, Brooks DJ (1997) The effect of movement frequency on cerebral activation: a positron emission tomography study. *J Neurol Sci* 151:195-205.

Jenkins IH, Jahanshahi M, Jueptner M, Passingham RE, Brooks DJ (2000) Self-initiated versus externally triggered movements II: the effect of movement predictability on regional cerebral blood flow. *Brain* 123:1216-1228.

Jirsa VK, Friedrich R, Haken H, Kelso JAS (1994) A theoretical model of phase transitions in the human brain. *Biol Cybern* 71:27-35.

Johnson KA, Cunnington R, Bradshaw JL, Phillips JG, Iansek R, Rogers MA (1998) Bimnaual coordination in Parkinson's disease. *Brain* 121:743-753.

Josephson BD (1962) Possible new effects in superconductive tunneling. *Phys Lett* 1:251-253.

Jueptner M, Stephan KM, Frith CD, Brooks DJ, Frackowiak RSJ, Passingham RE (1997) Anatomy of motor learning. I. Frontal cortex and attention to action. *J Neurophysiol* 77:1313-1324.

Kelso JAS (1984) Phase transitions and critical behavior in human bimanual coordination. *Am J Physiol* 246:R1000-R1004.

Kelso JAS (1994) The informational character of self-organized coordination dynamics. *Hum Mov Sci* 13:393-413.

Kelso JAS (1995) *Dynamic Patterns: The Self-Organization of Human Brain and Behavior*. MIT Press, Cambridge, MA.

Kelso JAS, Kay BA (1987) Information and control: A macroscopic analysis of perception-action coupling. In: Heuer H, Sanders AF (eds.) *Perspectives on Perception and Action*. Lawrence Erlbaum, Hillsdale, NJ, pp 3-32.

Kelso JAS, Scholz JP (1985) Cooperative phenomena in biological motion. In: Haken H (ed.) *Complex Systems: Operational Approaches in Neurobiology, Physical Systems and Computers.* Springer-Verlag, Berlin, pp 124-149.

Kelso JAS, Scholz JP, Schöner G (1988) Dynamics governs switching among patterns of coordination in biological movement. *Phys Lett A* 134(1):8-12.

Kelso JAS, DelColle JD, Schöner G (1990) Action-perception as a pattern formation process. In: Jeannerod M (ed.) *Attention and Performance XIII.* Lawrence Erlbaum, Hillsdale, NJ, pp 139-169.

Kelso JAS, Bressler SL, Buchanan S, DeGuzman GC, Ding M, Fuchs A, Holroyd T (1991) Cooperative and critical phenomena in the human brain revealed by multiple SQuIDs. In: Duke D, Pritchard W (eds.) *Measuring Chaos in the Human Brain.* World Scientific, Teaneck, NJ, pp 97-112.

Kelso JAS, Bressler SL, Buchanan S, DeGuzman GC, Ding M, Fuchs A, Holroyd T (1992) A phase transition in human brain and behavior. *Phys Lett A* 169:134-144.

Kelso JAS, Fuchs A, Lancaster R, Holroyd T, Cheyne D, Weinberg H (1998) Dynamic cortical activity in the human brain reveals motor equivalence. *Nature* 392:814-818.

Kermadi I, Liu Y, Tempini A, Rouiller EM (1997) Effects of reversible inactivation of the supplementary motor area (SMA) on unimanual grasp and bimanual pull and grasp performance in monkeys. *Somatosensory & Motor Research* 14(4): 268-280.

Kirk RE (1968) *Experimental Design: Procedures for the Behavioral Sciences.* Brooks/Cole, Belmont, CA, pp 88-90.

Kitamura J, Shibasaki H, Takagi A, Nabeshime H, Yamaguchi A (1993) Enhanced negative slope of cortical potentials before sequential as compared with simultaneous extensions of two fingers. *Electroencephalogr Clin Neurophysiol* 86:176-182.

Kornhuber HH, Deecke L (1965) Hirnpotentialänderungen bei Willkürbewegungen und passiven Bewegungen des Menschen: Bereitschaftspotential und reafferente Potentiale. *Pflügers Arch* 284:1-17.

Kornhuber HH, Deecke L, Lang W, Lang M, Kornhuber A (1989) Will, volitional action, attention and cerebral potentials in man: Bereitschaftspotential, performance-related potentials, directed action potential, EEG spectrum changes. In: Hershberger W (ed.) *Volitional Action.* Elsevier, Amsterdam, pp. 107-168.

Kristeva R, Cheyne D, Deecke L (1991) Neuromagnetic fields accompanying unilateral and bilateral voluntary movements: topography and analysis of cortical sources. *Electroencephalogr Clin Neurophysiol* 81:284-298.

Kristeva-Feige R, Feige B, Makeig S, Ross B, Elbert T (1993) Oscillatory brain activity during a motor task. *NeuroReport* 4:1291-1294.

Kristeva-Feige R, Walter H, Lütkenhöner B, Hampson S, Ross B, Knorr U, Steinmetz H, Cheyne D (1994) A neuromagnetic study of the functional organization of the sensorimotor cortex. *European Journal of Neuroscience* 6:632-639.

Kristeva-Feige R, Rossi S, Pizzella V, Sabato A, Tecchio F, Feige B, Romani G-L, Edrich J, Rossini PM (1996) Changes in movement-related brain activity during transient deafferentation: a neuromagnetic study. *Brain Research* 714:201-208.

Lang W, Lang M, Podreka I, Steiner M, Uhl F, Suess E, Müller C, Deecke L (1988) DC-potential shifts and regional cerebral blood flow reveal frontal cortex involvement in human visuomotor learning. *Exp Brain Res* 71:353-364.

Lang W, Zilch O, Koska C, Lindinger G, Deecke L (1989) Negative cortical DC shifts preceding and accompanying simple and complex sequential movements. *Exp Brain Res* 74:99-104.

Lang W, Obrig H, Lindinger G, Cheyne D, Deecke L (1990) Supplementary motor area activation while tapping bimanually different rhythms in musicians. *Exp Brain Res* 79:504-514.

Lang W, Cheyne D, Kristeva R, Beisteiner R, Lindinger G, Deecke L (1991) Three-dimensional localization of SMA activity preceding voluntary movement. A study of electric and magnetic fields in a patient with infarction of the right supplementary motor area. *Experimental Brain Research* 87(3):688-695.

Lang W, Cheyne D, Höllinger P, Gerschlager W, Lindinger G (1996) Electric and magnetic fields of the brain accompanying internal simulation of movement. *Cog Brain Res* 3:125-129.

Larsson J, Gulyás B, Roland PE (1996) Cortical representation of self-paced finger movement. *Neuroreport* 7:463-468.

Lee DN, Craig CM, Grealy MA (1999) Sensory and intrinsic coordination of movement. *Proceedings of the Royal Society of London*, B266: 2029-2035.

Lejeune H, Maquet P, Bonnet M, Casini L, Ferrara A, Macar F, Pouthas V, Timsit-Berthier M, Vidal F (1997) The basic pattern of activation in motor and sensory temporal tasks: Positron emission tomography data. *Neurosci Lett* 235:21-24

Leocani L, Toro C, Manganotti P, Zhuang P, Hallett M (1997) Event-related coherence and event-related desynchronization/synchronization in the 10 Hz and 20 Hz EEG during self-paced movements. *Electroencephalogr Clin Neurophysiol* 104:199-206.

Lins OG, Picton TW (1995) Auditory steady-state responses to multiple simultaneous stimuli. *Electroencephalogr Clin Neurophysiol* 96:420-432.

Liu L, Ioannides AA, Taylor JG (1998) Observation of quantization effects in human auditory cortex. *NeuroReport* 9:2679-2690.

Lopes da Silva FH (1991) Neural mechanisms underlying brain waves: from neural membranes to networks. *Electroencephalogr Clin Neurophysiol* 79:81-93.

Lopes da Silva FH, van Rotterdam A, Storm van Leeuwen W, Tielen AM (1970) Dynamic characteristics of visual evoked potentials in the dog. II. Beta frequency selectivity in evoked potentials and background activity. *Electroencephalogr Clin Neurophysiol* 29:260-268.

MacKay WA (1997) Synchronized neuronal oscillations and their role in motor processes. *Trends Cog Sci* 1(5):176-183.

Malapani C, Dubois B, Rancurel G, Gibbon J (1998) Cerebellar dysfunctions of temporal processing in the seconds range in humans. *NeuroReport* 9:3907-3912.

Manganotti P, Gerloff C, Toro C, Katsuta H, Sadato N, Zhuang P, Leocani L, Hallet M (1998) Task-related coherence and task-related spectral power changes during sequential finger movements. *Electroencephalogr Clin Neurophysiol* 109:50-62.

Mayville JM, Bressler SL, Fuchs A, Kelso JAS (1999) Spatiotemporal reorganization of electrical activity in the human brain associated with a timing transition in rhythmic auditory-motor coordination. *Exp Brain Res* 127:371-381.

Mayville JM, Fuchs A, Ding M, Cheyne D, Deecke L, Kelso JAS (submitted) Event-related changes in neuromagnetic activity associated with syncopation and synchronization timing tasks. *Submitted to Human Brain Mapping*.

Mayville JM, Fuchs A, Kelso JAS (in preparation) Neuromagnetic beta (15-30 Hz) rhythm associated with transitions in overt and imagined sensorimotor coordination.

Murthy VN, Fetz EE (1992) Coherent 25-30 Hz oscillations in the sensorimotor cortex of awake behaving monkeys. *Proc Natl Acad Sci USA* 89:5670-5674.

Mushiake H, Inase M, Tanji J (1991) Neuronal activity in the primate premotor, supplementary, and precentral motor cortex during visually guided and internally determined sequential movements. *J Neurophysiology* 66(3):705-718.

Näätänen R, Picton T (1987) The N1 wave of the human electric and magnetic response to sound: a review and an analysis of the component structure. *Psychophysiology* 24(4):375-425.

Nashmi R, Mendonça AJ, MacKay WA (1994) EEG rhythms of the sensorimotor region during hand movements. *Electroencephalogr Clinical Neurophysiol* 91:456-467.

Nunez PL (1981) *Electric Fields of the Brain: The Neurophysics of EEG*. Oxford University Press, New York.

O'Boyle DJ, Freeman JS, Cody FWJ (1996) The accuracy and precision of timing of self-paced, repetitive movements in subjects with Parkinson's disease. *Brain* 119:51-70.

Oldfield, RC (1971) The assessment and analysis of handedness: the Edinburgh inventory. *Neuropsychologia* 9:97-11.

Orgogozo JM, Larsen B (1979) Activation of the SMA during voluntary movements in man suggests it works as a supramotor area. *Science* 206:847-850.

Pastor MA, Artieda J, Jahanshahi M, Obeso JA (1992a) Performance of repetitive wrist movements in Parkinson's disease. *Brain* 115:875-891.

Pastor MA, Artieda J, Jahanshahi M, Obeso JA (1992b) Time estimation and reproduction is abnormal in Parkinson's disease. *Brain* 115:225.

Penhune VB, Zatorre RJ, Evans AC (1998) Cerebellar contributions to motor timing: a PET study of auditory and visual rhythm reproduction. *J Cog Neurosci* 10(6):752-765.

Pfurtscheller G (1981) Central beta rhythm during sensory motor activities in man. *Electroencephalogr Clin Neurophysiol* 51:253-264.

Pfurtscheller G (1992) Event-related synchronization (ERS): an electrophysiological correlate of cortical areas at rest. *Electroencephalogr Clin Neurophysiol* 83:62-69.

Pfurtscheller G, Aranibar A (1977) Event-related cortical desynchronization detected by power measurements of scalp EEG. *Electroencephalogr Clin Neurophysiol* 2:817-826.

Pfurtscheller G, Berghold A (1989) Patterns of cortical activation during planning of voluntary movement. *Electroencephalogr Clin Neurophysiol* 72:250-258.

Pfurtscheller G, Lopes da Silva FH (1999) Event-related EEG/MEG synchronization and desynchronization: basic principles. *Clin Neurophysiol* 110:1842-1857.

Pfurtscheller G, Neuper C (1992) Simultaneous EEG 10 Hz desynchronization and 40 Hz synchronization during finger movements. *NeuroReport* 3:1057-1060.

Pfurtscheller G, Neuper C (1997) Motor imagery activates primary sensorimotor area in humans. *Neurosci Lett* 239:65-68.

Pfurtscheller G, Stancák A Jr., Neuper C. (1996) Post-movement beta synchronization. A correlate of an idling motor area? *Electroencephalogr Clin Neurophysiol* 98:281-293.

Pfurtscheller G, Zalaudek K, Neuper C (1998) Event-related beta synchronization after wrist, finger and thumb movement. *Electroencephalogr Clin Neurophysiol* 109:154-160.

Platel H, Price C, Baron J-C, Wise R, Lambert J, Frackowiak B, Lechevalier B, Eustache F (1997) The structural components of music perception: A functional anatomical study. *Brain* 120:229-243.

Praamstra P, Stegeman DF, Horstink MWIM, Cools AR (1996) Dipole source analysis suggests selective modulation of the supplementary motor area contribution to the readiness potential. *Electroencephalogr Clin Neurophysiol* 98:468-477.

Pribram KH (1991) *Brain and Perception.* Lawrence Erlbaum, Hillsdale, NJ.

Quintana J, Yajeya J, Fuster JM (1988) Prefrontal representation of stimulus attributes during delay tasks. 1. Unit activity in cross-temporal integration of sensory and sensory-motor integration. *Brain Res* 474:211-221.

Rammsayer TH (1999) Neuropharmacological evidence for different timing mechanisms in humans. *Quarterly Journal of Experimental Psychology Section B – Comparative and Physiological Psychology* 52(3):273-386.

Rao SM, Binder JR, Bandettini PA, Hammeke TA, Yetkin FZ, Jesmanowicz A, Lisk LM, Morris GL, Mueller WM, Estkowski LD, Wong EG, Haughton VM, Hyde JS (1993) Functional magnetic resonance imaging of complex human movements. *Neurology* 43:2311-2318.

Rao SM, Bandettini PA, Binder JR, Bobholz JA, Hammeke TA, Stein EA, Hyde JS (1996) Relationship between finger movement rate and functional magnetic

resonance signal change in human primary motor cortex. *J Cerebral Blood Flow Metabol* 16:1250-1254.

Rao SM, Harrington DL, Haaland KY, Bobholz JA, Cox RW, Binder JR (1997) Distributed neural systems underlying the timing of movements. *J Neurosci* 17(14):5528-5535.

Roland PE, Larsen B, Lassen NA, Skinhøj E (1980) Supplementary motor area and other cortical areas in the organization of voluntary movements in man. *J Neurophysiology* 43(1):118-136.

Rothwell J (1994) *Control of Human Voluntary Movement, 2ⁿᵈ Ed.* Chapman & Hall, London.

Ryding E, Decety J, Sjöholm H, Stenberg G, Ingvar DH (1993) Motor imagery activates the cerebellum regionally: a SPECT rCBF study with ⁹⁹ᵐTc-HMPAO. *Cog Brain Res* 2:94-99.

Sadato N, Campbell G, Ibañez V, Deiber MP, Hallett M (1996) Complexity affects regional cerebral blood flow change during sequential finger movements. *J Neurosci* 16:2693-2700.

Sadato N, Ibañez V, Campbell G, Deiber MP, Le Bihan D, Hallett M (1997) Frequency-dependent changes of regional cerebral blood flow during finger movements: functional MRI compared to PET. *J Cerebral Blood Flow Metabol* 17:670-679.

Salmelin R, Hari R (1994) Spatiotemporal characteristics of sensorimotor neuromagnetic rhythms related to thumb movement. *Neuroscience* 60:537-550.

Scholz JP, Kelso JAS (1990) Intentional switching between patterns of bimanual coordination depends on the intrinsic dynamics of the patterns. *J Mot Behav* 22(1):98-124.

Schubotz RI, Friederici AD, Yves von Cramon D (2000) Time perception and motor timing: a common cortical and subcortical basis revealed by fMRI. *Neuroimage* 11:1-12.

Shibasaki H, Sadato N, Lyshkow H, Yonekura Y, Honda M, Nagamine T, Suwazono S, Magata Y, Ikeda A, Miyazaki M, Fukuyama H, Asato R, Konishi J (1993) Both primary motor cortex and supplementary motor area play an important role in complex finger movement. *Brain* 116:1387-1398.

Simonetta M, Clanet M, Rascol O (1991) Bereitschaftspotential in a simple movement or in a motor sequence starting with the same simple movement. *Electroencephalogr Clin Neurophysiol* 81:129-134.

Stančák A Jr., Feige B, Lücking CH, Kristeva-Feige R (2000) Oscillatory cortical activity and movement-related potentials in proximal and distal movements. *Clin Neurophysiol* 111:636-650.

Talairach J, Tournoux P (1988) Co-planar Stereotaxic Atlas of the Brain. New York: Thieme.

Tallal P, Miller S, Fitch R (1993) Neurobiological basis of speech: a case for the preeminence of temporal processing. In: Tallal P, Galaburda AM, Llinas RR, von Euler C (eds.) *Temporal Information Processing in the Nervous System: Special Reference to Dyslexia and Dysphasia.* Annals of the New York Academy of Sciences, *Vol 682*, pp 27-47.

Tanji J, Shima K (1994) Role for supplementary motor area cells in planning several movements ahead. *Nature* 371:413-416.

Temprado JJ, Zanone PG, Monno A, Laurent M (1999) Attentional load associated with performing and stabilizing preferred bimanual patterns. *J Exp Psychol Hum Percept Perform* 25(6):1579-1594.

Tesche CD, Karhu JJT (2000) Anticipatory cerebellar responses during somatosensory omission in man. *Human Brain Mapping* 9:119-142.

Toro C, Deuschl G, Thatcher R, Sato S, Kufta C, Hallett M (1994) Event related desynchronization and movement-related cortcial potentials on EcoG and EEG. *Electroencephalogr Clin Neurophysiol* 93:390-403.

Truelle JL, Le Gall D, Joseph PA, Aubin G, Derouesné C, Lezak MD (1995) Movement disturbances following frontal lobe lesions: qualitative analysis of gesture and motor programming. *Neuropsychiatry Neuropsychol Behav Neurol* 8(1):14-19.

Tuller B, Kelso JAS (1989) Environmentally-elicited patterns of movement coordination in normal and split-brain subjects. *Exp Brain Res* 75:306-316.

Vanni S, Portin K, Virsu V, Hari R (1999) Mu rhythm modulation during changes of visual percepts. *Neuroscience* 91(1):21-31.

Wallenstein GV, Kelso, JAS, Bressler, SL (1995) Phase transitions in spatiotemporal patterns of brain activity and behavior. *Physica D* 20:626-634.

Walter WG, Cooper R, Aldridge VJ, McCallum WC, Winter AL (1964) Contingent negative variation: an electrical sign of sensorimotor association and expectancy in the human brain. *Nature* 203:380-384.

Warren WH, Kelso JAS (1985) Report of the work group on perception and action. In: Warren WH, Shaw RE (eds.) *Persistence and Change: Proceedings of the First International Conference on Event Perception.* Lawrence Erlbaum, Hillsdale, NJ, pp 269-281.

Warren WH Jr. (1998) Visually controlled locomotion: 40 years later. *Ecological Psychology* 10(3-4):177-219.

Wessel K, Zeffiro T, Toro C, Hallett M (1997) Self-paced versus metronome-paced finger movements. *J Neuroimag* 7:145-151.

Wing AM, Kristofferson AB (1973) Response delays and the timing of discrete motor responses. *Percept Psychophys* 14:5-12.

Wing AM, Keele SW, Margolin DI (1984) Motor disorder and the timing of repetitive movements. In: Gibbon J, Allen L (eds.) *Annals of the New York Academy of Sciences: Vol 423. Timing and Time Perception.* NY Academy of Sciences, New York, pp 183-192.

Wimmers RH, Beek PJ, van Wieringen PCW (1992) Phase transitions in rhythmic tracking movements: a case of unilateral coupling. *Hum Mov Sci* 11:217-226.

CURRICULUM VITAE

Justine M Mayville

Personal Information:

Date of Birth:	10/18/71
Age:	28
Sex:	Female
Citizenship:	United States

Work Address:	Center for Complex Systems and Brain Sciences
	Florida Atlantic University
	Innovation Center 2
	3834 FAU Boulevard, Suite 210
	Boca Raton, FL 33431

Home Address:	112 Palamino Circle
	Boca Raton, FL 33487

Phone:	(561) 297-2230 – work / (561) 999-9447 – home
Fax:	(561) 297-3634
E-mail:	mayville@walt.ccs.fau.edu

Major Research Interests:

The use of human neuroimaging techniques (electroencephalography-EEG, magnetoencephalography-MEG, magnetic resonance imaging-MRI, and functional MRI) to investigate the spatiotemporal dynamics of brain activity. Especially sensorimotor integration in a rhythmic context and the emergence of instability in coordinative behavior.

Education:

1994-Current:	Pre-Doctoral Fellow. Center for Complex Systems and Brain Sciences. Florida Atlantic University. Boca Raton, FL.
1993:	Bachelor of Arts (Psychology/Sociology), Wake Forest University. Winston-Salem, NC

Awards and Honors:

1996-1997: Newell Fellowship Award, Florida Atlantic University

1994-1997: NIMH Predoctoral Trainee, Award #MH19116

1993: B.A. in Psychology, Magna Cum Laude

1989-1993: Dean's List, all eight semesters, Wake Forest University

Research Experience:

1994-present: Research assistant in the EEG lab, Human Brain and Behavior Laboratory, Center for Complex Systems and Brain Sciences, Florida Atlantic University. Using EEG to characterize the human cortical response to transitions in coordinative timing.

1999-present: Research assistant at University MRI, Boca Raton, FL. Using MRI/fMRI to assess cortical/subcortical involvement in auditory-motor function.

Publications:

Journal Articles:

Mayville JM, Fuchs A, Ding M, Cheyne D, Deecke L, Kelso JAS. Event-related changes in neuromagnetic activity associated with syncopation and synchronization timing tasks. Submitted to *Human Brain Mapping*.

Fuchs A, **Mayville JM**, Cheyne D, Weinberg H, Deecke L, Kelso JAS (in press) Spatiotemporal analysis of neuromagnetic events underlying the emegence of coordinative instabilities. *Neuroimage*.

Mayville JM, Bressler SL, Fuchs A, Kelso JAS (1999) Spatiotemporal reorganization of electric activity in the human brain associated with a timing transition in rhythmic auditory-motor coordination. *Experimental Brain Research* 127: 371-381.

Posters:

Fuchs A, **Mayville JM**, Purcott KL, Steinberg F, Kelso JAS. Cerebellar activity distinguishes sensorimotor task difficulty in fMRI. Submitted to *Society for Neuroscience Abstracts*.

Mayville JM, Cheyne D, Deecke L, Ding M, Fuchs A, Kelso JAS. Desynchronization of MEG (15-30 Hz) associated with overt and imagined sensorimotor coordination reflects task difficulty. Submitted to *Society for Neuroscience Abstracts*.

Carver FW, Fuchs A, Mayville JM, Davis SW, Kelso JAS (1999) Systematic investigation of the human brain's response to rhythmic auditory stimulation. *Dynamical Neuroscience VII, Integration Across Multiple Imaging Modalities*, Delray Beach, FL.

Fuchs A, Purcott KL, Nair DG, Mayville JM, Owens S, Steinberg F, Kelso JAS (1999) Brain activity in perception-motor coordination revealed by functional fMRI. *Dynamical Neuroscience VII, Integration Across Multiple Imaging Modalities*, Delray Beach, FL.

Kelso JAS, Fuchs A, Mayville JM, Nash AJ, Cheyne D, Weinberg H, Deecke L (1999) Decomposition of brain signals into physiological events underlying phase transitions in the human brain. *Society for Neuroscience Abstracts* 25(1): 1137.

Nair DG, Purcott KL, Fuchs A, Mayville JM, Steinberg F, Kelso JAS (1999) Comparing motor and imaginary related activation in the brain: a functional MRI study in normal subjects and a stroke patient. *Dynamical Neuroscience VII, Integration Across Multiple Imaging Modalities*, Delray Beach, FL.

Mayville JM, Wallenstein GV, Nash A, Fuchs A, Bressler SL, Kelso JAS (1996) Cortical dynamics of the human EEG associated with behavioral phase transitions in an auditory-motor task. *Society for Neuroscience Abstracts* 22(2): 890.